Test and Evaluation of TRUST: Tools for Recognizing Useful Signals of Trustworthiness

Jamie R. Lukos
Matthew A. Yanagi
Wayne Ensign
Patrick Longhini
Visarath In

SSC Pacific
San Diego, CA 92152-5001

The citation of trade names and names of names of manufacturers is not to be construed as official government endorsement or approval of commercial products or services referenced in this report.

MATLAB® is a registered trademark of The MathWorks.

RP

ACKNOWLEDGMENTS

EXECUTIVE SUMMARY

   The purpose of this project was to test and evaluate a new research method for measuring and requiring trust between individuals. The task was adapted from a well-evaluated game theory paradigm (Prisoner's Dilemma) that puts participants in a situation where they must decide to trust or not trust an assigned partner. Their decisions, and the decisions of their partners, to trust or not trust, determined the amount of monetary compensation they were given at the end of the experimental session. The goal of the study was to evaluate the extent to which particular behavioral, psychological, physiological, and neural signals are related to trust between two people. The measures described in this report include frontal alpha power asymmetry, electroencephalography (EEG), high- and low-frequency and RR interval of heart rate, electrocardiography (ECG), skin conductance levels and Galvanic Skin Response (GSR), oxytocin and cortisol concentrations, and psychological state (questionnaires). These dependent measures were investigated using three different methodological transformations: one examining raw signals, and two adjusting the signals to baseline: [minus baseline] and divided by baseline.

[Six hypotheses were derived from the Social Exchange Model (SEM):]

- H1: Do measures change (relative to baseline) in accordance with SEM *before trust* interactions?
- H2: Do measures change (relative to baseline) in accordance with SEM *after trust* interactions?
- H3: Do measures change (relative to baseline) in accordance with SEM *before distrust* interactions?
- H4: Do measures change (relative to baseline) in accordance with SEM *after distrust* interactions?
- H5: Do measures differ *between trust and distrust* decisions in accordance with SEM *before* interactions?
- H6: Do measures differ *between trust and distrust* decisions in accordance with SEM *after* interactions?

   For each hypothesis, sub-hypotheses were stated relating how the individual measures of interest would change as predicted by the SEM.

   Using standard repeated measures of analysis of variance (ANOVA) with multiple comparisons, we found inconsistent significant changes across measures, hypotheses and methodologies. This result may be due to the ambitious goal of measuring trust in a psychophysiological context in an inherently noisy ecological setting, or due to the type of methodologies and measures evaluated. But importantly, these data highlight the complexity of understanding the nature of trust: there is no single measure or simple answer to such an interconnected human process. A conglomerate of multimodal measures, regardless of their individual significance, is the first attempt at building a holistic representation of the psychophysiological basis of the decision to trust. In turn, this project will act as an important benchmark for future efforts into understanding trust and the social dynamics of human interactions.

SYMBOLS, ABBREVIATIONS, AND ACRONYMS

*	Significant (as defined by particular analyses)
A	Ability (in reference to Mayer-ABI)
ACTH	Adrenal Corticotropic Hormore
ANOVA	Analysis of Variance
ANS	Autonomic Nervous System
ATRQ	Attitude Toward Risk Questionnaire
B	Benevolence (in reference to Mayer-ABI)
bpm	Beats per Minute
CI	Confidence Interval
CDC	Centers for Disease Control and Prevention
coeff	Coefficient
CT	Cortisol
dB	Decibels
ECG	Electrocardiography
EDA	Electrodermal Activity
EEG	Electroencephalography
EOG	Electrooculography
FFT	Fast Fourier Transform
fMRI	Functional Magnetic Resonance Imaging
GSR	Galvanic Skin Response
GSS	Gene Suspicion Scale
HC	hydrocortisol
HF	High Frequency
HFnorm	High Frequency normalized
HR	Heart Rate
HRV	Heart Rate Variability
Hz	Hertz
I	Integrity (in reference to Mayer-ABI)
IARPA	Intelligence Advanced Research Projects Activity
IBI	Inter-beat Interval
IC	Independent Component
ICA	Independent Component Analysis
ICD	Informed Consent Document
IV	Intravenous
LSD	Least Square Difference
LF	Low Frequency
LFnorm	Low Frequency normalized
log	Logarithm
MANOVA	Multivariate Analysis of Variance
Mayer-ABI	Mayer trust scale for partner's Ability, Benevolence, and Integrity
Mayer-P	Mayer trust scale for Propensity
ml	Milliliter

ms	milliseconds
uS	Microsiemens
n	Number of values
nS	Nanosiemens
n.s.	Not significant
n.s.*	Significant, but in opposition to the SEM hypothesis
n.u.	No unit
NEO	Neuroticism-Extraversion-Openness Personality Scale
NEO-FFI-3	Neuroticism-Extraversion-Openness-Five Factor Inventory-3
Nfft	Length of Fast Fourier Transform
ODNI	Office of the Director of National Intelligence
OSHA	Occupational Safety and Health Administration
OT	Oxytocin
PANAS	Positive and Negative Affect Schedule
Pg	picogram
PD	Prisoner's Dilemma
PNS	Parasympathetic Nervous System
PSD	Power Spectral Density
R	A point corresponding to the peak of the QRS complex of the ECG
RR interval	The interval between successive R's as shown on an electrocardiogram
R^2	Coefficient of determination
RCI-R	Relationship Closeness Inventory-Revised
RN	Registered nurse
RQ	Relationship Questionnaire
SAS	Stress Appraisal Scale
SCL	Skin Conductance Level
SCR	Skin Conductance Response
SE	Standard Error
SEM	Social Exchange Model
SMAS	Stephenson Multigroup Acculturation Scale
SNK	Student-Newman-Keuls
SNS	Sympathetic nervous system
SPSS	Statistical Package for the Social Sciences
SS	Sharing Secrets
STAI-S	State-Trait Anxiety Inventory
Trapz	Trapezoidal Numerical Integration Function
T&E	Test and Evaluation
TRUST	Tools for Recognizing Useful Signals of Trustworthiness
µg	micrograms
USD	United States Dollar
µS	microsiemens
µV	microvolts
α	Alpha wave; cortical frequency band of 8-13 Hz
β	Beta wave; cortical frequency band of 13-20 Hz

γ	Gamma wave; cortical frequency band of 35-55 Hz
θ	Theta wave; cortical frequency band 4-7 Hz

CONTENTS

Figures

Tables

1. INTRODUCTION AND BACKGROUND

1.1 GOAL

The goal of this project was to test a new experimental protocol for manipulating and measuring interpersonal trust using neural, physiological, behavioral, and psychological test instruments with research participants of varying acculturation levels.

We tested whether two versions of a novel paradigm, the "Sharing Secrets (SS)" protocol, described below is a construct, face, and ecologically valid way to measure interpersonal trust between two people. The two individuals were either familiar or unfamiliar to each other and may or may not share significant cultural traits. In this study, trust was tested in a situation in which two individuals worked together to complete an interview-based task in order to keep a monetary endowment they earned at the beginning of the study.

The SS protocol was part of the Tools for Recognizing Useful Signals of Trustworthiness (TRUST) Program (Phase 1), sponsored by the Office of the Director of National Intelligence's Intelligence Advanced Research Projects Activity (IARPA). The TRUST program goals were to develop means of assessing trust in varying contexts and environments, independent of stress or deception. A key component to the test and evaluation (T&E) of TRUST was the design and development of unique and ecologically-valid paradigms that measure trust in larger protocols with external validity. During these protocols, participants were measured using various neural, physiological, behavioral, and psychological tools to assess trustworthiness. This was done by measuring and interpreting a person's own emitted signals to access a corresponding partner's own trustworthiness.

1.2 BACKGROUND

Although definitions of trust vary, there are common themes within the body of trust research. One recent meta-analysis (Castaldo, 2008) pulled together 72 different published definitions of trust from a variety of academic disciplines to examine what they have in common, and how they differ. Most of the definitions have elements that reference: (1) a subject, (2) an action/behavior, and (3) a future action (i.e., an intention) and/or expectation (i.e., a belief). The future element, which involves predicting or anticipating another's actions is a distinctive and critical feature of trust. Common themes across these and dozens of other trust definitions suggest that interpersonal trust operates under conditions of acknowledged interdependence, and is characterized by a willingness to accept vulnerability and risk based on confident expectations that another person's future actions will produce some positive result (Bigley and Pearce, 1998; Hosmer, 1995; Kramer, 1999; Mayer, Davis, and Schoorman, 1995; Rousseau, Sitkin, Burt, and Camerer, 1998; and Zand, 1972). The definition of trust that has driven the conceptual design of the protocol to be tested is "the willingness to make oneself vulnerable to another party. This is usually with positive expectations regarding the other's competence or intentions, under conditions in which the negative consequences of abuse of that trust far outweigh any potential gain."

Published trust literature has explored potential determinants or antecedents of interpersonal trustworthiness. Three determinants of trustworthiness that have stood the test of time, posited by

Aristotle and continuing through the writings of contemporary authors (Kasperson, 1986; Kasperson, Golding, and Tuler, 1992) are competence, benevolence, and integrity (Mayer, Davis and Shoorman, 1995; Peters, Covello, and MacCallum, 1997). When evaluating their partner's trustworthiness (and deciding on their own state of trust), an individual will evaluate their partners competence, benevolence, and integrity. While researchers have attempted to design tasks to separate these three components, in the real world, these are all intertwined to form the basis for our evaluation of another person's trustworthiness.

Given the complexity of interpersonal trust and the importance of vulnerability, it is perhaps surprising that previous research has relied on simple tasks with low consequences. Techniques used to measure trust have included survey-style assessments and behavioral economic games such as the Prisoner's Dilemma Game and the Trust Game. In these games, subjects make abstract yes/no decisions that result in small rewards, typically less than one U.S. dollar (USD) per choice. Social dilemma games are particularly favored by researchers who view trust as an economic decision because the utilities (or payoffs) of each decision can be very clearly specified. Limitations of these approaches include an over-reliance on anonymous, single-shot interactions or responses. These often have low stakes and evoke behavioral responses of trust that are difficult to disentangle from general processes like cooperation or altruism.

Although trust researchers have identified some determinants of trust, and key behaviors trust predicts, only a small number of studies have examined the neurophysiology of such behaviors, and only while employing social dilemma games. Several successful fMRI studies have been conducted, but the physical limitations of MRI equipment have resulted in studies that exhibit all of the flaws mentioned above as well as preventing natural, face-to-face interaction.

Another marker used to indicate an individual's state of trust is neuropeptide oxytocin (OT). Oxytocin is a naturally occurring neuropeptide found in most mammals. It is synthesized in the hypothalamus. Oxytocin is implicated in a diverse array of physiological and psychological processes including birthing, lactation, sexual arousal, blood pressure, anxiety, and social behaviors (Gimpl and Fahrenholz, 2001; Barberis and Tribollet, 1996). It appears to facilitate the forming of social bonds and attachments (Carter, 1998; Insel and Young, 2001). It appears to speed the healing of physical wounds and enhance positive communications and perceived social support (Gouin et al., 2010). Oxytocin has been found to mitigate the stress-response effects of social anxiety and social stressors (Heinrichs, Baumgartner, Kirschbaum, and Ehlert, 2003). In several recent experiments, intranasal administration of exogenous oxytocin leads to increases in cooperative and trust-like behaviors (Baumgartner et al., 2008; Kosfeld et al., 2005). Professor Ernst Fehr (Fehr, Fischbacher, and Kosfeld, 2005; Fehr, 2008, 2009) from the University of Zurich and Dr. Paul Zak (2005, 2007, 2008), director of the Center for Neuroeconomics Studies at Claremont Graduate University, have led efforts to explore the role of oxytocin in interpersonal trust and relationships.

In previous experiments using the Trust Game, researchers found that oxytocin levels naturally and consistently rise in the player who was the beneficiary of a trust decision. Oxytocin's role in this signal of being trusted was confirmed when researchers administered doses of oxytocin, and players tended to show more reciprocity in their game behavior; that is, they were both more likely to give money back and to return a greater amount of their benefit to the other player. With the boost of oxytocin, reciprocity and generosity increases, even when risk-taking itself (i.e., playing against the

odds in a gambling or probability task) does not change, suggesting oxytocin's effects are very specific and sensitive to social context (Kosfeld et al., 2005).

The social exchange model (SEM) builds on Social Exchange Theory in that a trust-building process is predicated on prosocial behavior (such as bonding and affiliation), which reduces the perceived costs – both material (resources, time) and immaterial (cognitive load, stress, etc.) - of interaction in order to foster relationships, and generally requires positive emotion experienced toward others, as well as approach-type motivations (Blau, 1986; Cox, 2002, 2004; Cox and Deck, 2005).

The SEM proposed and being tested suggests that social behaviors involve the principle that one person provides something of value to another with the expectation of some future return, not necessarily specified in advance. Because an appropriate return for what was given is not guaranteed, social exchange requires trust—the belief that others will follow through on their obligations. The model includes the beliefs that:

- Interpersonal trust in a relationship will increase over time via recurrent reciprocity of benefits.
- Costs are likely to be perceived as greater between strangers than between friends, because the lack of a history of previous interchanges between strangers makes it more difficult to judge the likelihood and value of potential benefits.
- People make decisions for their behavior in interactions based on (not entirely conscious) assessments of benefits and costs relative to those benefits. The benefits exchanged include not only material benefits and explicit favors (such as items with monetary value or actions that confer social status), but also emotional comfort, such as that provided by expressions of congeniality and supportiveness. Often the perceived costs and benefits are relative to individuals' expectations.
- Social and cultural norms have a large influence on expectations, which help to comparatively evaluate other's behavior and provide a more secure foundation for judgment.

1.3 COMBINED ACCESSMENT OF TRUSTWORTHINESS

The assessment of another person's trustworthiness will involve differing combinations of competence ("can do"), benevolence ("want to do"), and integrity ("will do). The combinations will differ due to context, personalities, prior experience, perceived consequences, etc. But the hypothesis is that, while people use social exchange to try and assess whom to trust for different reasons , trust-up and trust-down will be reliably associated with certain neurophysiological "states." Research plan

The main goal of the proposed research was to validate a new protocol for measuring trust. This protocol improves significantly on the limitations of previous trust research discussed in Section 1.2. Limitations addressed in Section 1.2 are summarized as lack of ecological validity, serious consequences, cultural diversity, and limited measurement tools. The SS protocol focused on engaging pairs of subjects in interactions that had high ecological validity by interacting with both familiar and unfamiliar subjects. Subjects were motivated to accurately assess the trustworthiness of their partner. Meaningful consequences for trusting or not trusting their partner were put in place. Paired subjects were either familiar or unfamiliar to each other. In either case, they may not have

shared significant cultural traits. Familiar subjects were more likely to have similar cultural backgrounds than unfamiliar subjects. If successful, the results of the research would be a significant advance in the measurement and understanding of interpersonal trust. The proposed SS protocol was based on an interactive task derived from the well-known Prisoner's Dilemma (PD) (Poundstone, 1992).

In the classic PD task, two partners-in-crime are isolated and told the consequences of either confessing or not confessing to a crime. The penalties for confessing or not confessing are structured so that a rational decision-maker should decide to confess. Consequently, on rational grounds both individuals should confess even though both would suffer a lesser penalty if both did not confess. In the SS protocol, subjects first earned an endowment and then responded to a moral dilemma question. The two subjects then interacted to learn the other's answer to the moral dilemma. The answer was recorded on a small piece of paper and placed in a mutually agreed upon secret compartment (1 of 10). Subjects were told to keep the location of the compartment secret. They were then told they would be interviewed individually and asked to reveal their partner's secret (location of the hidden answer in the box with 10 compartments). Prior to the interview they are told the consequences of either revealing their partner's secret or not revealing it. All choices involved losses of part of their endowment. As in the PD situation, the rational choice for each partner based on the consequences was to reveal the other partner's secret. On the other hand, if partners trust each other, both subjects could choose to reduce their potential losses by not revealing their partners secret.

Many of the cognitive factors that can influence trust decisions are based on a deeper knowledge of the other person, and the stability of the other's behavior across time and contexts. Trust was deemed more likely to occur in extended relationships (Rousseau et al., 1998). In the SS protocol, this idea was explored by engaging subjects in interactions with an individual they identified as a trusting friend or family member. The interaction was then repeated with an unfamiliar partner with whom they had no prior history. The goal of this manipulation was to use the signals collected while interacting with the familiar partner as a standard to compare the interactions with the unfamiliar partner. The temporal element implicit in the relational model was addressed by having subjects engage in multiple sessions with an interviewer where they had to choose whether or not to protect their partner's secrets. This allowed subjects to build a shared history and presented an opportunity to test the trustworthiness of their partner, and move towards a relational base of trust. Details of the tasks conducted are provided in Section 2.2.

Utilizing the SS protocol, we sought in our testing to converge evidence that changes in observable neural, physiological, behavioral, and psychological signals are consistent with predictions of the consequences of being a recipient of trusting or non-trusting behavior.

1.4 EXPERIMENTAL MEASURES

Provided in this section are four areas that were addressed as part of our study: neural signals, physiological signals, behavior measures, and psychological measures.

1.4.1 Neural Signals

Electroencephalography (EEG) was used to measure changes in electric potentials associated with neural activity, particularly in the frontal cortex. An analysis of each of the frequency bands was

4

performed, with the main focus on alpha power 8–12 Hz. Studies suggest that an increase in alpha power in the left frontal cortex, relative to the right, is part of the neurophysiology related to approach behaviors and positive affect rather than avoidance behaviors (Ahern and Schwartz, 1985; Davidson, 1984, 1988; Davidson et al., 1990). Using an increase in the left frontal alpha band as a signal of evolving and increasing trust is consistent with the concept that trust is dependent on prosocial and positive interactions that require approach behaviors to foster the development of relationships over time (Blau, 1986). To increase ecological validity by permitting natural interaction, neurophysiological recording was limited to systems that were as nonintrusive as possible in a laboratory environment.

1.4.2 Physiological Signals

Peripheral physiological measures were taken while subjects were interacting and performing the SS task. The peripheral measures of heart rate, respiration, and skin conductance, which are regulated by the automatic nervous system (ANS) and neural connections originating in the brainstem, were used as indicators of relative activation of the sympathetic nervous system (SNS) and parasympathetic nervous systems (PNS) in response to, or in preparation for, a partner's actions and decisions, or a subject's own actions and decisions. The SNS, traditionally known as the fight or flight system, and the PNS are the complementary circuits that modulate peripheral physiology and may aid in facilitating or disrupting social exchanges that foster the development of trust. We hypothesized in our study that ANS activity is correlated with interpersonal trust. Broadly speaking, the trust interactions require suppression of the fight or flight response. Note, the degree to which ANS activity specifically predicts trust is unknown.

Cortisol and oxytocin were measured at various points in the task. Cortisol levels are reported to be inversely correlated with oxytocin levels (Bodenmann et al., 2009). Levels of oxytocin are hypothesized to be correlated with self-reported trust, as well as the other measures described in this protocol. It was important to determine if oxytocin played an important role in interpersonal trust when the interactions were dynamic and lasted hours, rather than in response to rapid decisions in economic games as previously studied.

1.4.3 Behavioral Measures

In the SS protocol, trusting behavior is evidenced by a subject choosing to not reveal a partner's secret. Non-trusting behavior is evidenced by a subject choosing to reveal a partner's secret and/or choosing to buy insurance to protect against endowment losses.

1.4.4 Psychological Measures

In addition to these neural, behavioral, and physiological measures of trust, each subject was given a battery of subjective questionnaires to measure baseline traits and states. Their behavioral decisions were followed up during the testing sessions. The psychological measures assessed: propensity to trust, dispositional trust, personality, state, and trait-based affect and anxiety, motivation, tolerance for uncertainty and risk, risk seeking, social orientation (pro-self vs. pro-other), perceived stress, acculturation and cultural identity, and perceived trustworthiness of their partner. In the SS protocol we used the choices that a subject made were not based on an explicit judgment of

their partner's trustworthiness, but on their assessment of their partner's competence, benevolence, and integrity and their own willingness to take a risk. As described above, these judgments are consistent with the working definition of trust; thus, results indicated whether the protocol has construct validity. The suite of measurements applied provided converging evidence enabling an informed decision about the validity of the SS protocol.

2. MATERIALS AND METHODS

2.1 SUBJECTS

Eighty-four subjects (39 male, 45 females; average age 35.69 ±8.47 years) participated in this study. All subjects passed a phone screen given by an experimenter to determine if they met the following qualifications:

Subject screening qualifications are as follows:

- Can read and write English at a middle school level
- 21 to 49 years old
- Not employed by the military or US government
- Must weigh more than 110 pounds
- Not pregnant
- Willing to take a pregnancy test
- Comfortable giving blood or being instrumented for monitoring devices
- Never participated in other research protocols such as JD and SS
- Smokes no more than packs of cigarettes or drinks no more than three alcoholic drinks a day
- No medical condition currently or during the previous year including mental illness
- Consider themselves in good mental and physical health
- Not taking (certain) prescription or over-the-counter drugs
- No history of allergies to latex
- No history of rashes or hives associated with a medical examination
- No aversion to having their chest hair shaved for electrode placement
- Not diagnosed with high blood pressure (140/90)
- No physical disabilities preventing travel to the testing center, moving around the testing facility or sitting in a chair for ~ 60 minutes
- Regular consistent sleep pattern
- Must have U.S. citizenship or a permanent visa
- Must be physically present at the testing facility for ~ 8 hours (8:30 am–4:30 pm PST/PDT)
- Both the subject and parent born in or out of the United States

The experiment was broken down into two protocols. In Protocol 1, two pairs of familiar trusted partners were scheduled. Each subject interacted with both their familiar partner and an unfamiliar partner. In protocol 2, four subjects were scheduled independently and each subject interacted with two unfamiliar partners. All subjects signed an Informed Consent Document (ICD) approved by the Institutional Review Board at Space and Naval Warfare Systems Center (SSC Pacific) and in accordance with the Declaration of Helsinki.

2.2 EXPERIMENTAL PROCEDURES

The experiment consisted of a testing session (approximately 7 to 8 hours) completed in one visit to the testing center starting at 8:30 am on the scheduled testing date. Each subject was assigned to an individual testing room and experimenter. The experimenter gave a brief introduction of themselves and the study, and then read aloud the Privacy Act Statement and ICD as the subject followed along on his/her copy. Once all questions about the experiment and ICD were sufficiently answered by the

experimenter, subjects completed a 14-question ICD comprehension questionnaire to ensure that they understood their rights as a research subject, the risks involved, and their ability to withdraw from the study at any time. Any comprehension questions that were answered incorrectly were discussed with the experimenter to resolve the misunderstanding. If subjects wished to comply, they then signed and dated the ICD. A copy of the ICD signed by the subject, the principle investigator, and the experimenter was kept by the experimenter as well as given to the subject. Subjects were also given a copy of the State of California Bill of Rights document.

Following the signing of the ICD, subjects completed the baseline questionnaire packet consisting of the Stephenson Multigroup Acculturation Scale (SMAS), Positive and Negative Affect Schedule (PANAS), Attitude Toward Risk Questionnaire (ATRQ), Relationship Closeness Inventory-Revised (RCI-R) [Protocol 1 only], Mayer trust scale for Propensity (MAYER-P), Neuroticism-Extraversion-Openness Personality Scale (NEO), Relationship Questionnaire (RQ), Stress Appraisal Scale (SAS), and the State-Trait Anxiety Inventory (STAI-S). (For more details, see Section 2.5.4). These paper and pencil subjective measurements were completed by subjects in their individual testing rooms with the investigator present to answer or clarify any questions they may have.

Next, a California licensed registered nurse (RN) placed a peripheral intravenous (IV) catheter (20 g) in a forearm vein using standard antiseptic procedures. The catheter remained in place no longer than necessary to complete the study, at maximum ~ 7 hours. This is well below the Centers for Disease Control and Prevention (CDC) recommended maximum of 96 hours. The first 1–2 mL of each blood collection was drawn into a separate tube and discarded to prevent saline dilution. Two additional blood samples were collected. One blood sample was collected using a 5-mL orange top tube containing Hemogard Stopper and thrombin (cortisol). The second blood sample was collected using a 5-ml K_2EDTA purple top tube (oxytocin) after blood collection, 100 µl (0.76 mg) of the protease inhibitor aprotinin was added to the purple top K_2 EDTA tube. Each tube was mixed by inversion several times. The oxytocin sample tube was placed on ice and the cortisol sample was kept at room temperature and allowed to clot before processing. All blood samples were collected using a Becton Dickinson vacutainer with a luer lock access device. Twelve blood draws were performed throughout the course of the day's experimental testing, requiring approximately 168 mL of blood from each subject. All samples were handled in accordance with Occupational Safety and Health Administration (OSHA) bloodborne pathogen guidelines and training.

The subjects were subsequently instrumented with the psychophysiological recording equipment used to measure EEG, electrooculography (EOG), electrocardiography (ECG), and GSR/electrodermal activity (EDA).

Once subjects were fully outfitted with the physiological equipment in their separate rooms, they began an endowment earning task which asked subjects to guess the average population's response to questions related to a moral quandary. This was defined as the Baseline Epoch. Each subject continued guessing the answers until the targeted $120 endowment was earned. This task is intended to establish a sense of ownership of the money to be used in the main task.

The subjects watched a brief video of the task followed by a practice version administered by the experimenter. The task was as follows:

For Protocol 1, subjects were then randomly united with either a familiar partner (the person they came with) or an unfamiliar partner (a person they do not know). For Protocol 2, subjects were united only with an unfamiliar partner. With both subjects in the same room, they were presented with a Moral Dilemma question . Each subject was given a box separated into 10 compartments. After the experimenter left the room, subjects had to discuss the moral dilemma and decide whether the action performed by Joe, the character in the dilemma, was morally acceptable. The answer to this question is the subject's secret. Then subjects decide to hide their partner's secret in one of their 10 boxes. This interaction time was defined as the Pre-Decision Epoch.

Then each subject returned to his/her individual testing room. An interviewer (someone other than the subject's experimenter to avoid any bias or habitual behaviors) asked subjects which box contained their partner's secret. Subjects were told that if they chose not reveal their partner's secret, the interviewer would still guess a compartment randomly, therefore having a 10% chance of being correct. The payout matrix Table 1 shows the consequences of their decisions to either reveal their partner's secret or not reveal it. This was explained by the experimenter prior to the interview until subjects fully understood the implications of their decisions.

Table 1. Payout matrix.

		YOU	
		You DID NOT GIVE UP the secret and Your Interviewer Guessed INCORRECTLY	You GAVE UP your secret OR Your Interviewer Guessed CORRECTLY
YOUR PARTNER	Your Partner DID NOT GIVE UP the secret and the Interviewer guessed INCORRECTLY	You and Partner LOSE $30	You Lose $0 Your Partner Loses $60
	Your Partner GAVE UP the secret OR Your Partner's Interviewer Guessed CORRECTLY	Your Partner Loses $0 You Lose $60	You and your Partner LOSE $45

The Payout Matrix shows the consequences in terms of lost endowment for choosing to either reveal a partner's secret or not reveal a partner's secret. If both partners A (the main partner) and B (the supporting partner) trust each other and choose not to reveal the other's secret, then both lose $15. If neither partner trusts the other and both choose to reveal the other's secret then both lose $45. If A trusts B and chooses not to reveal B's secret when B does not trust A and chooses to reveal A's secret, then A loses $60 and B loses $0. If A does not trust B and chooses to reveal B's secret while B trusts A and chooses not to reveal A's secret, then A loses $0 and B loses $60.

After the interview, subjects either were informed of the outcome of their partner's interview on a computer display (Protocol 1) or this information was not revealed until after the second interview

later in the session (Protocol 2). Next, subjects were again brought together in the same room to discuss the previous interview. This was defined at the Post-Decision Epoch. Then, either subjects' endowments were adjusted based on the payout matrix and the outcome of the interview (Protocol 1), or the endowment adjustment was not done until after the second interview later in the session (Protocol 2).

The moral dilemma task was repeated a second time (Round 2) followed by a second interview. At this point in Protocol 2, subjects were shown the outcome of their partner's interviews and their endowment is adjusted appropriately. Then, in both protocols, subjects were asked to complete a hypothetical game (Round 3) in which they were asked whether they would play this game with the same partner again. After the reveal of their partner's response to this question, an open-ended debrief questionnaire was given, and then the session was complete.

Figure 1 shows an overview of the scheduled study efforts during a day. After a 30-minute lunch break, alone in their individual testing rooms, subjects repeated the entire protocol (beginning with a new endowment earning task), but with a different partner. The RN periodically collected blood samples and questionnaires were administered at specific times throughout the course of the task After the afternoon session, subjects completed a final debrief questionnaire and received their payment (hourly plus remaining endowment from both rounds). After payment and debriefing, subjects were unhooked from the physiological recording equipment, the RN removed the catheter, and subjects were excused from the testing center.
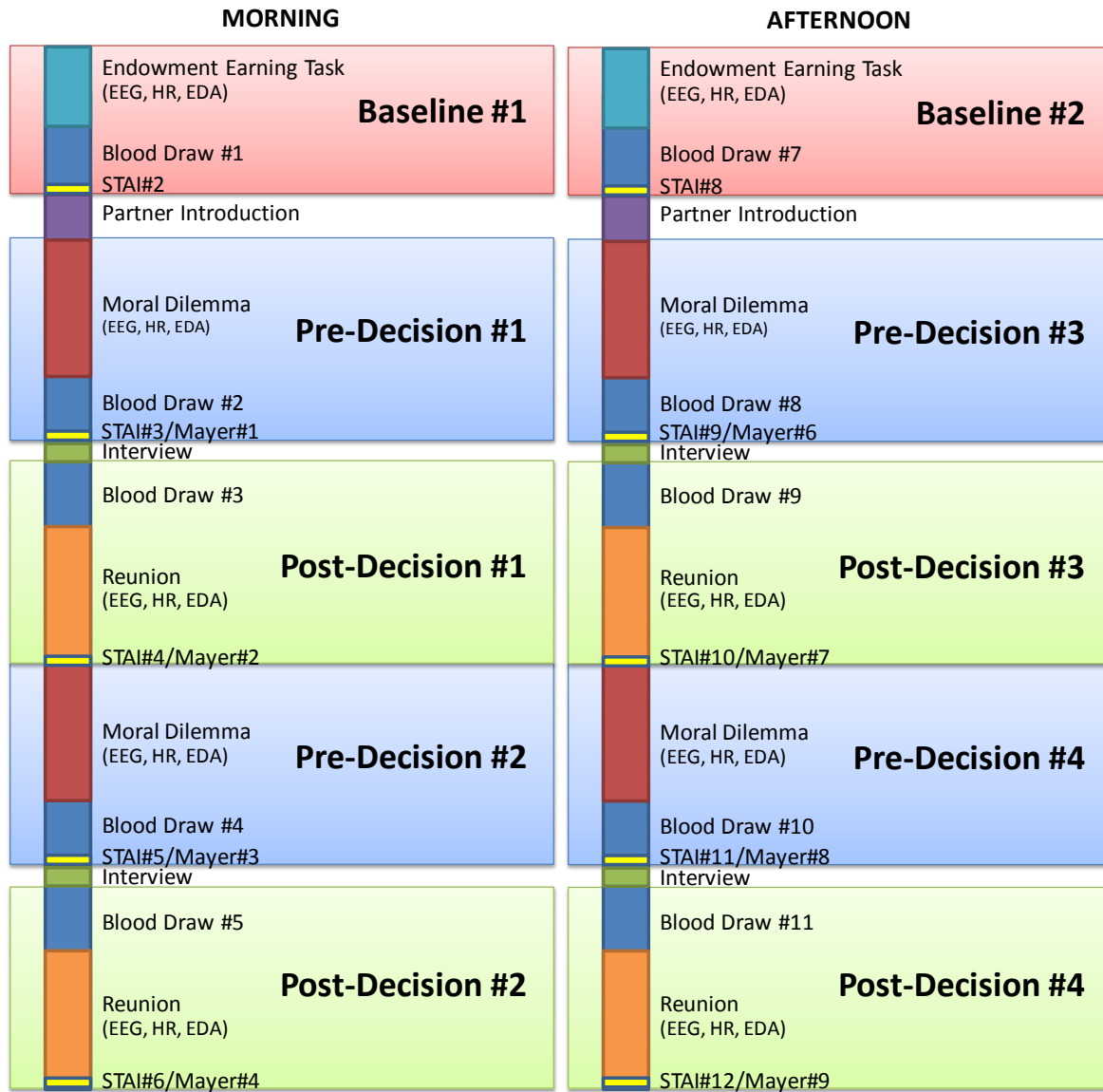
Figure 1. Time course and measures of protocol.

The time course measures presented in this report are shown above for the morning and afternoon sessions (left and right chart, respectively).

2.3 PHYSIOLOGICAL RECORDINGS

Subjects were outfitted with a standard 16-channel active electrode cap (BioSemi) for collection of EEG during the task.

Other recording sources included the following:

- Two electrodes were placed on the left and right mastoid. After data collection, the average mastoid signal was used to reference the data collected.
- Four electrodes were placed beneath and to the side of each eye to record EOG activity. The data was used to remove eye-movement artifacts from the cortical activity (see below).

- Two electrodes placed directly under the left clavicle and in the middle of the sternum to record ECG.
- Two electrodes were placed on the index and middle finger of the non-dominant hand to obtain skin conductance levels, GSR.

All channels were simultaneously recorded at 2048 Hz and time-synchronized to event triggers which designated epochs of interest (see below).

2.4 DATA PROCESSING

2.4.1 Tasks of Interest

Data were epoched based on the event triggers initiated during each experimental session (i.e., morning and afternoon). This was done at specified relevant time-points with reference to the decision to trust or not trust the working partner. The tasks were as follows:

- Baseline
- Pre-decision 1
- Post-decision 1
- Pre-decision 2
- Post-decision 2

For each task, we exacted a 2-minute interval to normalize the time compared across epochs. The baseline epoch was taken during the endowment earning task since it was in this time period that subjects had not yet met their partner. Pre-decision epochs were taken during the moral dilemma tasks. This was the closest time period before the actual decision to trust or not trust (i.e., the interview) in which subjects were interacting with each other. The post-decision epochs were taken during the reunion period since this was the closest time after the decision in which subjects were interacting with each other. For baseline and pre-decision tasks, the 2-minute interval was centered on middle of epoch. For the post-decision tasks, the first 2 minutes of interval was used. The difference in intervals extracted was to obtain data closest to behaviorally relevant time periods.

2.4.2 Defining Trust

Data were then differentiated based on whether each subject interaction represented trust or distrust. An interaction was considered trust if subjects: (1) kept the secret, or (2) followed the agreed-upon strategy with their partner (to the extent this can be confirmed).

Figure 2 details the determination of trust cycle. Each subject performed two trust decisions in the morning and afternoon making a total of four trust decisions made. Note that a different baseline value (i.e., during the endowment earning task) was used for the morning and afternoon sessions. A flowchart showing underlying logic for coding a decision as trust or distrust is shown in Figure 2.
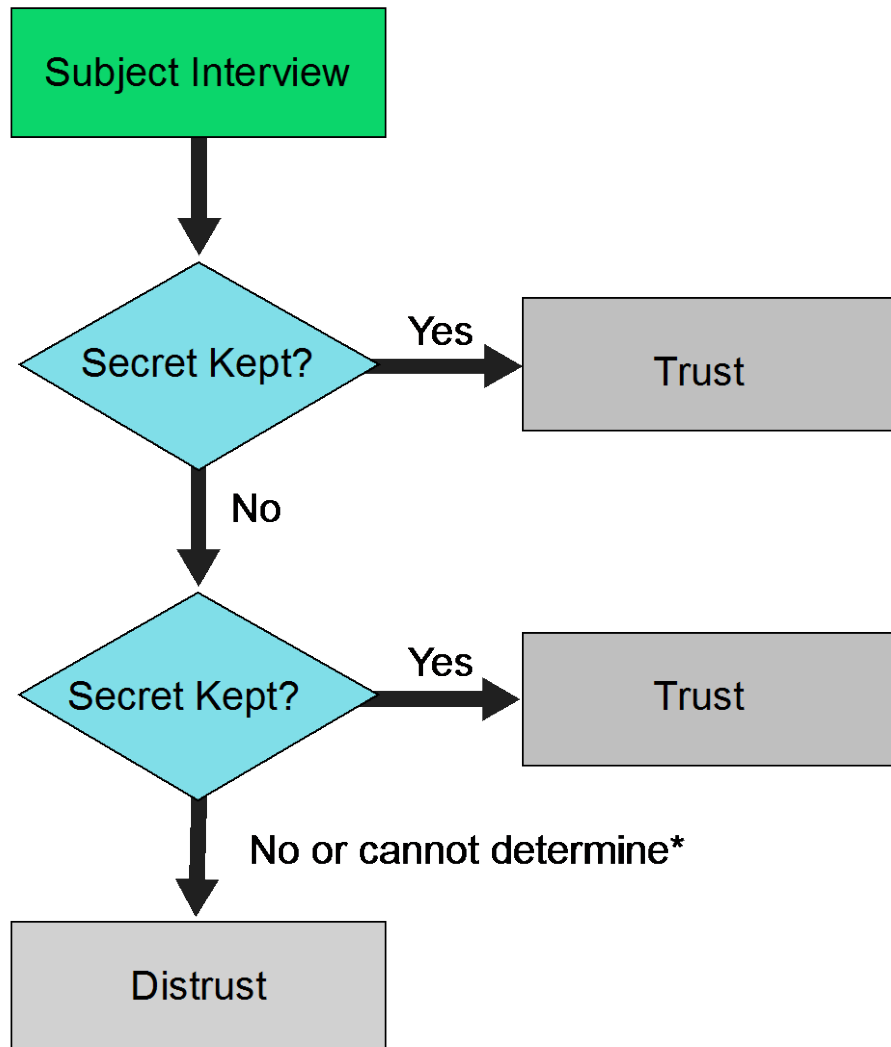
Figure 2. Determination of trust.

2.4.3 Electroencephalography (EEG)

EEG data were processed using MATLAB® with the EEGLab plug-in toolbox (Swartz Center for Computational Neuroscience, UCSD). The data were referenced to the average mastoids and then run through a high-pass filter with a 1-Hz cutoff and low-pass filter with a 55-Hz cutoff. To remove non-physiological artifacts from the data, we applied an independent component (IC) analysis (Delorme and Makeig, 2004; Hammon et al., 2008). Components that exhibited artifact characteristics, based on visual inspection of scalp topography and frequency spectra, were removed. EEG data were then reconstructed by back-projecting the time course of the remaining ICs to the surface electrodes to obtain a clean (i.e., cortically relevant) signal.

2.4.4 Electrocardiography (ECG)

A peak detection algorithm was used to detect the peaks present in the ECG signal (Chernenko, 2012). The detected peaks and the measured data were plotted together and compared. This data could then be evaluated to determine whether the data was noisy and/or erratic and if the peaks could be found accurately. The corrupted data was then discarded. This step was repeated for all subjects and all tasks. Next, we calculated the inter-beat interval (IBI) in milliseconds from the peaks of the good data. We accomplished this by calculating the difference between the time steps of two consecutive R peaks. The next IBI time series was found by using the instantaneous time scale of IBI, e.g., $t_1,\ldots,t_{(n-1)}$, where n = length of the IBI vector.

2.4.5 Galvanic Skin Response (GSR)

Data epochs were down-sampled to 32 Hz using the MATLAB® decimate function (factor of 64), then processed using Ledalab version 3.4.1 (Ledalab, Graz, Austria), an open-source MATLAB® toolbox for analysis of skin conductance signals. GSR data, which were recorded in nanosiemens, were converted to microsiemens. Then, data were smoothed using Gaussian smoothing at six samples (187.5 ms), analyzed using continuous decomposition analysis (with six optimization attempts) to extract the underlying temporal characteristics of the signal (Benedek, and Kaernbach, 2010). This decomposes the data into phasic and tonic components that are used to calculate the skin conductance response and level (see below).

2.4.6 Oxytocin and Cortisol

After the cortisol sample tubes were sufficiently clotted and the oxytocin K_2 EDTA tubes were thoroughly chilled. All samples were centrifuged at 3000 rpm for 15 minutes on a tabletop centrifuge (Hettich® Lab Technology ROTOFIX 32 A). The serum and plasma was harvested, placed into freezer vials, and stored in a -20 °F refrigerator. Within 1 week after collection, the samples were subsequently shipped (on dry ice) to the Air Force Research Laboratory to determine the cortisol (serum) and oxytocin (plasma) concentrations.

2.5 DATA ANALYSES

2.5.1 EEG Frequency Analysis

Figure 3 *shows* a periodogram of with a Hann smoothing window was used to extract the one-sided n-point (n = sampling frequency, 2048 Hz) power spectral density (PSD) corresponding to the frequencies present within each channel of data. The mean-square power spectrum was calculated by taking the Fourier transform of the autocorrelated data. A 2 second sliding window (with 50% overlap per iteration) across each 2-minute task interval was applied for each of the 16 data channels. The power spectral density was normalized by taking log base 10 of the data. Frequency bands of interest, known to be associated with cortical responses, were extracted (Figure 3, top left plot).

For all channels, power was averaged across the following frequency bands:

- Theta: 4–7 Hz
- Alpha: 8–13 Hz
- Beta: 14–30 Hz
- Gamma: 31–40 Hz

The presence of asymmetrical power in the alpha (α) band frequencies (8–13 Hz) in the frontal left vs. right hemispheres was an important indicator of motivation and emotion (Davidson, 1993, 1998; Coan and Allen, 2004). The EEG hypotheses specific to this study focused on the extent to which the alpha power of channels F3 and F4 differed depending on subjects trust. Greater right frontal power (relative to left) shows been associated with greater response to a positive stimuli (Coan and Allen, 2003), thus it was hypothesized to be correlated with trust behavior. An example of this difference is shown in the right-hand plots (Figure 3) that display channel F4–F3 hemispheric asymmetry.
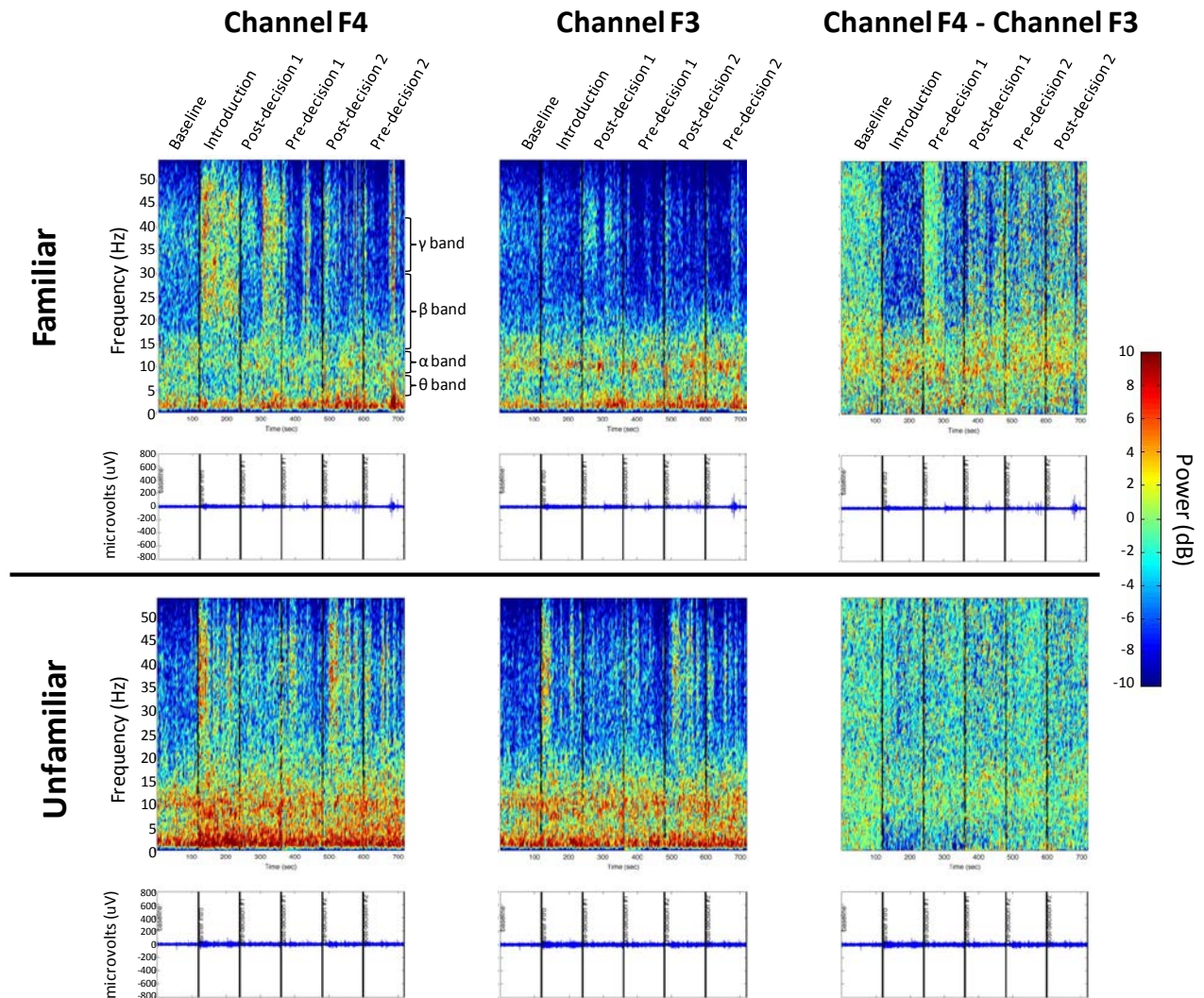
Figure 3. EEG power spectral density (alpha asymmetry example).

The familiar condition (top plot) shows greater relative power in the right hemisphere in the α frequency band (seen as more red in the color spectrum), compared to the unfamiliar condition (bottom plot). Left, middle, and right plots show average PSD across all subjects for right (channel F4), left (channel F3) frontal hemisphere signals, and the difference between them (F4–F3) for one subject of Protocol 1 during the familiar and unfamiliar conditions. For each condition and channel, there is a plot of the PSD and the activity from which the PSD was derived (top and bottom plots). Frequencies are displayed along the y-axis and time/event along the x-axis. Note that the time displayed is not continuous, but the 2-minute window designated for each event of interest. The power of each frequency is represented in color, as labeled by the color bar on the right. The θ, α, β, and γ frequency bands are labeled in the top left plot.

2.5.2 ECG Frequency Analysis

Based on previous work (Baker, Colrain, and Trinder, 2008; Trinder et al., 2001), a third order (spline) interpolation was applied to the IBI data to asynchronously resample the IBI time series for each event to 4 Hz by adjusting the sampling period of the time scale of the IBIs to ¼ second. The resampled data were then detrended using a third-order polynomial fit (Baker, Colrain, and Trinder, 2008; Mitov, 1998). Each 2-minute event was multiplied by a Hanning window to remove artifacts in the spectra due to signal truncation. Then the Power Spectral Density (PSD) was computed using 0.00024 Hz resolution with n-point fast Fourier transform of 2^14 and sampling rate of Fs = 4 Hz. Specifically,

$$PSD \ = \ (abs(FFT)^2) \times \frac{\text{sampling period}}{\text{Hanning coeff} * \text{nfft}} \ ,$$

where Hanning coeff (Coefficient) = 0.5.

Low-frequency (LF) and high-frequency (HF) power was then extracted by finding the maximum peak of the PSD found in step within the given band, and then searching for half-power peaks to the left and the right of the peak. The power between the maximum peak and the first peak among half-power peaks [5] was found using the trapezoidal rule for integration of PSD over the bands of interest LF band = 0.003–0.15 Hz; HF band = 0.15–0.4 Hz. Additionally, LF norm and HF norm were calculated as LF/(LF+HF) and HF/(LF+HF).

2.5.3 Skin Conductance Response (SCR) and Skin Conductance Level (SCL)

GSR was used to calculate two separate variables: (1) skin conductance level (SCL), where 50 uA was constant, and the current reflection could be measured based on properties of the skin, and (2) skin conductance response (SCR), where the fastest could be measured and phasic nature of spikes were used to detect the intensity and amplitude of the current reflection, as opposed to SCL's slower/tonic signal.

SCL, as a more generalized level of arousal over gross intervals, rather than SCR's more variable wave, were both calculated using Ledalab version 3.4.1 (Ledalab, Graz, Austria). SCL was calculated as the tonic data's mean value over the 2-minute window:

$$SCL = \frac{SCL_{observed} - SCL_{minimum}}{SCL_{maximum} - SCL_{minimum}} \ .$$

SCR was calculated using MATLAB's trapezoidal numerical integration function (trapz) as an approximation for the area under curve, allowing the capture of both amplitude and temp oral changes of the signal in one value:

$$SCR = \frac{SCR_{observed}}{SCL_{maximum}} \ .$$

2.5.4 Questionnaire Scoring

Subjects were asked to complete several baseline questionnaires:

- State-Trait Anxiety Inventory-State (STAI-S) (Spielberger, Gorsuch, and Lushene, 1970)
- Stress Appraisal Scale (SAS) (Schneider, 2008)
- Relationship Questionnaire (RQ) (Bartolomew and Horowitz, 1991)
- Mayer Trust Scale for Propensity (Mayer, and Davis, 1999)
- Attitudes Toward Risk Questionnaire (ATRQ) (Franken, Gibson, and Rowland, 1991)
- Positive and Negative Affect Schedule (PANAS) (Watson, Clark, and Tellegan, 1988)
- Stephenson Multi-group Acculturation Scale (SMAS) (Stephenson, 2000)
- Relationship Closeness Inventory-Revised (RCI-R) (Berscheid, Snyder, and Omoto. 2004)
- The Neuroticism-Extraversion-Openness-Five Factor Inventory-3 (NEO-FFI-3) (Costa and McCrae, 1992)

At the beginning of the study to determine their specific view on trust between people and basic personality traits. These baseline questionnaires measured several areas: each subject's social status and psychological state, the closeness of the relationship with their familiar partner, the degree to which they have adopted the behaviors typical of the culture they live in, their willingness to believe in the positive attributes of other people in general, their level of anxiety, motivation, tolerance for uncertainty and risk, and the degree to which they tend to be oriented toward their own welfare rather than the welfare of others.

During each session, subjects were asked to answer four repeated questionnaires: STAI-S seven times, Mayer-Ability-Benevolence (B)-Integrity (I)-Revised (Mayer-ABI-R) (Mayer and Davis, 1999) five times, SAS three times, and Gene Suspicion Scale (GSS) two times. These repeated questionnaires were used to evaluate the subject's anxiety level, their view on their partner's trustworthiness, how much stress they are feeling, and how suspicious they are toward their partner. All of the questionnaires were evaluated and scored as indicated in their specific manual/reference article cited above.

2.6 SCIENTIFIC APPROACH

Based on the analysis specifications outlined by IAPRA for each signal, we computed the value immediately before (H1a-j, H3a-j, and H5a-j) and after (H2a-j, H4a-j, and H6a-j) the relevant decision point when a person chooses to trust/distrust another. Data was assessed in three different ways: (1) raw (un-normalized) values, (2) values with baseline subtracted, and (3) values divided by baseline. We then determined whether signal amplitude changes relative to baseline as predicted by the Social Exchange Model using the following analyses. (Note that data from Protocol 1 and Protocol 2 are combined for the following analyses and outlier values were removed from the analysis so as not to skew the statistical outcome.)

2.6.1 Analysis 1: Binary Aggregate of Data

Analysis 1 included a binary aggregate of data (i.e., yes or no, does the amplitude of the signal follow that which was hypothesized?). Data are reported in a table as percentages (and absolute ratios) calculated for each sub-hypothesis. The protocol will be considered valid if the proposed hypotheses are confirmed in 80% of the specified trust decisions made. For sub-hypothesis k (all the above signals change simultaneously), data are reported as the percentage of decisions in which all variables changed (from baseline) in the direction stated in the SEM.

2.6.2 Analysis 2: Comparison of Pre- and Post-decisions Relative to Baseline

Analysis 2 included a comparison of data relative to baseline (i.e., did signals surrounding the decision point change compared to baseline levels?). To evaluate raw data, signal amplitude from baseline measures was compared to pre- and post-decision measures by performing a one-way repeated measures ANOVA with a post-hoc multiple comparison analysis least square difference, (LSD) to determine significant group differences. Resulting data was reported in a table as a mean difference [trust–distrust] ±standard error (SE) and p-value of mean difference between comparisons for each sub-hypothesis (note that statistical significance was not adjusted for multiple comparisons). To evaluate normalized signals, the 95% confidence intervals were calculated. For signals with baseline subtracted, if the confidence window did not include 0, the mean value was considered significantly different from the baseline. For signals divided by baseline, if the confidence window did not include one, the mean value was considered significantly different from the baseline. Data are reported in a table as 95% confidence intervals for each sub-hypothesis.

For Analyses 1 and 2, the validity of the protocol was assessed separately for trust and distrust decisions.

2.6.3 Analysis 3: Comparison of Trust vs. Distrust Interactions

Analysis 3 determined whether signal amplitude when a person chose to trust another was significantly different than the changes in signal amplitude when a person chose to distrust another. Data samples were statistically analyzed by performing one-way repeated measures using ANOVA with a post-hoc multiple comparison analysis LSD to determine significant group differences. Data was populated in a table as the mean difference [trust–distrust] (±SE) and the p-value of the result was the mean difference between comparisons for each sub-hypothesis (note that statistical significance was not adjusted for multiple comparisons).

3. RESULTS

3.1 HYPOTHESIS 1 (H1)

Immediately *before* a decision point when one person chooses to *trust* another, the following changes in signal amplitude (relative to baseline) are evident and discussed in Sections 3.1.1 through 0:

3.1.1 Hypothesis 1: Binary Aggregate Across All Decisions (Analysis 1)

Table 2 shows percentages (and absolute ratios) calculated for the signal of each sub-hypothesis:

Table 2. Hypothesis 1: Binary Aggregate Across all decisions.

Specific Hypothesis	Percentage of Decisions That Agree With the Hypothesis
H1a: [F4 – F3] Frontal alpha power asymmetry increases	54% (150/280)
H1b: RR interval increases	26% (34/131)
H1c: High-frequency Heart Rate Variability (HRV) increases	HF: 38% (51/133) HFnorm: 33% (44/135)
H1d: Low-frequency HRV decreases	LF: 33% (44/135) LFnorm: 33% (44/132)
H1e: Skin conductance level decreases	SCL: 15% (37/258) SCR: 31% (74/242)
H1f: Oxytocin concentration increases	50% (106/211)
H1g: Cortisol concentration decreases	75% (171/227)
H1h: Mayer score increases	N/A (no baseline measure)
H1i: STAI score decreases	41% (122/297)
H1j: SAS score decreases	68% (199/294)
H1k: All the above signals change simultaneously	2% (7/297)

There were no variables that support the validity of the protocol to measure trust (i.e., < 80% of decisions agree with hypothesis).

3.1.2 Hypothesis 1: Raw Signals (Analysis 2)

Table 3 shows the mean difference was calculated [baseline - pre-decision] (±SE) and the p-value was calculated using the one-way ANOVA. See Section 2.6 for all sub-hypotheses.

Table 3. Hypothesis 1: Raw signals.

Specific Hypothesis for Trust Condition	Mean difference [baseline – pre-decision] (±SE); *p*-value of mean difference
H1a: [F4 – F3] Frontal alpha power asymmetry increases	-0.030 ± 0.212, p = 0.889; n.s.
H1b: RR interval increases	22.378 ± 14.285, p = 0.146; n.s.
H1c: High-frequency HRV increases	HF: -0.357 ± 0.430,p = 0.407; n.s. HFnorm: 0.102 ± 0.025,p = 0.000; n.s.*
H1d: Low-frequency HRV decreases	LF-1.552 ±0.680,p = 0.023; n.s.* LFnorm: -0.102 ±0.025,p = 0.000; n.s.*
H1e: Skin conductance level decreases	SCL:-1.337 ±0.413,p = 0.001; n.s.* SCR:-5.612 ±1.510,p = 0.000; n.s.*

Table 3. Hypothesis 1: Raw signals (continued).

Specific Hypothesis for Trust Condition	Mean difference [baseline – pre-decision] (±SE); *p*-value of mean difference
H1f: Oxytocin concentration increases	1.645 ± 0.518, p = 0.002; *
H1g: Cortisol concentration decreases	1.645 ±0.518,p = 0.002; *
H1h: Mayer score increases	N/A (no baseline measure)
H1i: STAI score decreases	0.658 ±0.893,p = 0.461; n.s.
H1j: SAS score decreases	0.174 ±0.060,p = 0.004; *

* = significant of the proposed SEM hypothesis

n.s. = not significant

n.s.* = significant but in the opposite direction of the proposed SEM hypothesis

Note that skin conductance level, skin conductance response, normalized high-frequency and low-frequency (raw and normalized) were all different from baseline, but in the direction opposite to that which was hypothesized.

Variables that support the validity of the protocol for trust (i.e., measure is different from baseline):

Cortisol, cortisol concentrations decreased when comparing pre-decision to baseline levels.

SAS, SAS scores decreased when comparing pre-decision to baseline levels.

3.1.3 Hypothesis 1: Signals Minus Baseline (Analysis 2)

Table 4 shows 95% confidence intervals for the signal of each sub-hypothesis.

Table 4. Hypothesis 1: Signals minus baseline.

Specific Hypothesis for Trust Condition	95% Confidence Interval (CI) for Mean
H1a: [F4–F3] Frontal alpha power asymmetry increases	[-0.236 0.183]; n.s.
H1b: RR interval increases	[-50.218 -24.667]; n.s.*
H1c: High-frequency HRV increases	HF: [-0.165 1.202]; n.s. HFnorm: [-0.156 -0.074]; n.s.*
H1d: Low-frequency HRV decreases	LF: [0.421 2.629]; n.s.* LFnorm: [0.0741 0.156]; n.s.*
H1e: Skin conductance level decreases	SCL: [1.038 1.391]; n.s.* SCR: [3.683 6.809]; n.s.*
H1f: Oxytocin concentration increases	[-0.280 0.072]; n.s.
H1g: Cortisol concentration decreases	[-1.864 -0.937]; *
H1h: Mayer score increases	N/A (no baseline measure)
H1i: STAI score decreases	[-1.30 -0.11]; *
H1j: SAS score decreases	[-0.232 -0.170]; *

* = significant of the proposed SEM hypothesis

n.s. = not significant

n.s.* = significant but in the opposite direction of the proposed SEM hypothesis

Note that RR interval, skin conductance level, skin conductance response, normalized high-frequency and low-frequency (raw and normalized) were all different from baseline, but in the direction opposite to that which was hypothesized.

Variables that support the validity of the protocol for trust (i.e., measure is different from baseline. [confidence interval does not include 0]):

Cortisol. Cortisol concentrations decreased when comparing pre-decision to baseline levels.

STAI. STAI scores decreased when comparing pre-decision to baseline levels.

SAS. SAS scores decreased when comparing pre-decision to baseline levels.

3.1.4 Hypothesis 1: Signals Divided by Baseline (Analysis 2)

Table 5 shows 95% confidence intervals for the signal of each sub-hypothesis.

Table 5. Hypothesis 1: Signals divided by baseline.

Specific Hypothesis for Trust Condition	95% Confidence Interval for Mean
H1a: [F4–F3] Frontal alpha power asymmetry increases	[-2.771 1.646]; n.s.
H1b: RR interval increases	[0.948 0.976]; n.s.*
H1c: High-frequency HRV increases	HF: [1.335 4.007]; * HFnorm: [0.835 1.304]; n.s.
H1d: Low-frequency HRV decreases	LF: [2.754 4.517]; n.s.* LFnorm: [1.249 1.539]; n.s.*
H1e: Skin conductance level decreases	SCL: [1.316 1.452]; n.s.* SCR: [3.864 7.530]; n.s.*
H1f: Oxytocin concentration increases	[1.051 1.202]; *
H1g: Cortisol concentration decreases	[0.856 0.962]; *
H1h: Mayer score increases	N/A (no baseline measure)
H1i: STAI score decreases	[0.97 1.01]; n.s.
H1j: SAS score decreases	[0.898 0.942]; *

* = significant of the proposed SEM hypothesis

n.s. = not significant

n.s.* = significant but in the opposite direction of the proposed SEM hypothesis

Note that RR interval, skin conductance level, skin conductance response, and low-frequency (raw and normalized) were all different from baseline, but in the direction opposite to that which was hypothesized.

Variables that support the validity of the protocol for trust (i.e., measure is different from baseline [confidence interval does not include 1]):

High-frequency HRV. HF increased when comparing pre-decision to baseline levels.

Oxytocin. Oxytocin concentrations increased when comparing pre-decision to baseline levels.

Cortisol. Cortisol concentrations decreased when comparing pre-decision to baseline levels.

STAI. STAI scores decreased when comparing pre-decision to baseline levels.

3.2 HYPOTHESIS 2 (H2)

Immediately *after* a decision point when one person chooses to *trust* another, the changes in signal amplitude (relative to baseline) are evident discussed in sections 3.2.1 through 3.2.4:

3.2.1 Hypothesis 2: Binary Aggregate Across All Decisions (Analysis 1)

Table 6 shows percentages (and absolute ratios) calculated for the signal of each sub-hypothesis.

Table 6. Hypothesis 2: Binary aggregate across all decisions.

Specific Hypothesis	Percentage of Decisions That Agree With The Hypothesis
H2a: [F4–F3] Frontal alpha power asymmetry increases	56% (155/277)
H2b: RR interval increases	46% (52/114)
H2c: High-frequency (HF) HRV increases	HF: 51% (59/115) HFnorm: 42% (49/118)
H2d: Low-frequency (LF) HRV decreases	LF: 39% (45/114) LFnorm: 42% (49/118)

Table 6. Hypothesis 2: Binary aggregate across all decisions (continued).

Specific Hypothesis	Percentage of Decisions That Agree With The Hypothesis
H2e: Skin conductance level decreases	SCL: 17% (44/256) SCR: 30% (73/241)
H2f: Oxytocin concentration increases	53% (114/216)
H2g: Cortisol concentration decreases	82% (187/227)
H2h: Mayer score increases	N/A (no baseline measure)
H2i: STAI score decreases	44% (130/296)
H2j: SAS score decreases	N/A (no post-decision measure)
H2k: All the above signals change simultaneously	*4% (12/297)*

Variables that support the validity of the protocol to measure trust (i.e., < 80% of decisions agree with hypothesis):

Cortisol. Cortisol concentrations decreased after the decision to trust was made in 82% of the cases (n = 187/227).

3.2.2 Hypothesis 2: Raw Signals (Analysis 2)

Table 7 shows the mean difference [baseline – post-decision] (±SE) and the p-value calculated by the one-way ANOVA Section 2.6 for all sub-hypotheses.

Table 7. Hypothesis 2: Raw signals.

Specific Hypothesis for Trust Condition	Mean Difference [Baseline – Pre-Decision] (±SE); *p*-Value Of Mean Difference
H2a: [F4–F3] Frontal alpha power asymmetry increases	-0.099 ±0.213, p = 0.643; n.s.
H2b: RR interval increases	12.224 ±15.402, p = 0.428; n.s.
H2c: High-frequency HRV increases	HF: -0.143 ±0.431, p = 0.740; n.s. HFnorm: 0.041 0.025, p = 0.109; n.s.
H2d: Low-frequency HRV decreases	LF: -0.855 ±0.681, p = 0.210; n.s. LFnorm: -0.041 ±0.025, p = 0.109; n.s.
H2e: Skin conductance level decreases	SCL: -1.319 ±0.413, p = 0.001; n.s.* SCR: -6.223 ±1.508, p = 0.000; n.s.*
H2f: Oxytocin concentration increases	-0.708 ±0.524, p = 0.177; n.s.
H2g: Cortisol concentration decreases	2.244 ±0.517, p = 0.000; *
H2h: Mayer score increases	N/A (no baseline measure)
H2i: STAI score decreases	0.961 ±0.893, p = 0.282; n.s.
H2j: SAS score decreases	N/A (no post-decision measure)

* = significant of the proposed SEM hypothesis

n.s. = not significant

n.s.* = significant but in the opposite direction of the proposed SEM hypothesis

Note that skin conductance level and skin conductance response were different from baseline, but in the direction opposite to that which was hypothesized.

Variables that support the validity of the protocol for trust (i.e., measure is different from baseline):

Cortisol. Cortisol concentrations decreased when comparing post-decision to baseline levels.

3.2.3 Hypothesis 2: Signals minus Baseline (Analysis 2)

Table 8 shows 95% confidence intervals for the signal of each sub-hypothesis.

Table 8. Hypothesis 2: Signals minus baseline.

Specific Hypothesis for Trust Condition	95% Confidence Interval for Mean
H2a: [F4–F3] Frontal alpha power asymmetry increases	[-0.182 0.220]; n.s.
H2b: RR interval increases	[-25.709 -1.084]; n.s.*
H2c: High-frequency HRV increases	HF: [-0.226 0.830]; n.s. HFnorm: [-0.108 -0.003]; n.s.*
H2d: Low-frequency HRV decreases	LF: [-0.233 1.802]; n.s. LFnorm: [0.003 0.108]; n.s.*
H2e: Skin conductance level decreases	SCL: [1.018 1.421]; n.s.* SCR: [3.491 7.093]; n.s.*
H2f: Oxytocin concentration increases	[-0.265 0.138]; n.s.
H2g: Cortisol concentration decreases	[-2.526 -1.631]; *
H2h: Mayer score increases	N/A (no baseline measure)
H2i: STAI score decreases	[-1.69 -0.35]; *
H2j: SAS score decreases	N/A (no post-decision measure)
H2f: Oxytocin concentration increases	[-0.265 0.138]; n.s.
H2g: Cortisol concentration decreases	[-2.526 -1.631]; *
H2h: Mayer score increases	N/A (no baseline measure)
H2i: STAI score decreases	[-1.69 -0.35]; *
H2j: SAS score decreases	N/A (no post-decision measure)

* = significant of the proposed SEM hypothesis

n.s. = not significant

n.s.* = significant but in the opposite direction of the proposed SEM hypothesis

Note that RR interval, skin conductance level, skin conductance response, high-frequency normalized (HFnorm) and low-frequency normalized (LFnorm) all were different from baseline, but in the direction opposite to that which was hypothesized.

Variables that support the validity of the protocol for trust (i.e., measure is different from baseline [confidence interval does not include 0]):

Cortisol. Cortisol concentrations decreased when comparing post-decision to baseline levels.

STAI. STAI scores decreased when comparing post-decision to baseline levels.

3.2.4 Hypothesis 2: Signals Divided by Baseline (Analysis 2)

Table 9 shows 95% confidence intervals for the signal of each sub-hypothesis.

Table 9. Hypothesis 2: Signals divided by baseline.

Specific Hypothesis for Trust Condition	95% Confidence Interval for Mean
H2a: [F4–F3] Frontal alpha power asymmetry increases	[-6.337 1.032], n.s.
H2b: RR interval increases	[0.973 1.002], n.s.
H2c: High-frequency HRV increases	HF: [1.649 3.366], * HFnorm: [1.114 1.984], *
H2d: Low-frequency HRV decreases	LF: [2.300 5.169], n.s.* LFnorm: [1.128 1.543], n.s.*

Table 9. Hypothesis 2: Signals divided by baseline (continued).

Specific Hypothesis for Trust Condition	95% Confidence Interval for Mean
H2c: High-frequency HRV increases	HF: [1.649 3.366], * HFnorm: [1.114 1.984], *
H2d: Low-frequency HRV decreases	LF: [2.300 5.169], n.s.* LFnorm: [1.128 1.543], n.s.*
H2e: Skin conductance level decreases	SCL: [1.332 1.484], n.s.* SCR: [4.165 9.516], n.s.*
H2f: Oxytocin concentration increases	[1.017 1.107], *
H2g: Cortisol concentration decreases	0.799 0.903], *
H2h: Mayer score increases	N/A (no baseline measure)
H2i: STAI score decreases	0.96 1.00], n.s.
H2j: SAS score decreases	N/A (no post-decision measure)

 * = significant of the proposed SEM hypothesis

n.s. = not significant

n.s.* = significant but in the opposite direction of the proposed SEM hypothesis

Note that skin conductance level, skin conductance response, and low-frequency (raw and normalized) were all different from baseline, but in the direction opposite to that which was hypothesized.

Variables that support the validity of the protocol for trust (i.e., measure is different from baseline [confidence interval does not include 1]):

High-frequency HRV. HF, and HFnorm increased when comparing post-decision to baseline levels.

Oxytocin. Oxytocin concentrations increases when comparing post-decision to baseline levels.

Cortisol. Cortisol concentrations decreased when comparing post-decision to baseline levels.

3.3 HYPOTHESIS 3 (H3)

Immediately *before* a decision point when one person chooses to *distrust* another, the following changes in signal amplitude (relative to baseline) are evident and discussed in Sections 3.1.1 through 0:

3.3.1 Hypothesis 3: Binary Aggregate Across All Decisions (Analysis 1)

Table 10 shows percentages (and absolute ratios) calculated for the signal of each sub-hypothesis.

Table 10. Hypothesis 3: Binary aggregate across all decisions.

Specific Hypothesis	Percentage of decisions that agree with the Hypothesis
H3a: [F4–F3] Frontal alpha power asymmetry decreases	46% (7/38)
H3b: RR interval decreases	91% (10/11)
H3c: High-frequency HRV decreases	HF: 78% (7/9) HFnorm: 64% (7/11)
H3d: Low-frequency HRV increases	LF: 73% (8/11) LFnorm: 64% (7/11)
H3e: Skin conductance level increases	SCL: 88% (28/32) SCR: 81% (22/27)

Table 10. Hypothesis 3: Binary aggregate across all decisions (continued).

Specific Hypothesis	Percentage of decisions that agree with the Hypothesis
H3f: Oxytocin concentration decreases	56% (15/27)
H3g: Cortisol concentration increases	35% (9/26)
H3h: Mayer score decreases	N/A (no baseline measure)
H3i: STAI score increases	44% (17/39)
H3j: SAS score increases	39% (15/38)
H3k: All the above signals change simultaneously	5% (2/39)

Variables that support the validity of the protocol to measure distrust (i.e., < 80% of decisions agree with hypothesis):

Skin Conductance Levels: Skin conductance levels increased before the decision to distrust was made in 88% of the cases (n = 28/32) and skin conductance response increased before the decision to distrust was made in 88% of the cases (n = 22/27).

There were no variables that support the validity of the protocol to measure distrust (i.e. measure is different from baseline for this test.

3.3.2 Hypothesis 3: Raw Signals (Analysis 2)

Table 11 shows the mean difference [baseline – pre-decision] ($\pm$SE) and the *p*-value calculated by the one-way ANOVA Section 2.6 for all sub-hypotheses.

Table 11. Hypothesis 3: Raw signals.

Specific Hypothesis for Distrust Condition	Mean Difference [Baseline – Pre-Decision] ($\pm$SE); *p*-Value of Mean Difference
H3a: [F4–F3] Frontal alpha power asymmetry decreases	0.232 ± 0.535,p = 0.664; n.s.
H3b: RR interval decreases	68.677 ± 44.658,p = 0.125; n.s.
H3c: High-frequency HRV decreases	HF: -0.153 ± 1.280,p = 0.905; n.s. HFnorm: 0.117 ± 0.074,p = 0.116; n.s.
H3d: Low-frequency HRV increases	LF: -2.901 ± 2.008,p = 0.149; n.s. LFnorm: -0.117 ± 0.074,p = 0.116; n.s.
H3e: Skin conductance level increases	SCL: -1.578 ± 1.061,p = 0.137; n.s. SCR: -1.432 ± 4.098,p = 0.727; n.s.
H3f: Oxytocin concentration decreases	0.172 ±1.357,p = 0.899; n.s.
H3g: Cortisol concentration increases	-0.138 ±1.387,p = 0.921; n.s.
H3h: Mayer score decreases	N/A (no baseline measure)
29H3i: STAI score increases	0.593 ±2.281,p = 0.795; n.s.
H3j: SAS score increases	0.222 ±0.167,p = 0.109; n.s.

n.s. = not significant

There were no Variables that supported the validity of the protocol to measure distrust (i.e., measure is different from baseline):

3.3.3 Hypothesis 3: Signals minus Baseline (Analysis 2)

Table 12 shows 95% confidence intervals for the signal of each sub-hypothesis.

Table 12. Hypothesis 3: Signals minus baseline.

Specific Hypothesis for Distrust Condition	95% Confidence Interval for Mean
H3a: [F4–F3] Frontal alpha power asymmetry decreases	[-0.112 0.355], n.s.
H3b: RR interval decreases	[-122.219 -24.943], *
H3c: High-frequency HRV decreases	HF: [-2.249 1.265], n.s. HFnorm: [-0.258 0.113], n.s.
H3d: Low-frequency HRV increases	LF: [-0.538 6.779], n.s. LFnorm: [-0.113 0.258], n.s.
H3e: Skin conductance level increases	SCL: [1.335 3.141], * SCR: [1.45 3 10.652], *
H3f: Oxytocin concentration decreases	[-0.372 0.686], n.s.
H3g: Cortisol concentration increases	[-2.552 0.232], n.s.
H3h: Mayer score decreases	N/A (no baseline measure)
H3i: STAI score increases	[-3.79 2.56], n.s.
H3j: SAS score increases	[-0.224 -0.054], n.s.*

 * = significant of the proposed SEM hypothesis

n.s. = not significant

Variables that support the validity of the protocol to measure distrust (i.e., measure is different from baseline [confidence interval does not include 0])

RR interval. RR interval decreased when comparing pre-decision to baseline levels.

Skin Conductance Level. Skin conductance levels and skin conductance response increased when comparing pre-decision to baseline levels.

3.3.4 Hypothesis 3: Signals Divided by Baseline (Analysis 2)

Table 13 shows 95% confidence intervals for the signal of each sub-hypothesis.

Table 13. Hypothesis 3: Signals divided by baseline.

Specific Hypothesis for Distrust Condition	95% Confidence Interval for Mean
H3a: [F4–F3] Frontal alpha power asymmetry decreases	[-0.017 2.449], n.s.
H3b: RR interval decreases	[0.871 0.971], *
H3c: High-frequency HRV decreases	HF: [0.347 1.140], n.s. HFnorm: [-0.022 3.528], n.s.
H3d: Low-frequency HRV increases	LF: [0.928 3.824], n.s. LFnorm: [0.896 1.523], n.s.

Table 13. Hypothesis 3: Signals divided by baseline (continued).

Specific Hypothesis for Distrust Condition	95% Confidence Interval for Mean
H3e: Skin conductance level increases	SCL: [1.315 1.706], * SCR: [1.110 17.283], *
H3f: Oxytocin concentration decreases	[0.866 1.108], n.s.
H3g: Cortisol concentration increases	[0.809 1.204], n.s.
H3h: Mayer score decreases	N/A (no baseline measure)
H3i: STAI score increases	[0.93 1.08], n.s.
H3j: SAS score increases	[0.906 1.045], n.s.

* = significant of the proposed SEM hypothesis

n.s. = not significant

Variables that support the validity of the protocol for distrust (i.e., measure is different from baseline [confidence interval does not include 1]):

Skin Conductance Level. Skin conductance levels and skin conductance response increased when comparing pre-decision to baseline levels.

3.4 HYPOTHESIS 4 (H4)

Immediately *after* a decision point when one person chooses to *distrust* another, the following changes in signal amplitude (relative to baseline) are evident and discussed in Sections 3.4.1through 3.4.4:

3.4.1 Hypothesis 4: Binary Aggregate Across All Decisions (Analysis 1)

Table 14 shows percentages (and absolute ratios) calculated for the signal of each sub-hypothesis.

Table 14. Hypothesis 4: Binary aggregate across all decisions.

Specific Hypothesis	Percentage of decisions that agree with the Hypothesis
H4a: [F4–F3] Frontal alpha power asymmetry decreases	39% (14/36)
H4b: RR interval decreases	76% (13/17)
H4c: High-frequency HRV decreases	HF: 47% (8/17) HFnorm: 71% (12/17)
H4d: Low-frequency HRV increases	LF: 82% (14/17) LFnorm: 71% (12/17)
H4e: Skin conductance level increases	SCL: 87% (27/31) SCR: 85% (22/26)
H4f: Oxytocin concentration decreases	50% (14/28)
H4g: Cortisol concentration increases	30% (8/27)
H4h: Mayer score decreases	N/A (no baseline measure)
H4i: STAI score increases	41% (16/39)
H4j: SAS score increases	N/A (no post-decision measure)
H4k: All the above signals change simultaneously	10% (4/39)

Variables that support the validity of the protocol to measure distrust (i.e., < 80% of decisions agree with hypothesis):

Low-frequency. Average low frequency of heart rate inter-beat intervals increased after the decision to distrust was made in 82% of the cases (n = 14/17).

Skin Conductance Levels: Skin conductance levels increased after the decision to distrust was made in 87% of the cases (n = 27/31) and skin conductance response increased after the decision to distrust was made in 85% of the cases (n = 22/26).

3.4.2 Hypothesis 4: Raw Signals (Analysis 2)

Table 15 shows the mean difference [baseline – post-decision] (±SE) and the p-value calculated by the one-way ANOVA Section 2.6 for all sub-hypotheses.

Table 15. Hypothesis 4: Raw signals.

Specific Hypothesis for distrust condition	Mean difference [baseline – post-decision] (±SE); *p*-value of mean difference
H4a: [F4–F3] Frontal alpha power asymmetry decreases	0.137 ±0.538,p = 0.799; n.s.
H4b: RR interval decreases	40.493 ±41.227,p = 0.327; n.s.
H4c: High-frequency HRV decreases	HF: -0.095 ±1.173,p = 0.935; n.s. HFnorm: 0.135 ±0.069,p = 0.050; *
H4d: Low-frequency HRV increases	LF: -4.885 ±1.839,p = 0.008; * LFnorm: -0.135 ±0.069,p = 0.050; *
H4e: Skin conductance level increases	SCL: -1.298 ±1.067,p = 0.224; n.s. SCR: -2.147 ±4.124,p = 0.603; n.s.
H4f: Oxytocin concentration decreases	0.635 ±1.348,p = 0.638; n.s.
H4g: Cortisol concentration increases	0.257 ±1.377,p = 0.852; n.s.
H4h: Mayer score decreases	N/A (no baseline measure)
H4i: STAI score increases	1.285 ±2.281,p = 0.573; n.s.
H4j: SAS score increases	N/A (no post-decision measure)

 * = significant of the proposed SEM hypothesis

n.s. = not significant

Variables that support the validity of the protocol for distrust (i.e., measure is different from baseline):

High-frequency HRV. HFnorm decreased when comparing post-decision to baseline levels.

Low-frequency HRV. LF and LFnorm increased when comparing post-decision to baseline levels.

3.4.3 Hypothesis 4: Signals minus Baseline (Analysis 2)

Table 16 shows 95% confidence intervals for the signal of each sub-hypothesis.

Table 16. Hypothesis 4: Signals minus baseline.

Specific Hypothesis for distrust condition	95% Confidence Interval for Mean
H4a: [F4–F3] Frontal alpha power asymmetry decreases	[-0.040 0.442], n.s.
H4b: RR interval decreases	[-101.998 -7.922], *
H4c: High-frequency HRV decreases	HF: [-0.526 0.950], n.s. HFnorm: [-0.199 -0.008], *
H4d: Low-frequency HRV increases	LF: [-0.319 8.682], n.s. LFnorm: [0.057 0.118], *
H4e: Skin conductance level increases	SCL: [1.200 3.050], * SCR: [2.121 11.784], *

Table 16. Hypothesis 4: Signals minus baseline (continued).

Specific Hypothesis for distrust condition	95% Confidence Interval for Mean
H4c: High-frequency HRV decreases	HF: [-0.526 0.950], n.s. HFnorm: [-0.199 -0.008], *
H4d: Low-frequency HRV increases	LF: [-0.319 8.682], n.s. LFnorm: [0.057 0.118], *
H4e: Skin conductance level increases	SCL: [1.200 3.050], * SCR: [2.121 11.784], *
H4f: Oxytocin concentration decreases	[-0.891 0.291], n.s.
H4g: Cortisol concentration increases	[-3.248 -0.332], n.s.*
H4h: Mayer score decreases	N/A (no baseline measure)
H4i: STAI score increases	[-4.74 2.13], n.s.
H4j: SAS score increases	N/A (no post-decision measure)

 * = significant of the proposed SEM hypothesis

n.s. = not significant

n.s.* = significant but in the opposite direction of the proposed SEM hypothesis

Variables that support the validity of the protocol for distrust (i.e., measure is different from baseline [confidence interval does not include 0])

High-frequency HRV. HFnorm decreased when comparing post-decision to baseline levels.

Low-frequency HRV. LFnorm increased when comparing post-decision to baseline levels.

Skin Conductance Level. Skin conductance levels and skin conductance response increased when comparing post-decision to baseline levels.

3.4.4 Hypothesis 4: Signals Divided by Baseline (Analysis 2)

Table 17 shows 95% confidence intervals for the signal of each sub-hypothesis.

Table 17. Hypothesis 4: Signals divided by baseline.

Specific Hypothesis for Distrust Condition	95% Confidence Interval for Mean
H4a: [F4–F3] Frontal alpha power asymmetry decreases	[0.090 2.290], n.s.
H4b: RR interval decreases	[0.889 0.992], *
H4c: High-frequency HRV decreases	HF: [0.760 2.356], n.s. HFnorm: [0.461 1.615], n.s.
H4d: Low-frequency HRV increases	LF: [0.908 5.387], n.s. LFnorm: [0.993 1.629], n.s.
H4e: Skin conductance level increases	SCL: [1.294 1.709], * SCR: [-0.542 24.951], n.s.

Table 17. Hypothesis 4: Signals divided by baseline (continued).

Specific Hypothesis for Distrust Condition	95% Confidence Interval for Mean
H4f: Oxytocin concentration decreases	[0.886 1.166], n.s.
H4g: Cortisol concentration increases	[0.766 1.106], n.s.
H4h: Mayer score decreases	N/A (no baseline measure)
H4i: STAI score increases	[0.92 1.08], n.s.
H4j: SAS score increases	N/A (no post-decision measure)

n.s. = not significant

Variables that support the validity of the protocol for distrust (i.e., measure is different from baseline [confidence interval does not include 1]): .

Skin Conductance Level. Skin conductance levels increased when comparing post-decision to baseline levels.

3.5 HYPOTHESIS 5 (H5)

Compare distribution of each signal at times ***before*** a decision to ***trust*** to distribution of the signal at times ***before*** a decision to ***distrust***, the following changes in signal are evident and discussed in Sections 3.5.1 through 0.

3.5.1 Hypothesis 5: Raw Signals (Analysis 3)

Table 18 shows the mean difference [trust–distrust] (±SE) and the *p*-value calculated by the one-way ANOVA Section 2.6 for all sub-hypotheses.

Table 18. Hypothesis 5: Raw signals.

Specific Hypothesis for Trust Condition	Mean difference [trust–distrust] (±SE); *p*-value of mean difference
H5a: [F4–F3] Frontal alpha power asymmetry increases	0.339 ±0.356,p = 0.342; n.s.
H5b: RR interval increases	64.743 ±31.807,p = 0.042; *
H5c: High-frequency HRV increases	HF: 0.095 ±0.926,p = 0.919; n.s. HFnorm: -0.035 ±0.053,p = 0.514; n.s.
H5d: Low-frequency HRV decreases	LF: 0.542 ±1.453,p = 0.709; n.s. LFnorm: 0.035 ±0.053,p = 0.514; n.s
H5e: Skin conductance level decreases	SCL: -0.756 ±0.696,p = 0.278; n.s. SCR: -0.057 ±2.65,p = 0.983; n.s.
H5f: Oxytocin concentration increases	-0.296 ±0.911,p = 0.746; n.s.

Table 18. Hypothesis 5: Raw signals (continued).

Specific Hypothesis for Trust Condition	Mean difference [trust–distrust] (±SE); *p*-value of mean difference
H5g: Cortisol concentration decreases	-0.733 ±0.936,p = 0.434; n.s.
H5h: Mayer score increases	A: 0.82 ±0.130,p = 0.000; * B: 0.788 ±0.146,p = 0.000; * I: 0.627 ±0.120,p = 0.000; *
H5i: STAI score decreases	-1.676 ±1.497,p = 0.263; n.s.
H5j: SAS score decreases	-0.049 ±0.100,p = 0.629; n.s.

* = significant of the proposed SEM hypothesis

n.s. = not significant

Variables that support the validity of the protocol (i.e., p < 0.05 and amplitude direction agrees with hypothesis):

Mayer score. Average scores of Mayer A, B, and I were significantly different between trust and distrust decisions.before the decision was made.

3.5.2 Hypothesis 5: Signals minus Baseline (Analysis 3)

Table 19 shows the mean difference [trust–distrust] (±SE) and the *p*-value calculated by the one-way ANOVA. Section 2.6 for all sub-hypotheses.

Table 19. Hypothesis 5: Signals minus Baseline.

Specific Hypothesis for Trust Condition	Mean Difference [trust–distrust] (±SE); *p*-Value of Mean Difference
H5a: [F4–F3] Frontal alpha power asymmetry increases	-0.148 ±0.290,p = 0.610; n.s.
H5b: RR interval increases	36.138 ±22.598,p = 0.111; n.s.
H5c: High-frequency HRV increases	HF: 1.061 ±1.227,p = 0.388; n.s. HFnorm: -0.042 ±0.081,p = 0.605; n.s.
H5d: Low-frequency HRV decreases	LF: -1.595 ±1.946,p = 0.413; n.s. LFnorm: 0.042 ±0.081,p = 0.605; n.s.
H5e: Skin conductance level decreases	SCL: -1.202 ±0.314,p = 0.001; * SCR: -0.806 ±2.670,p = 0.763; n.s.
H5f: Oxytocin concentration increases	-0.261 ±0.288,p = 0.365; n.s.
H5g: Cortisol concentration decreases	-0.240 ±0.723,p = 0.740; n.s.
H5h: Mayer score increases	N/A (no baseline measure)
H5i: STAI score decreases	-0.088 ±1.066,p = 0.934; n.s.
H5j: SAS score decreases	-0.062 ±0.091,p = 0.493; n.s.

* = significant of the proposed SEM hypothesis

n.s. = not significant

Variables that support the validity of the protocol (i.e., p < 0.05 and amplitude direction agrees with hypothesis):

Skin Conductance Level. Skin conductance levels were significantly different between trust and distrust decisions before the decision was made.

3.5.3 Hypothesis 5: Signals Divided by Baseline (Analysis 3)

Table 20 shows the mean difference [trust–distrust] (±SE) and the *p*-value calculated by the one-way ANOVA.Section 2.6 for all sub-hypotheses.

Table 20. Hypothesis 5: Signals divided by baseline.

Specific Hypothesis for Trust Condition	Mean Difference [trust–distrust] (±SE); *p*-Value of Mean Difference
H5a: [F4–F3] Frontal alpha power asymmetry increases	-1.778 ±4.236,p = 0.675; n.s.
H5b: RR interval increases	0.041 ±0.025,p = 0.104; n.s.
H5c: High-frequency HRV increases	HF: 1.928 ±2.149,p = 0.370; n.s. HFnorm: -0.684 ±0.599,p = 0.255; n.s.
H5d: Low-frequency HRV decreases	LF: 1.259 ±1.961,p = 0.521; n.s. LFnorm: 0.184 ±0.302,p = 0.543; n.s.
H5e: Skin conductance level decreases	SCL: -0.127 ±0.109,p = 0.248; n.s. SCR: -3.500 ±3.865,p = 0.366; n.s.
H5f: Oxytocin concentration increases	0.139 ±0.111,p = 0.212; n.s.
H5g: Cortisol concentration decreases	-0.098 ±0.085,p = 0.248; n.s.
H5h: Mayer score increases	N/A (no baseline measure)
H5i: STAI score decreases	-0.018 ±0.030,p = 0.541; n.s.
H5j: SAS score decreases	-0.055 ±0.067,p = 0.405; n.s.

n.s. = not significant

There were no variables that supported the validity of the protocol (p) (i.e., p < 0.05 and amplitude direction agrees with hypothesis):

3.6 HYPOTHESIS 6 (H6)

Compare distribution of each signal at times *after* a decision to *trust* to distribution of the signal at times *after* a decision to *distrust*, the following changes in signal amplitude are evident:

3.6.1 Hypothesis 6: Raw Signals (Analysis 3)

Table 21 shows the mean difference [trust–distrust] (±SE) and the p-value calculated by the one-way ANOVA. See Section 2.6 for all sub-hypotheses.

Table 21. Hypothesis 6: Raw signals.

Specific Hypothesis for Trust Condition	Mean Difference [trust–distrust] (±SE); *p*-Value of Mean Difference
H6a: [F4–F3] Frontal alpha power asymmetry increases	0.313 ±0.361,p = 0.386; n.s.
H6b: RR interval increases	46.713 ±26.788,p = 0.082; n.s.
H6c: High-frequency HRV increases	HF: -0.062 ±0.772,p = 0.936; n.s. HFnorm: 0.044 ±0.045,p = 0.320; n.s.
H6d: Low-frequency HRV decreases	LF: -3.222 ±1.211,p = 0.008; * LFnorm: -0.044 ±0.44,p = 0.320; n.s.

Table 21. Hypothesis 6: Raw signals (continued).

Specific Hypothesis for Trust Condition	Mean Difference [trust–distrust] (±SE); *p*-Value of Mean Difference
H6e: Skin conductance level decreases	SCL: -0.494 ±0.705,p = 0.484; n.s. SCR: -0.160 ±2.692,p = 0.953; n.s.
H6f: Oxytocin concentration increases	0.995 ±0.894,p = 0.266; n.s.
H6g: Cortisol concentration decreases	-0.937 ±0.920,p = 0.309; n.s.
H6h: Mayer score increases	A: 0.778 ±0.134,p = 0.000; * B: 0.783 ±0.153,p = 0.000; * I: 0.620 ±0.126,p = 0.000; *
H6i: STAI score decreases	-1.287 ±1.498,p = 0.390; n.s.
H6j: SAS score decreases	N/A (no post-decision measure)

n.s. = not significant

Variables that support the validity of the protocol (i.e., p < 0.05 and amplitude direction agrees with hypothesis):

Low-frequency HRV. LF was significantly different between trust and distrust decisions.after the decision was made.

Mayer score. Average scores of Mayer A, B, and I were significantly different between trust and distrust decisions.after the decision was made.

Table 21. Hypothesis 6: Raw signals (continued).

Specific Hypothesis for Trust Condition	Mean Difference [Trust–Distrust] (±SE); *p*-Value of Mean Difference
H6b: RR interval increases	46.713 ±26.788,p = 0.082; n.s.
H6c: High-frequency HRV increases	HF: -0.062 ±0.772,p = 0.936; n.s. Fnorm: 0.044 ±0.045,p = 0.320; n.s.
H6d: Low-frequency HRV decreases	LF: -3.222 ±1.211,p = 0.008; * LFnorm: -0.044 ±0.44,p = 0.320; n.s.
H6e: Skin conductance level decreases	SCL: -0.494 ±0.705,p = 0.484; n.s. SCR: -0.160 ±2.692,p = 0.953; n.s.
H6f: Oxytocin concentration increases	0.995 ±0.894,p = 0.266; n.s.
H6g: Cortisol concentration decreases	-0.937 ±0.920,p = 0.309; n.s.
H6h: Mayer score increases	A: 0.778 ±0.134,p = 0.000; * B: 0.783 ±0.153,p = 0.000; * I: 0.620 ±0.126,p = 0.000; *
H6i: STAI score decreases	-1.287 ±1.498,p = 0.390; n.s.
H6j: SAS score decreases	N/A (no post-decision measure)

* = significant of the proposed SEM hypothesis

n.s. = not significant

Variables that support the validity of the protocol (i.e., p < 0.05 and amplitude direction agrees with hypothesis):

Low-frequency HRV. LF was significantly different between trust and distrust decisions.after the decision was made.

Mayer score. Average scores of Mayer A, B, and I were significantly different between trust and distrust decisions after the decision was made.

3.6.2 Hypothesis 6: Signals minus Baseline (Analysis 3)

Table 22 shows the mean difference [trust–distrust] (±SE) and the *p*-value calculated by the one-way ANOVA Section 2.6 for all sub-hypotheses.

Table 22. Hypothesis 6: Signals minus baseline.

Specific Hypothesis for Trust Condition	Mean Difference [trust–distrust] (±SE); *p*-Value of Mean Difference
H6a: [F4–F3] Frontal alpha power asymmetry increases	-0.182 ±0.294,p = 0.536; n .s.
H6b: RR interval increases	41.564 ±18.716,p = 0.027; *
H6c: High-frequency HRV increases	HF: 0.090 ±0.926,p = 0.923; n .s. HFnorm: 0.048 ±0.067,p = 0.480; n .s.
H6d: Low-frequency HRV decreases	LF: -3.408 ±1.612,p = 0.659; n .s. LFnorm: -0.048 ±0.067,p = 0.480; n .s.
H6d: Low-frequency HRV decreases	LF: -3.408 ±1.612,p = 0.659; n .s. LFnorm: -0.048 ±0.067,p = 0.480; n .s.
H6e: Skin conductance level decreases	SCL: -0.905 ±0.318,p = 0.005; * SCR: -1.660 ±2.717,p = 0.541; n .s.
H6f: Oxytocin concentration increases	0.237 ±0.283,p = 0.403; n .s.
H6g: Cortisol concentration decreases	-0.288 ±0.711,p = 0.685; n .s.
H6h: Mayer score increases	N/A (no baseline measure)
H6i: STAI score decreases	0.291 ±1.066,p = 0.785; n .s.
H6j: SAS score decreases	N/A (no post-decision measure)

* = significant of the proposed SEM hypothesis

n.s. = not significant

Variables that support the validity of the protocol (i.e., p < 0.05 and amplitude direction agrees with hypothesis):

RR-interval. Average RR-interval.was significantly different between trust and distrust decisions.after the decision was made.

Skin Conductance Level. Skin conductance levels were significantly different between trust and distrust decisions after the decision was made.

3.6.3 Hypothesis 6: Signals Divided by Baseline (Analysis 3)

Table 23 shows the mean difference [trust–distrust] (±SE) and the *p*-value calculated by the one-way ANOVA. Section 2.6 for all sub-hypotheses.

Table 23. Hypothesis 6: Signals divided by baseline.

Specific Hypothesis for Trust Condition	Mean Difference [trust–distrust] (±SE); *p*-Value of Mean Difference
H6a: [F4–F3] Frontal alpha power asymmetry increases	-3.842 ±4.290,p = 0.371; n.s.
H6b: RR interval increases	0.047 ±0.021,p = 0.026; *
H6c: High-frequency HRV increases	HF: 0.950 ±1.621,p = 0.558; n.s. HFnorm: 0.511 ±0.495,p = 0.304; n.s.
H6d: Low-frequency HRV decreases	LF: 0.587 ±1.624,p = 0.718; n.s. LFnorm: 0.024 ±0.250,p = 0.923; n.s.
H6e: Skin conductance level decreases	SCL: -0.093 ±0.111,p = 0.402; n.s. SCR: -5.364 ±3.912,p = 0.173; n.s.
H6f: Oxytocin concentration increases	0.0674 ±0.110,p = 0.539; n.s.
H6g: Cortisol concentration decreases	-0.085 ±0.083,p = 0.309; n.s.
H6h: Mayer score increases	N/A (no baseline measure)

Table 23. Hypothesis 6: Signals divided by baseline (continued).

Specific Hypothesis for Trust Condition	Mean Difference [trust–distrust] (±SE); *p*-Value of Mean Difference
H6i: STAI score decreases	-0.019 ±0.030,p = 0.529; n.s.
H6j: SAS score decreases	N/A (no post-decision measure)
H6h: Mayer score increases	N/A (no baseline measure)
H6i: STAI score decreases	-0.019 ±0.030,p = 0.529; n.s.
H6j: SAS score decreases	N/A (no post-decision measure)

* = significant of the proposed SEM hypothesis

n.s. = not significant

Variables that support the validity of the protocol (i.e., p < 0.05 and amplitude direction agrees with hypothesis):

RR-interval. Average RR-interval.was significantly different between trust and distrust decisions.after the decision was made.

3.7 BINARY AGGREGATE PLOTS

As described above, Analysis 1 counted the number of measures that changed from baseline in the direction that supported SEM.

3.7.1 Percentage of Decisions Supporting SEM

Figure 4 shows a graphic representation sub-hypotheses a–j of Hypothesis 1 (top plot, blue bars), Hypothesis 2 (bottom plot, blue bars), Hypothesis 3 (top plot, red bars), and Hypothesis 4 (bottom plot, red bars) for Analysis 1. Note that Hypotheses 5 and 6 could not be addressed since samples were not paired between trust and distrust. The dashed horizontal line at 80% was the threshold for determining the validity of protocol for measuring trust/distrust.
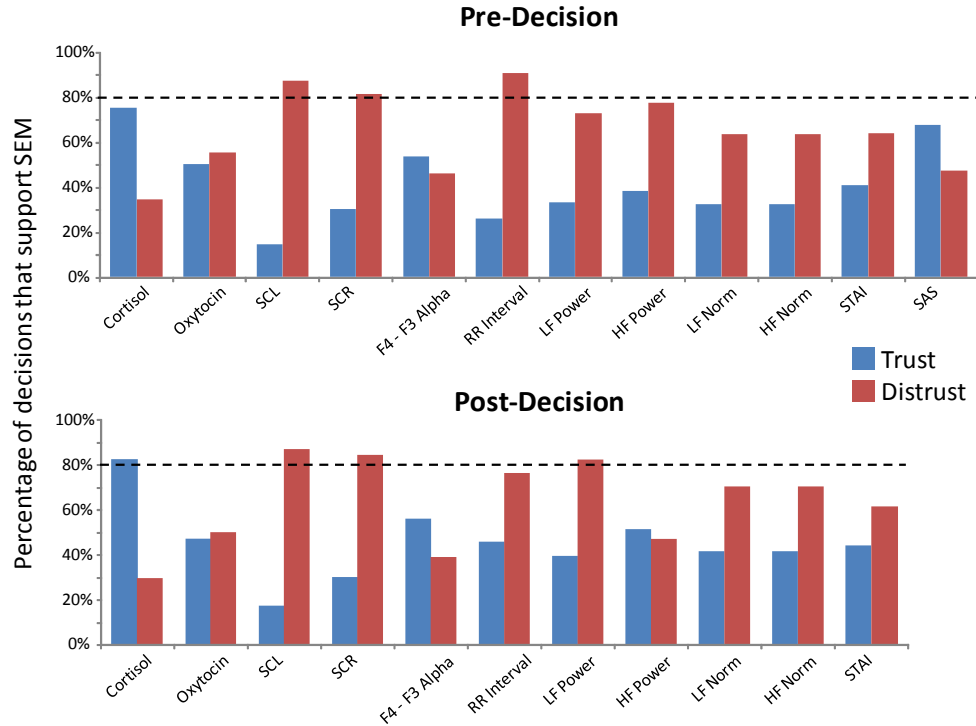
Figure 4. Percentage of decisions supporting SEM (all variables).

3.7.2 Simultaneous SIgnal Changes (Sub-hypothesis k)

Figure 5 details a histogram of percentage of measures supporting SEM. For each decision made, the percentage of measures supporting the SEM was computed (.i.e., if all the measures (from sub–hypotheses a–j) changed from baseline in the direction hypothesized, that would represent 100% support of the SEM for that decision). Alternatively, if only 2 of 10 measures supported the SEM, that decision would be labeled as 20%. Hypotheses 1 and 2 are represented by the left top and bottom plots. Hypotheses 3 and 4 are represented by the right top and bottom plots. Data were binned in 10% increments with the count of decisions shown on top of each bar. Note that Hypotheses 5 and 6 could not be addressed since samples were not paired between trust and distrust.

To address sub-hypothesis k (all signals change simultaneously), the binary (up/down) response for all measures was examined for each decision. The percentage of responses that agreed with SEM ranged from 100% (all measures agreed with SEM) to 0% (no measures agreed with SEM). A count of the decisions per 10% interval is displayed in Figure 5. We found that the percentage of measures that agreed with SEM varied greatly, with only a few instances where all measures had simultaneous directional changes consistent with SEM.
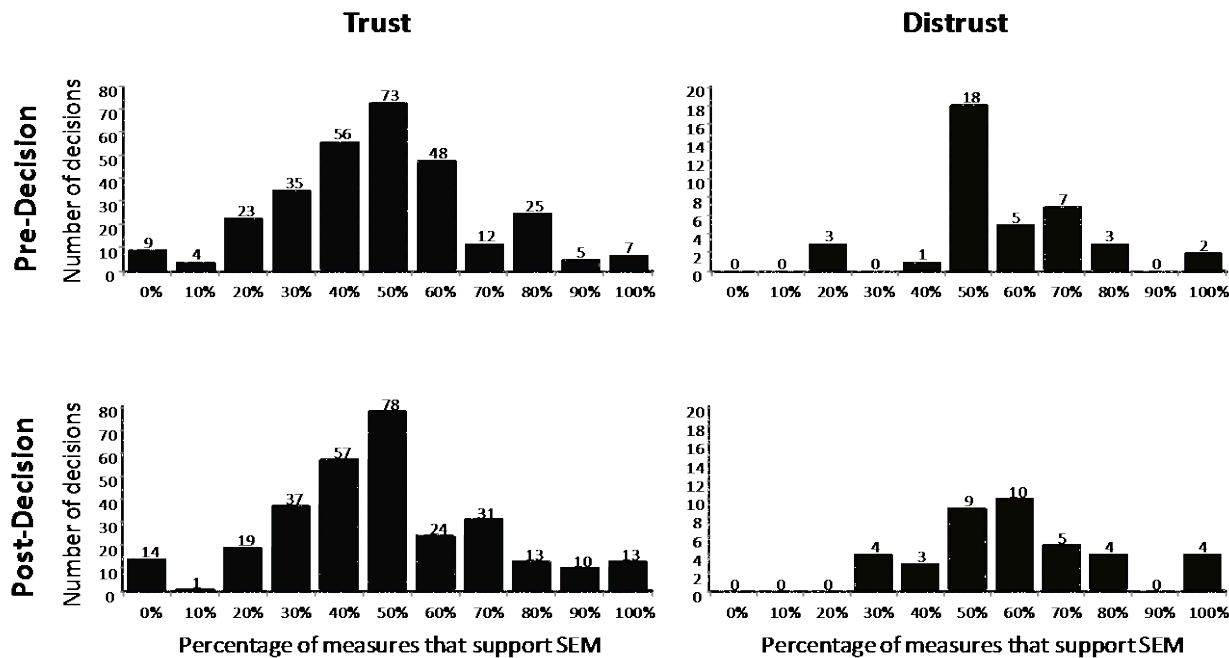
Figure 5. Histogram of percentage of measures supporting SEM.

Figure 6 lists numbers of decision for pre-and post-decision studies. An important issue when investigating sub-hypothesis k is that the number of measures associated with each decision is variable. This is due to the inability to extract all measures from all subjects (e.g., insufficient blood draws, EEG/HRV data too noisy, etc.). To further examine this, Figure 6 depicts data separated based on the number of measures present. This shows that not only is there a variable percentage of measures agreeing with SEM per decision (x–axis), but this does not seem to be correlated with the number of measures (y–axis).

Instances in which all measures had simultaneous directional changes in accordance with SEM (and also those in which no measures changed with SEM) may prove to be an interesting subset of individuals to further explore.

As the completeness of the dataset varied for each decision, these plots display the number of measures per decision (x-axis, 1–12 for pre-decision, 1–11 for post-decision) and how that correlated with the percentage of measure that supported SEM. The size and transparency of the circle is representative of the number of decisions that correspond to that particular point. The top graphs shows both trust and distrust interactions together for pre- and post-decisions (left and right plots). The bottom plots show trust and distrust interactions separately, with the number of decisions per point displayed in the center of each circle.

Below are statistical tables, summaries of results, bar plots of averaged data, and scatter plots of pre and post-decision data for all the individual measures stated in the SEM hypotheses. Note that the methods that adjusted for baseline levels (i.e., subtracting baseline and dividing by baseline), there is the effect of reducing the inherent variability of the signal, thus artificially narrowing the experimental

error. Therefore, outcomes for these methods may be a consequence of the adjustment rather than a true experimental outcome. Interpretations of these results are in Section 4.1.
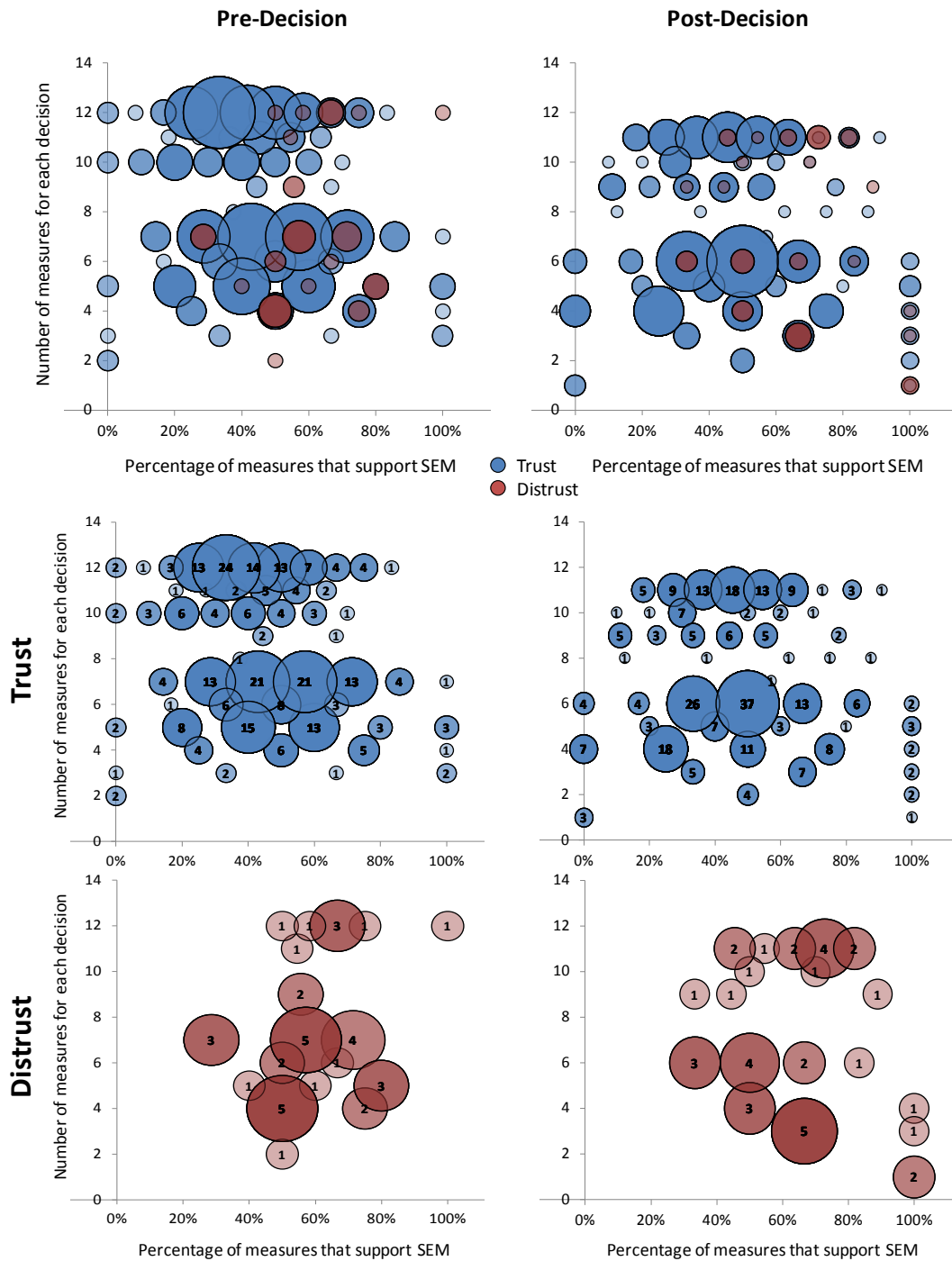

Figure 6. Number of measures per decision.

3.8 ALPHA ASYMMETRY

Table 24 shows all hypotheses and their corresponding statistical tests for alpha asymmetry.

Table 24. Alpha asymmetry statistical table.

Alpha Asymmetry

Specific Hypothesis	Percentage of decisions that agree with the Hypothesis	Raw Signal	Signal minus baseline	Signal divided by baseline
		Mean difference (±SE); p-value	95% Confidence Interval for Mean	95% Confidence Interval for Mean
H1a: [F4 – F3] alpha asymmetry increases TRUST: Baseline vs. Pre-decision	54% (150/280)	-0.030 ± 0.212 p = 0.889; n.s.	[-0.236 0.183] n.s.	[-2.771 1.646] n.s.
H2a: [F4 – F3] alpha asymmetry increases TRUST: Baseline vs. Post-decision	56% (155/277)	-0.099 ± 0.213 p = 0.643; n.s.	[-0.182 0.220] n.s.	[-6.337 1.032] n.s.
H3a: [F4 – F3] alpha asymmetry decreases DISTRUST: Baseline vs. Pre-decision	46% (7/38)	0.232 ± 0.535 p = 0.664, n.s.	[-0.112 0.355] n.s.	[-0.017 2.449] n.s.
H4a: [F4 – F3] alpha asymmetry decreases DISTRUST: Baseline vs. Post-decision	39% (14/36)	0.137 ± 0.538 p = 0.799; n.s.	[-0.040 0.442] n.s.	[0.090 2.290] n.s.
H5a: [F4 – F3] alpha asymmetry increases PRE-DECISION: Trust vs. Distrust		0.339 ± 0.356 p = 0.342; n.s.	-0.148 ± 0.290 p = 0.610; n.s.	-1.778 ± 4.236 p = 0.675; n.s.
H6a: [F4 – F3] alpha asymmetry increases POST-DECISION: Trust vs. Distrust		0.313 ± 0.361 p = 0.386; n.s.	-0.182 ± 0.294 p = 0.536; n.s.	-3.842 ± 4.290 p = 0.371; n.s.

n.s. = not significant

No significant differences for fontal alpha asymmetry were found for any of the hypotheses and methodologies, (despite the average data trending in the appropriate direction.

dark blue areas = specific hypothesis trust conditions studied.

light green = the area studied supports SEM (p<0.05; CJ.>95%).

pink = no support for SEM,

3.8.1 Average ±S.E.

Figures 7–9 show Average ±S.E. for alpha asymmetry. Areas are raw signal, signal minus baseline, and signal divided by baseline. Data details averages for baseline, pre-decision, and post-decision epochs, for trust and distrust interactions.
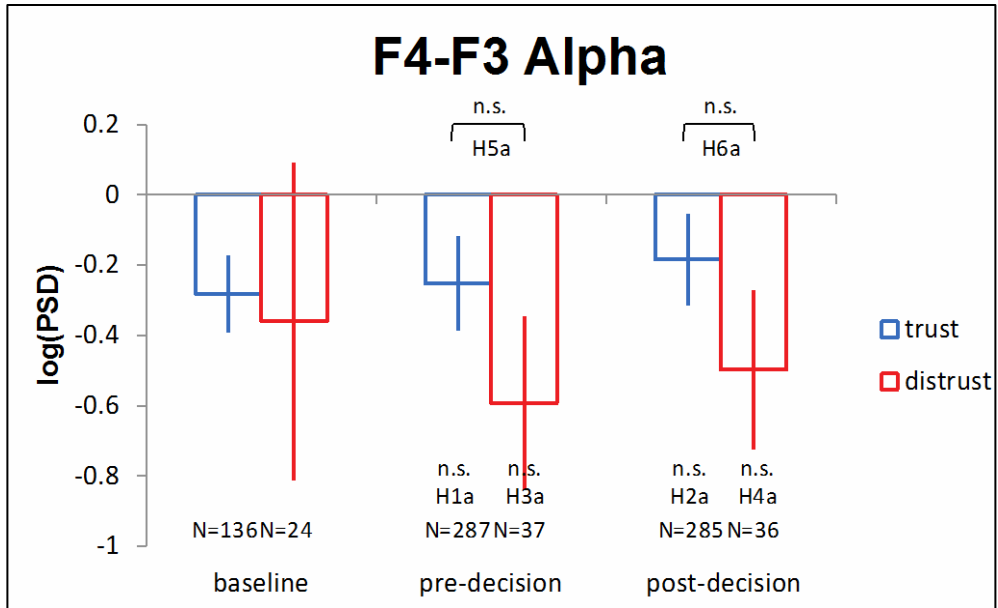
n.s. = not significant

N = the number of values per condition

Figure 7. Average ±S.E. for alpha asymmetry (raw signal).
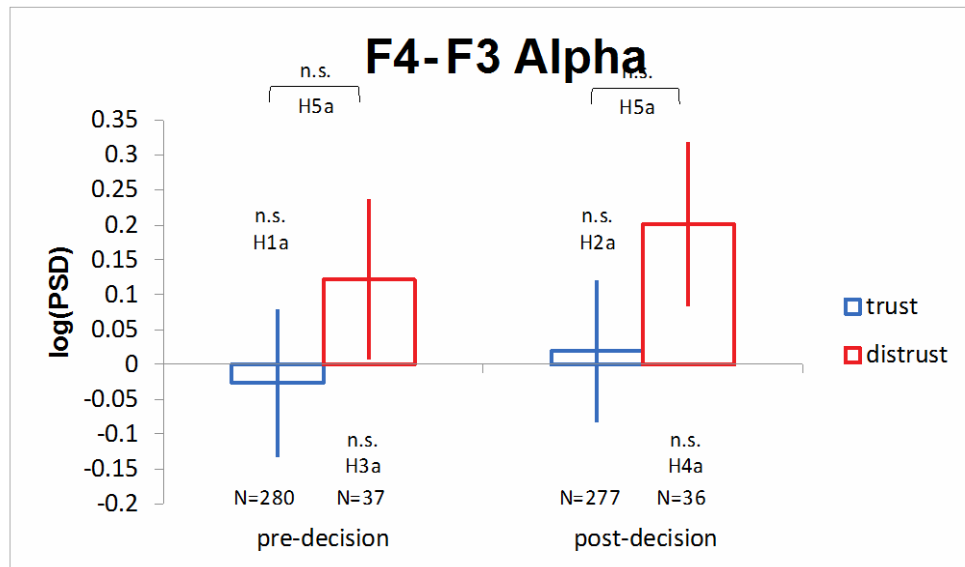
n.s. = not significant

N = the number of values per condition

Figure 8. Average ±S.E. for alpha asymmetry (signal minus baseline).

F4F3 Alpha

n.s. = not significant
N = the number of values per condition
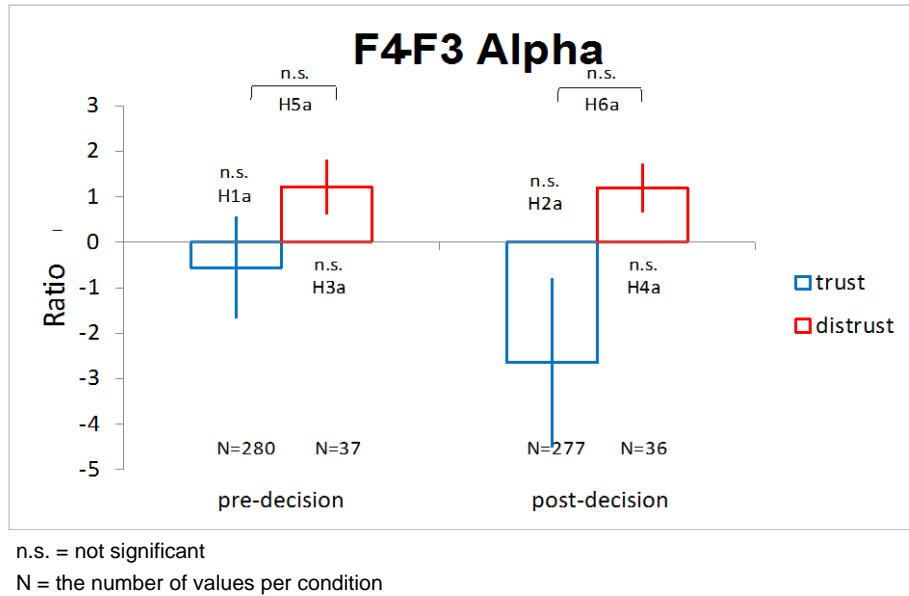
Figure 9. Average ±S.E. for alpha asymmetry (signal divided by baseline).

The sub-hypothesis addressed by specific parts of the plot see results in Figures 7–9.

3.8.2 Scatter Plots

Figures 10–12 show scatter plots for alpha asymmetry: raw signal, signal minus baseline, and signal divided by baseline. Values for pre-decision and post-decision epochs are displayed in the x-axis and y-axis, respectively. The equation and R2 value for the linear trendline is displayed for trust and distrust interactions in blue and red box.
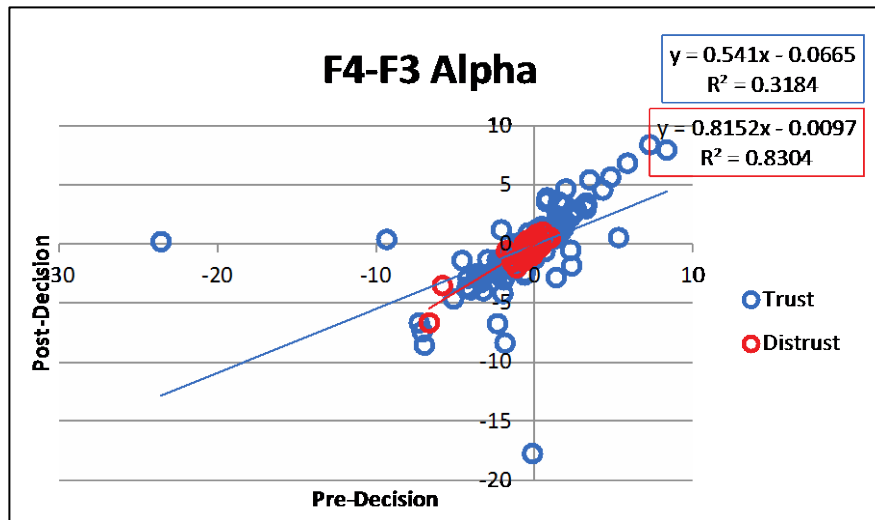
Values for pre-decision and post-decision epochs are displayed in the x-axis and y-axis.
The equation and R2 value for the linear trendline is displayed for trust and distrust interactions in blue and red box.

Figure 10. Scatter plot for alpha asymmetry (raw signal).
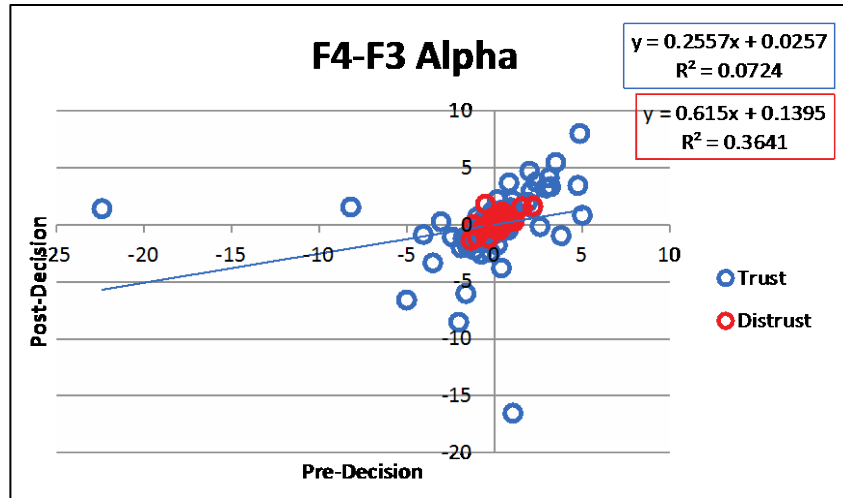
41

Values for pre-decision and post-decision epochs are displayed in the x-axis and y-axis.
The equation and R2 value for the linear trendline is displayed for trust and distrust interactions in blue and red box.

Figure 11. Scatter plot for alpha asymmetry (signal minus baseline).

Values for pre-decision and post-decision epochs are displayed in the x-axis and y-axis.
The equation and R2 value for the linear trendline is displayed for trust and distrust interactions in blue and red box.

Figure 12. Scatter plot for alpha asymmetry (signal divided by baselne).

3.9   RR INTERVAL

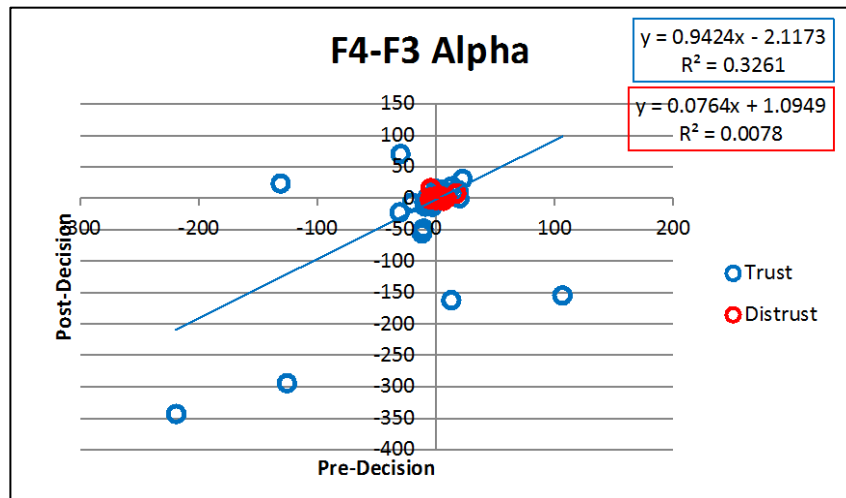Table 25 shows all hypotheses and their corresponding statistical tests for RR interval.

Table 25. RR interval statistical table.

Specific Hypothesis	Percentage of Decisions that Agree with the Hypothesis	Raw Signal	Signal Minus Baseline	Signal Divided by Baseline
		Mean Difference (±SE); p-value	95% Confidence Interval for Mean	95% Confidence Interval for Mean
H1b: RR interval increases TRUST: Baseline vs. Pre-decision	26% (34/131)	22.378 ±14.285 p= 0.146; n.s.	[-50.218 -24.667] n.s.*	[0.948 0.976] n.s.*
H2b: RR interval increases TRUST: Baseline vs. Post-decision	46% (52/114)	12.224 ±15.402 p = 0.428; n.s.	[-25.709 -1.084] n.s.*	[0.973 1.002] n.s.
H3b: RR interval decreases DISTRUST: Baseline vs. Pre-decision	91% (10/11)	68.677 ±44.658 p = 0.125; n.s.	[-122.219 -24.943] *	[0.871 0.971] *
H4b: RR interval decreases DISTRUST: Baseline vs. Post-decision	76% (13/17)	40.493 ±41.227 p = 0.327; n.s.	[-101.998 -7.922] *	[0.889 0.992] *
H5b: RR interval increases PRE-DECISION: Trust vs. Distrust		64.743 ±31.807 p = 0.042; *	36.138 ±22.598 p = 0.111; n.s.	0.041 ±0.025 p = 0.104; n.s.
H6b: RR interval increases POST-DECISION: Trust vs. Distrust		46.713 ±26.788 p = 0.082; n.s.	41.564 ±18.716 p = 0.027; *	0.047 ±0.021 p = 0.026; *

 * = significant of the proposed SEM hypothesis

n.s. = not significant

n.s.* = significant but in the opposite direction of the proposed SEM hypothesis.

dark blue areas   = specific hypothesis trust conditions studied.

light green = the area studied supports SEM (p<0.05; CJ.>95%).

pink = no support for SEM,

red = there was a significant opposite result found to SEM.

When evaluating the RR intervals (i.e., instantaneous heart rate, see Malik (1996) for the trust condition. There were no significant differences in the pre- or post-decision in the raw measures. When subtracting the baseline, both the pre- and post-decisions were significantly reduced; the same reduction was observed in the pre-decision measurement when dividing by the baseline. Adjusting for baseline in this instance significantly altered the RR intervals, but in the opposite direction of the SEM model (H1b).

Under conditions of distrust the reduction in the RR interval met the 80% threshold for the pre-decision measurement. The actual raw values were unchanged in both the pre- and post-decisions. When adjusting for the baseline (minus and dividing by the baseline), the RR interval was significantly altered in a direction supporting the SEM model. These findings indicate when an individual decides to distrust (at least when adjusting for baseline) the decision stimulated an increase in their heart rate (decreases in the RR interval).

Comparing the RR intervals changes between trust and distrust, there was a significant change in the RR interval in the pre-decision, but unchanged in the post-decision. When adjusting for baseline the significance pattern was reversed; the post-decision RR interval was significantly altered, whereas the pre-decision RR interval lacked significance.

3.9.1 Average ±S.E.

Figures 13–15 show average ±S.E. for RR intervals: raw signal, signal minus baseline, and signal divided by baseline plots respectively.

* = significant of the proposed SEM hypothesis

n.s. = not significant

N = the number of values per condition

Figure 13. Average ±S.E. for RR interval (raw signal).

* = significant of the proposed SEM hypothesis

n.s. = not significant

n.s.* = significant but in the opposite direction of the proposed SEM hypothesis

N = the number of values per condition

Figure 14. Average ±S.E. for RR interval (signal minus baseline).

Figure 15. Average ±S.E. for RR interval (signal divided by baseline).

Data shown in figures 13–15 are averages for baseline, pre-decision, and post-decision epochs, for trust and distrust interactions . The hypothesis addressed by specific parts of the plot are labeled as such.

3.9.2 Scatter Plots

Figures 16–18 show scatter plots for RR intervals: raw signal, signal minus baseline, and signal divided by baseline plots, respectively.
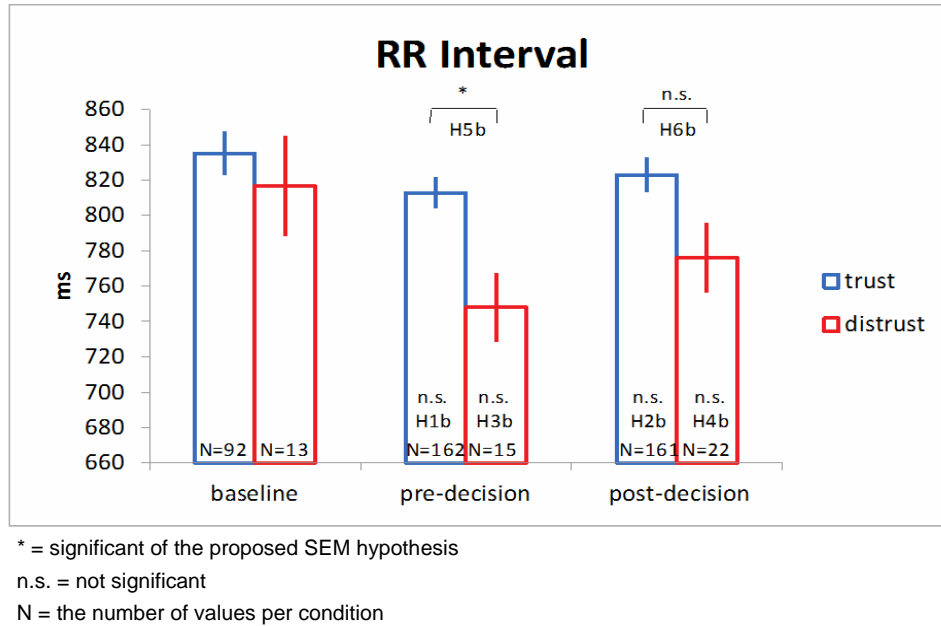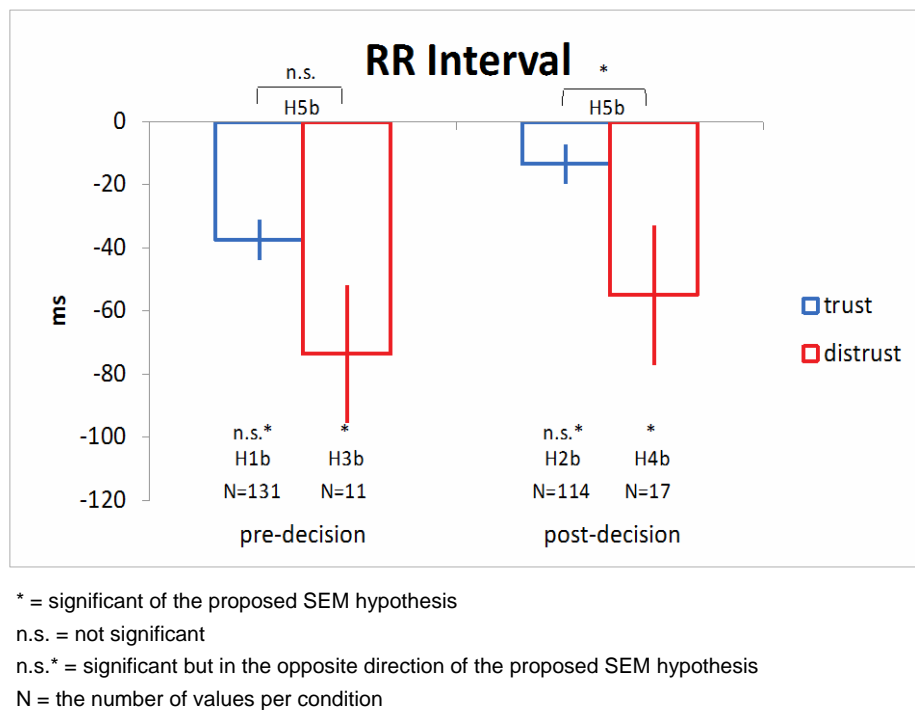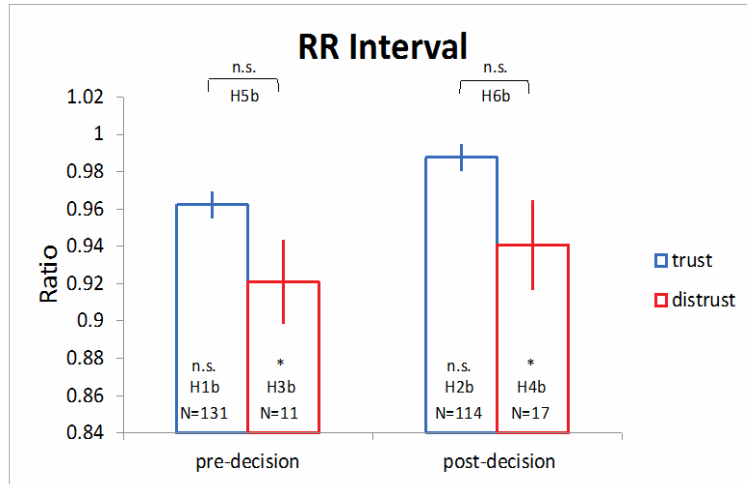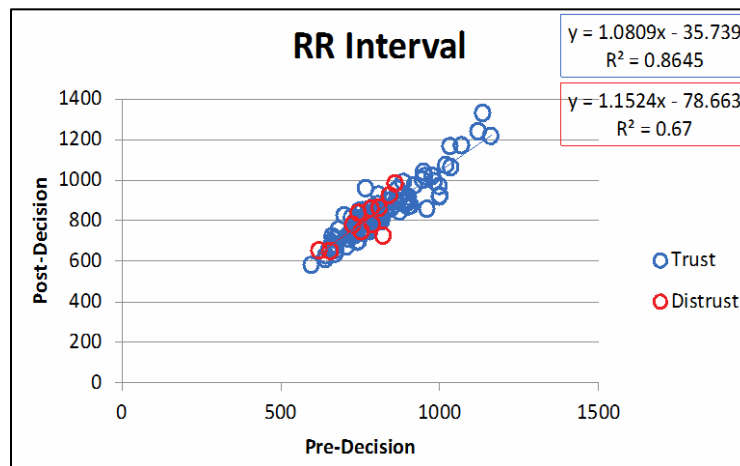

Figure 16. Scatter plot for RR interval (raw signal).

y = 0.6649x + 16.027
R² = 0.5623

y = 1.0305x + 49.726
R² = 0.5778

Values for pre-decision and post-decision epochs are displayed in the
x-axis and y-axis.

The equation and R2 value for the linear trendline is displayed for
trust and distrust interactions in blue and red box.

Figure 17. Scatter plot for RR interval (signal minus baseline).

y = 0.7415x + 0.28
R² = 0.5847

y = 1.1013x - 0.0366
R² = 0.5909

Values for pre-decision and post-decision epochs are displayed in the x-axis and
y-axis.

The equation and R2 value for the linear trendline is displayed for trust and distrust
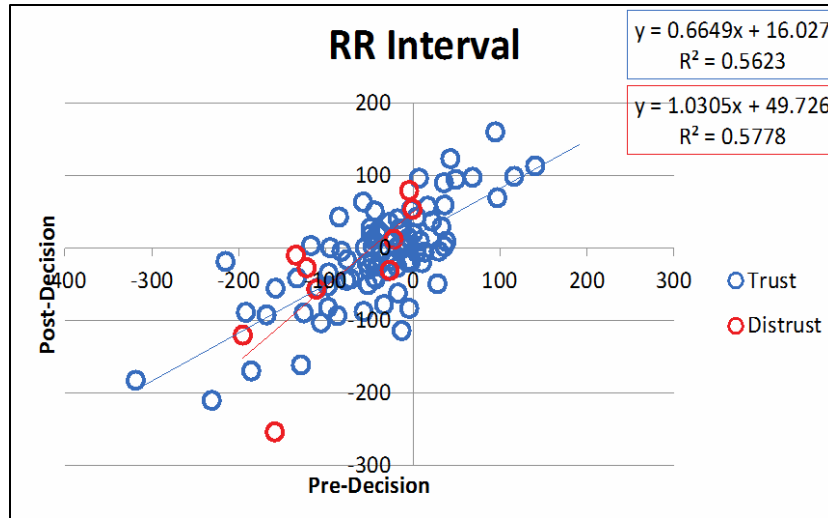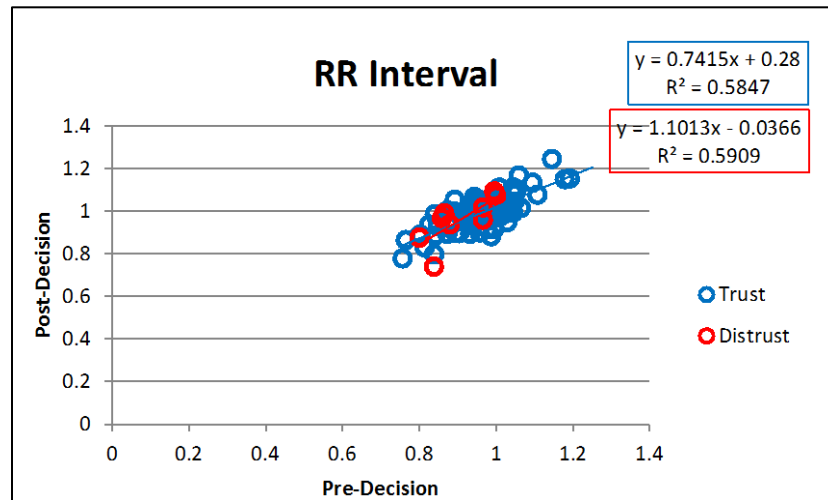interactions in blue and red box.

Figure 18. Scatter plot for RR interval (signal divided by baseline).

3.10 HIGH-FREQUENCY HRV POWER

Table 26 shows all hypotheses and their corresponding statistical tests for HF.

Table 26. High-frequency HRV statistical table.

Specific Hypothesis	Percentage of Decisions that Agree with the Hypothesis	Raw Signal Mean Difference (±SE); *p*-value	Signal Minus Baseline 95% Confidence Interval for Mean	Signal Divided by Baseline 95% Confidence Interval for Mean
H1c: High-frequency HRV increases TRUST: Baseline vs. Pre-decision	38% (51/133)	-0.357 ±0.430 p = 0.407; n.s.	[-0.165 1.202] n.s.	[1.335 4.007] *
H2c: High-frequency HRV increases TRUST: Baseline vs. Post-decision	51% (59/115)	-0.143 ±0.431 p = 0.740; n.s.	[-0.226 0.830] n.s.	[1.649 3.366] *
H3c: High-frequency HRV decreases DISTRUST: Baseline vs. Pre-decision	78% (7/9)	-0.153 ±1.280 p = 0.905; n.s.	[-2.249 1.265] n.s.	[0.347 1.140] n.s.
H4c: High-frequency HRV decreases DISTRUST: Baseline vs. Post-decision	47% (8/17)	-0.095 ±1.173 p = 0.935; n.s.	[-0.526 0.950] n.s.	[0.760 2.356] n.s.
H5c: High-frequency HRV increases PRE-DECISION: Trust vs. Distrust		0.095 ±0.926 p = 0.919; n.s.	1.061 ±1.227 p = 0.388; n.s.	1.928 ±2.149 p = 0.370; n.s.
H6c: High-frequency HRV increases POST-DECISION: Trust vs. Distrust		-0.062 ±0.772 p = 0.936; n.s.	0.090 ±0.926 p = 0.923; n .s.	0.950 ±1.621 p = 0.558; n.s.

 * = significant of the proposed SEM hypothesis
n.s. = not significant
dark blue areas = specific hypothesis trust conditions studied.
light green = the area studied supports SEM (p<0.05; CJ.>95%).
pink = no support for SEM,
red = there was a significant opposite result found to SEM.

There were no significant changes observed in any of the analyses for the HF power spectral density, with the exception of the trust decision when adjusting (dividing) by the baseline.

This change was noted as being in the direction predicted by the SEM (H1c, H2c). It is difficult to interpret experimental significance of a manipulated variable when the actual measurement was insignificant.

3.10.1 Average ±S.E.

Figures 19–21 show average ±S.E for HF power: raw signal, signal minus baseline, and signal divided by baseline. Data details averages for baseline, pre-decision, and post-decision epochs, for trust and distrust interactions.
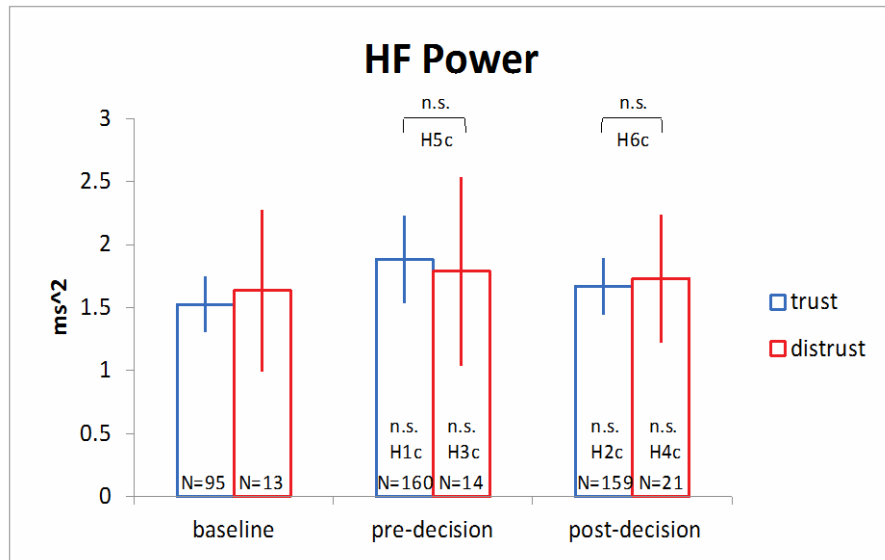
Figure 19. Average ±S.E. for HF power (raw signal).
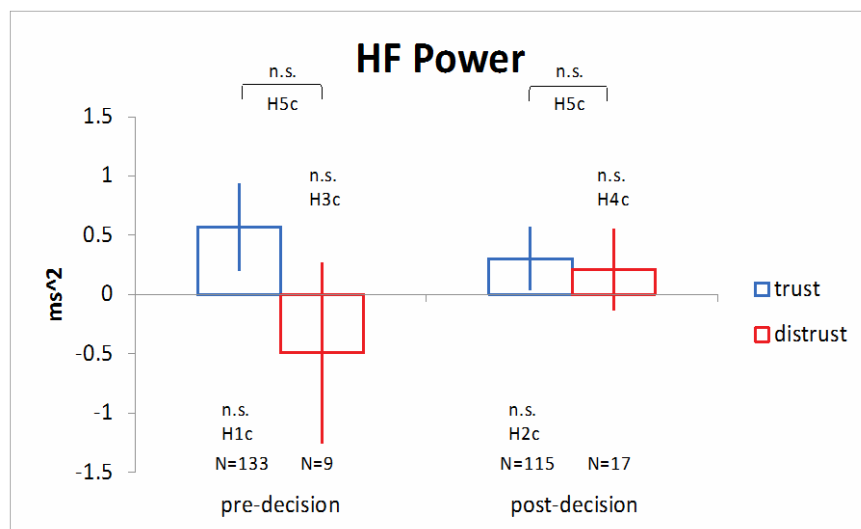
Figure 20. Average ±S.E. for HF power (signal minus baselne).
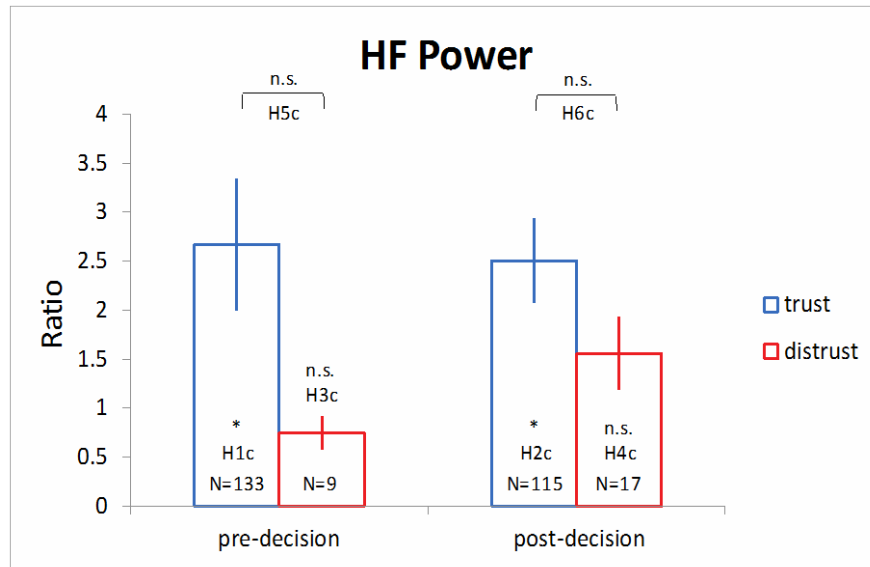
Figure 21. Average ±S.E. for HF power (signal divided by baselne).

* = significant of the proposed SEM hypothesis
n.s. = not significant
N = the number of values per condition

3.10.2 Scatter Plots

Figures 22–24 show scatter plots for HF power.for three areas: raw signal, signal minus baseline, and signal divided by baseline plots.
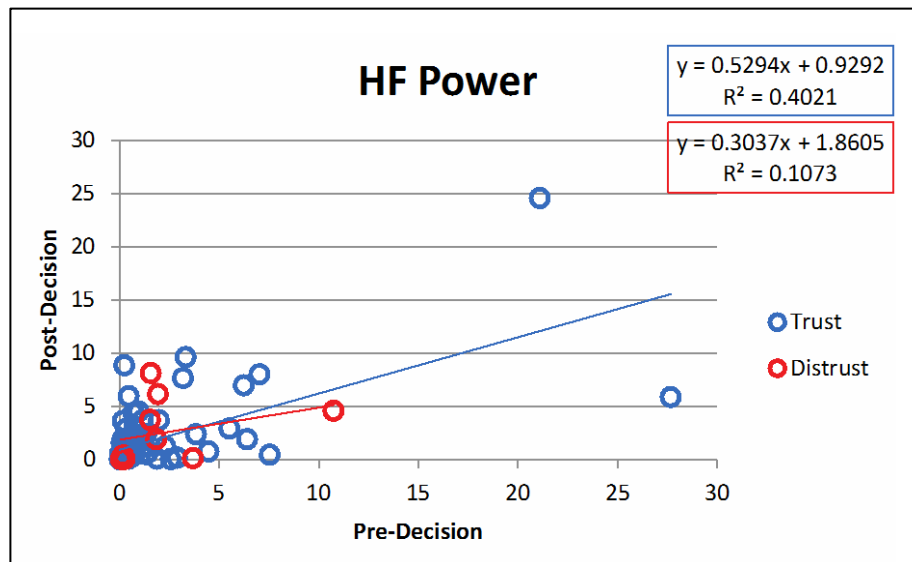
Values for pre-decision and post-decision epochs are displayed in the x-axis and y-axis.

The equation and R2 value for the linear trendline is displayed for trust and distrust interactions in blue and red box.

Figure 22. Scatter plot for HF power (raw signal).
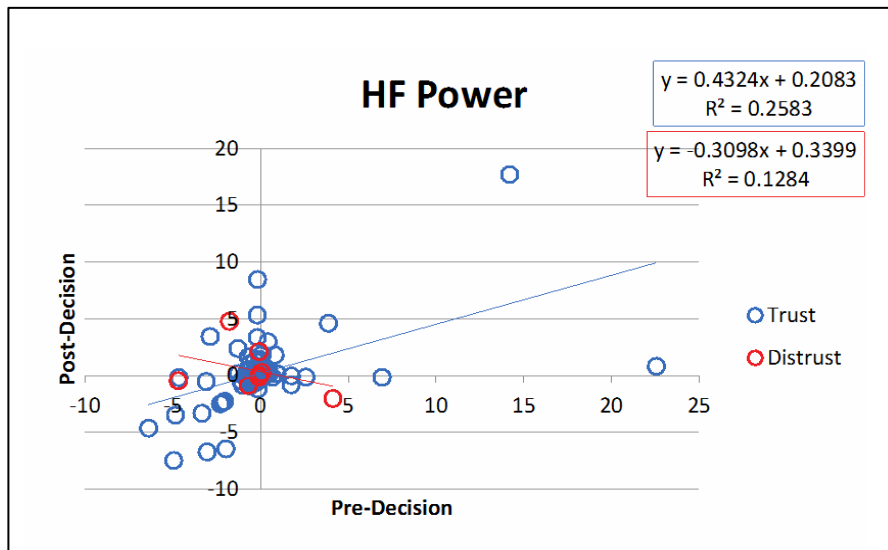
Values for pre-decision and post-decision epochs are displayed in the x-axis and y-axis.

The equation and R2 value for the linear trendline is displayed for trust and distrust interactions in blue and red box.

Figure 23. Scatter plot for HF power (signal minus baseline).
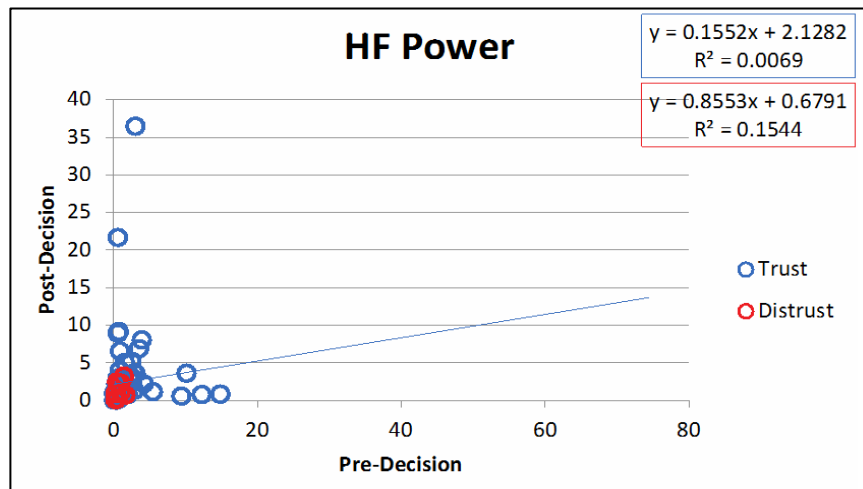
Values for pre-decision and post-decision epochs are displayed in the x-axis and y-axis.

The equation and R2 value for the linear trendline is displayed for trust and distrust interactions in blue and red box.

Figure 24. Scatter plot for HF power (signal divided by baseline).

3.11 NORMALIZED HIGH-FREQUENCY HRV POWER

Table 27 shows all hypotheses and their corresponding statistical tests for HFnorm.

Table 27. Normalized high-frequency HRV statistical table.

Specific Hypothesis	Percentage of Decisions that Agree with the Hypothesis	Raw Signal Mean Difference (±SE); p-value	Signal Minus Baseline 95% Confidence Interval for Mean	Signal Divided by Baseline 95% Confidence Interval for Mean
H1c: High-frequency HRV increases TRUST: Baseline vs. Pre-decision	33% (44/135)	0.102 ±0.025 p = 0.000; n.s.*	[-0.156 -0.074] n.s.*	[0.835 1.304] n.s.
H2c: High-frequency HRV increases TRUST: Baseline vs. Post-decision	42% (49/118)	0.041 ±0.025 p = 0.109; n.s.	[-0.108 -0.003] n.s.*	[1.114 1.984] *
H3c: High-frequency HRV decreases DISTRUST: Baseline vs. Pre-decision	64% (7/11)	0.117 ±0.074 p = 0.116; n.s.	[-0.258 0.113] n.s.	[-0.022 3.528] n.s.
H4c: High-frequency HRV decreases DISTRUST: Baseline vs. Post-decision	71% (12/17)	0.135 ±0.069 p = 0.050; *	[-0.199 -0.008] *	[0.461 1.615] n.s.
H5c: High-frequency HRV increases PRE-DECISION: Trust vs. Distrust		-0.035 ±0.053 p = 0.514; n.s.	-0.042 ±0.081 p = 0.605; n.s.	-0.684 ±0.599 p = 0.255; n.s.
H6c: High-frequency HRV increases POST-DECISION: Trust vs. Distrust		0.044 ±0.045 p = 0.320; n.s.	0.048 ±0.067 p = 0.480; n.s.	0.511 ±0.495 p = 0.304; n.s.

  * = significant of the proposed SEM hypothesis
n.s. = not significant
n.s.* = significant but in the opposite direction of the proposed SEM hypothesis.
dark blue areas = specific hypothesis trust conditions studied.
light green = the area studied supports SEM (p<0.05; CJ.>95%).
pink = no support for SEM,
red = there was a significant opposite result found to SEM.

Evaluation of the normalized HF HRV signal produced a different pattern of changes compared to raw HF. In the case of trust, there were significant differences in the pre-decision raw values as well as the adjusted (minus baseline) values (H1c). The post-decision for trust was also significantly different (H2c). The overall changes were contradictory to the SEM (Table 27). Note that dividing the raw normalized HF values by the baseline also produced a significant change in the post-decision trust measure. In this case, the change was consistent with the SEM (H2c). There were also significant differences noted in the post-decision normalized HF in the distrust measures in the raw data and in the minus baseline adjustment in the direction consistent with the SEM model.

In the main, the normalized data for the HF HRV signal seem to indicate that in the distrust condition HF is altered in a way that is consistent with the SEM (H4c), the HF alteration for trust on the other, are contradictory to the SEM (H1c, H2c). These changes in support of SEM when adjusting the data, make the results difficult to interpret.

3.11.1 Average ±S.E.

Figures 25–27 show average ±S.E. for HF normalized power: raw signal, signal minus baseline, and signal divided by baseline. Data details averages for baseline, pre-decision, and post-decision epochs, for trust and distrust interactions. The subhypothes is adressed by specific parts of the plot (see Figures 25–27) according to plot labels.
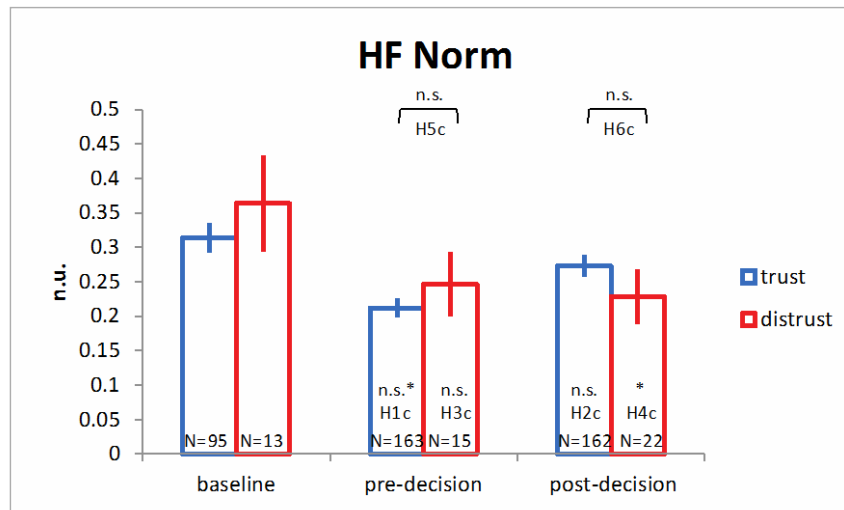

* = significant of the proposed SEM hypothesis
n.s. = not significant
n.s. * = significant but in the opposite direction of the proposed SEM hypothesis
N = the number of values per condition

Figure 25. Average ±S.E. for normalized HF power (raw signal).
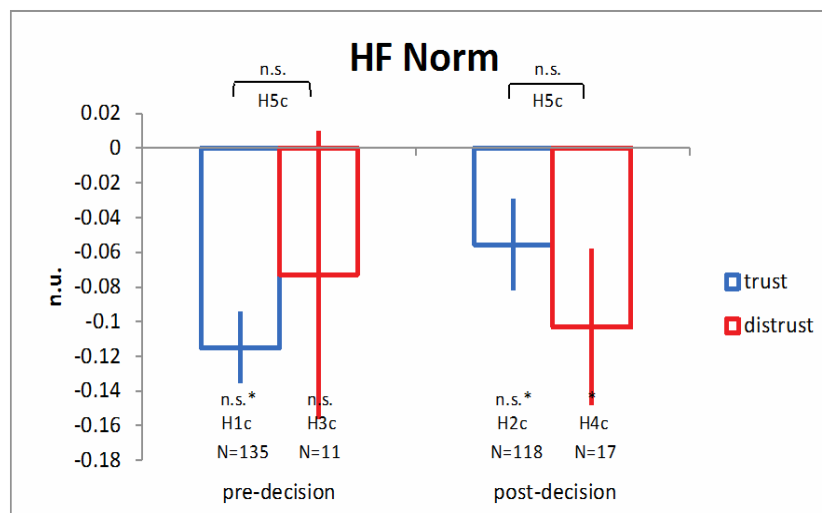
* = significant of the proposed SEM hypothesis
n.s. = not significant
n.s. * = significant but in the opposite direction of the proposed SEM hypothesis
N = the number of values per condition

Figure 26. Average ±S.E. for normalized HF power (signal minus baseline).
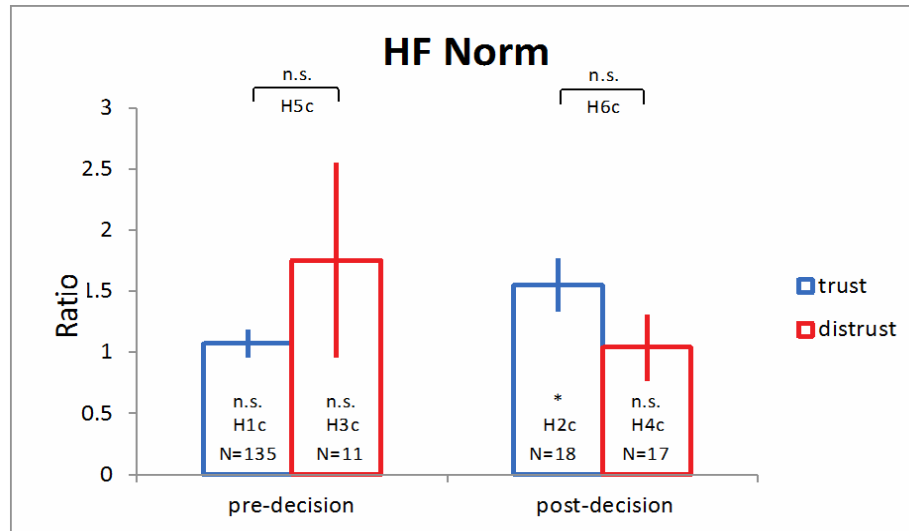
Figure 27. Average ±S.E. for normalized HF power (signal divided by baseline).

3.11.2 Scatter Plots

Figures 28–30 show scatter plots for normalized HF power: raw signal, signal minus baseline, and signal divided by baseline plots. Values for pre-decision and post-decision epochs are displayed in the x-axis and y-axis. The equation and R^2 value for the linear trendline is displayed for trust and distrust interactions in blue and red box.
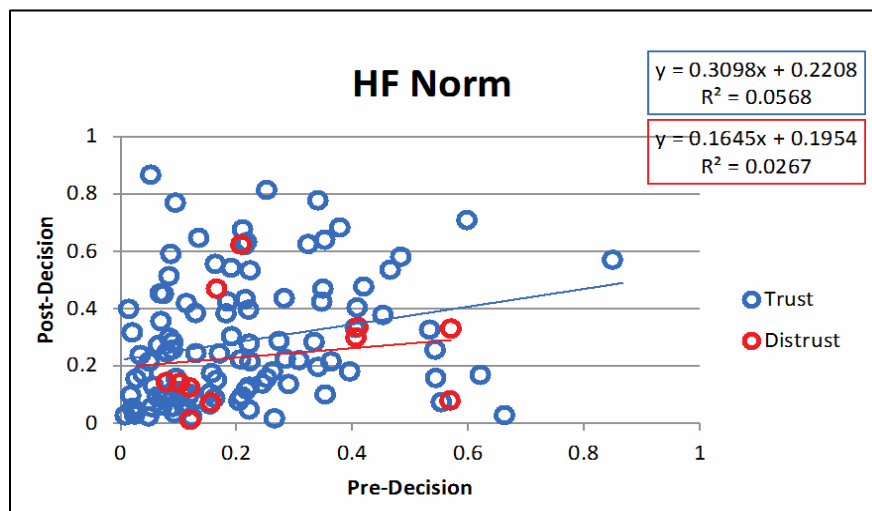
Values for pre-decision and post-decision epochs are displayed in the x-axis and y-axis.

The equation and R2 value for the linear trendline is displayed for trust and distrust interactions in blue and red box.

Figure 28. Scatter plot for normalized HF power (raw signal).
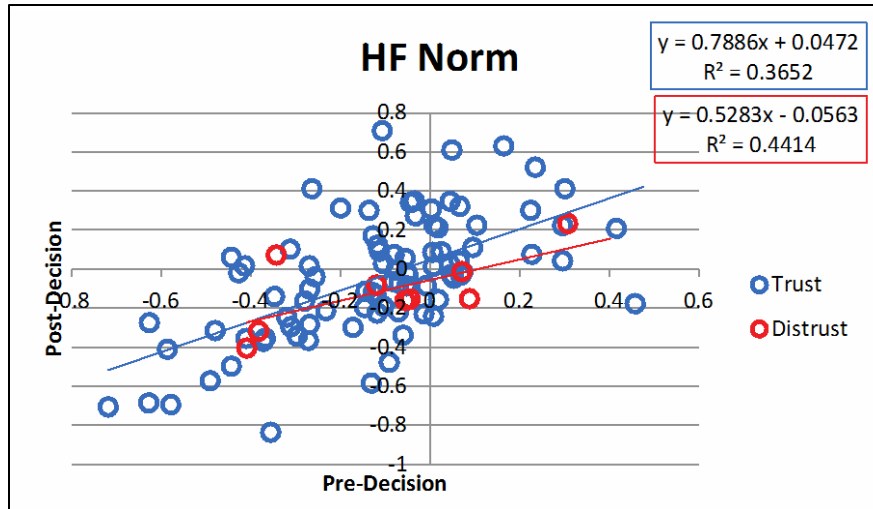
Values for pre-decision and post-decision epochs are displayed in the x-axis and y-axis.

The equation and R2 value for the linear trendline is displayed for trust and distrust interactions in blue and red box.

Figure 29. Scatter plot for normalized HF power (signal minus baseline).
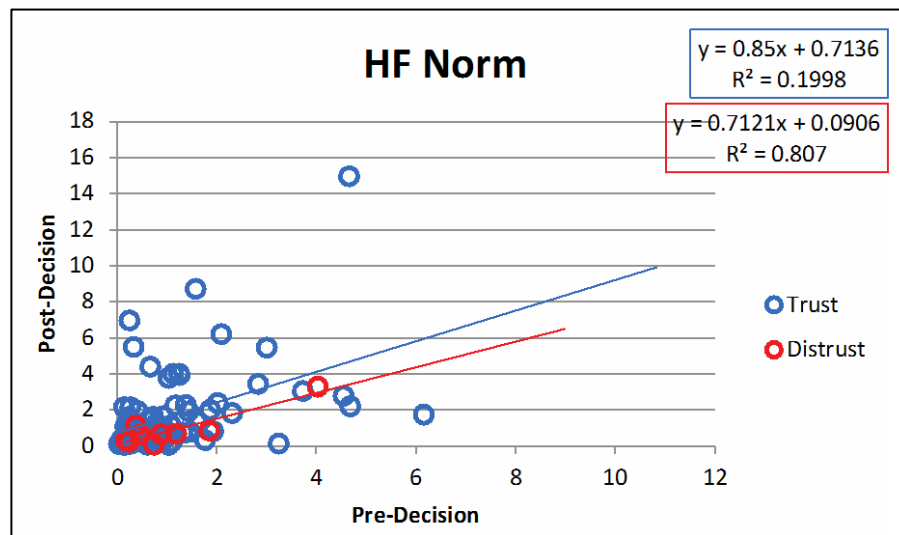
Values for pre-decision and post-decision epochs are displayed in the x-axis and y-axis.

The equation and R2 value for the linear trendline is displayed for trust and distrust interactions in blue and red box.

Figure 30. Scatter plot for normalized HF power (signal divided by baseline).

3.12 LOW-FREQUENCY HRV POWER

Table 28 shows all hypotheses and their corresponding statistical tests for LF.

Table 28. Low-frequency HRV statistical table.

| Specific Hypothesis	Percentage of Decisions that Agree with the Hypothesis	Raw Signal Mean Difference (±SE); p-value	Signal Minus Baseline 95% Confidence Interval for Mean	Signal Divided by Baseline 95% Confidence Interval for Mean
H1d: Low-frequency HRV decreases TRUST: Baseline vs. Pre-decision	33% (44/135)	-1.552 ±0.680, p = 0.023; n.s.*	[0.421 2.629] n.s.*	[2.754 4.517] n.s.*
H2d: Low-frequency HRV decreases TRUST: Baseline vs. Post-decision	39% (45/114)	-0.855 ±0.681 p = 0.210; n.s.	[-0.233 1.802] n.s.	[2.300 5.169] n.s.*
H3d: Low-frequency HRV increases DISTRUST: Baseline vs. Pre-decision	73% (8/11)	-2.901 ±2.008 p = 0.149; n.s.	[-0.538 6.779] n.s.	[0.928 3.824] n.s.
H4d: Low-frequency HRV increases DISTRUST: Baseline vs. Post-decision	82% (14/17)	-4.885 ±1.839 p = 0.008; *	[-0.319 8.682] n.s.	[0.908 5.387] n.s.
H5d: Low-frequency HRV decreases PRE-DECISION: Trust vs. Distrust		0.542 ±1.453 p = 0.709; n.s.	-1.595 ±1.946 p = 0.413; n.s.	1.259 ±1.961 p = 0.521; n.s.
H6d: Low-frequency HRV decreases POST-DECISION: Trust vs. Distrust		-3.222 ±1.211 p = 0.008; *	-3.408 ±1.612 p = 0.659; n.s.	0.587 ±1.624 p = 0.718; n.s.

 * = significant of the proposed SEM hypothesis

n.s. = not significant

n.s.* = significant but in the opposite direction of the proposed SEM hypothesis.

dark blue areas = specific hypothesis trust conditions studied.

light green = the area studied supports SEM (p<0.05; CJ.>95%).

pink = no support for SEM,

red = there was a significant opposite result found to SEM.

Analyses of the low-frequency (LF) component of the HRV signal produced significant changes in the raw values and the adjusted values in the baseline vs. pre-decision trust condition (H1d). The post-decision values for trust was also significantly increased (H2d). Both of these changes were opposite to the postulated changes of the SEM. In the distrust circumstances, there were significant changes in the binary data (80% threshold) and in the raw data values (H4d) as well as the direct comparison of the trust vs. distrust changes (H6d). In the case of distrust, these alterations were in a direction consistent with the SEM prediction (H4d).

The results of the LF HRV signals indicate the SEM model predicts distrust base on the experimental SS paradigm and SEM predicts the opposite changes for trust. In other words, LF increases regardless of whether subjects trusted or distrusted. Consistent with SEM, comparisons between trust vs. distrust indicate that LF is greater during distrust for the post-decision epoch.

3.12.1 Average ±S.E.

Figures 31–33 show average ±S.E. for LF power: raw signal, signal minus baseline, and signal divided by baseline plots. Data details averages for baseline, pre-decision, and post-decision epochs, for trust and distrust interactions. The sub-hypothesis addressed by specific parts of the plots are labeled as such.
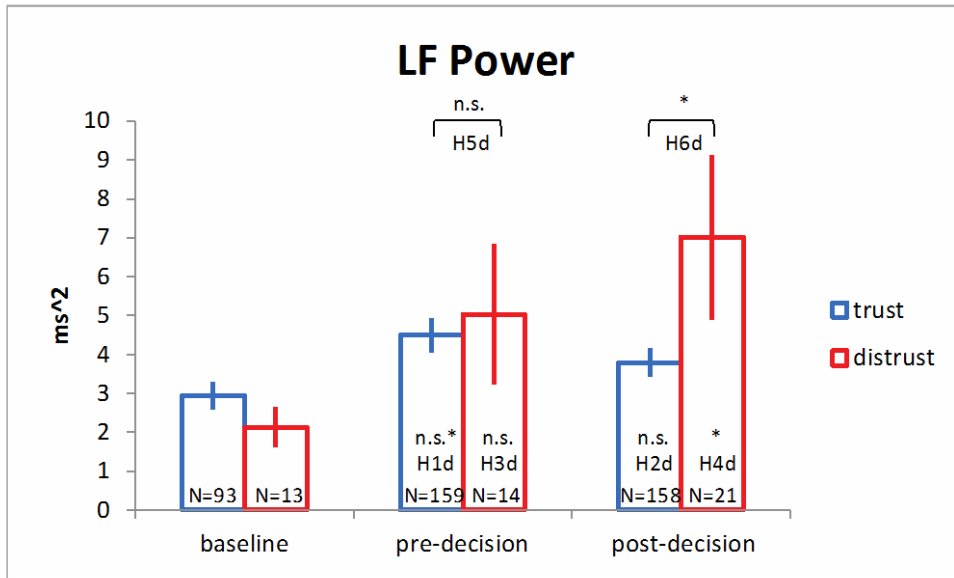
* = significant of the proposed SEM hypothesis

n.s. = not significant

n.s. * = significant but in the opposite direction of the proposed SEM hypothesis

N = the number of values per condition

Figure 31. Average ±S.E. for LF power (raw signal).
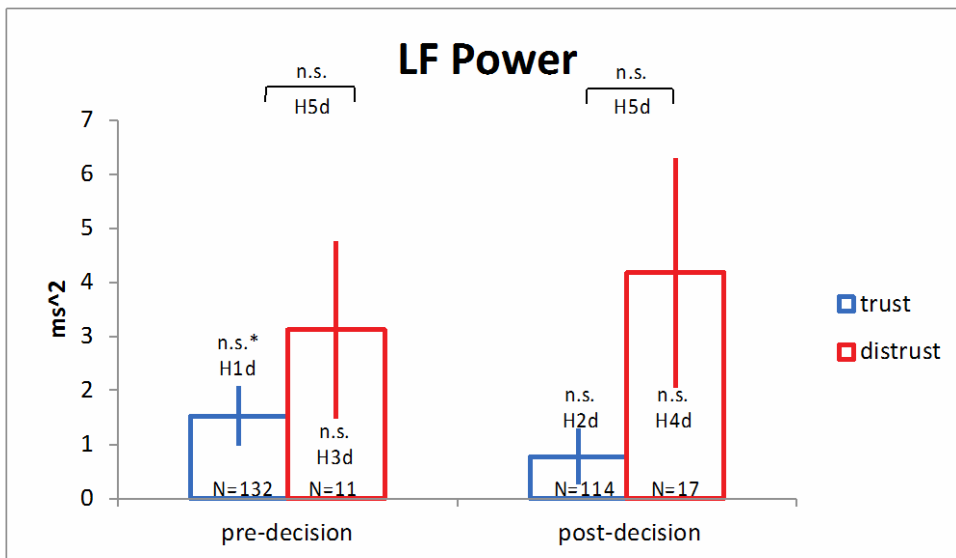
* = significant of the proposed SEM hypothesis

n.s. = not significant

n.s. * = significant but in the opposite direction of the proposed SEM hypothesis

N = the number of values per condition

Figure 32. Average ±S.E. for LF power (signal minus baseline).
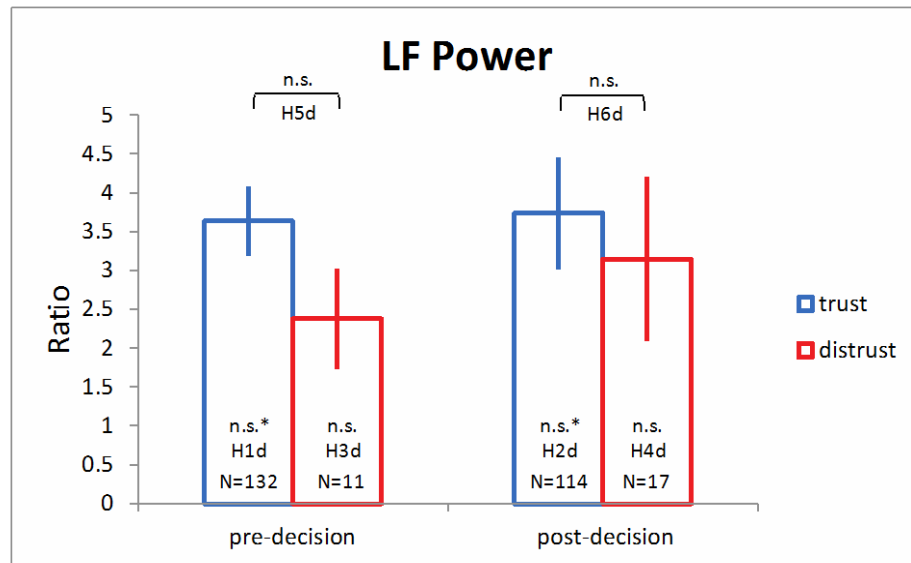
Figure 33. Average ±S.E. for LF power (signal divided by baseline).

* = significant of the proposed SEM hypothesis
n.s. = not significant
n.s. * = significant but in the opposite direction of the proposed SEM hypothesis
N = the number of values per condition

3.12.2 Scatter Plots

Figures 34–36 show scatter plots for LF power: raw signal, signal minus baseline, and signal divided by baseline plots.
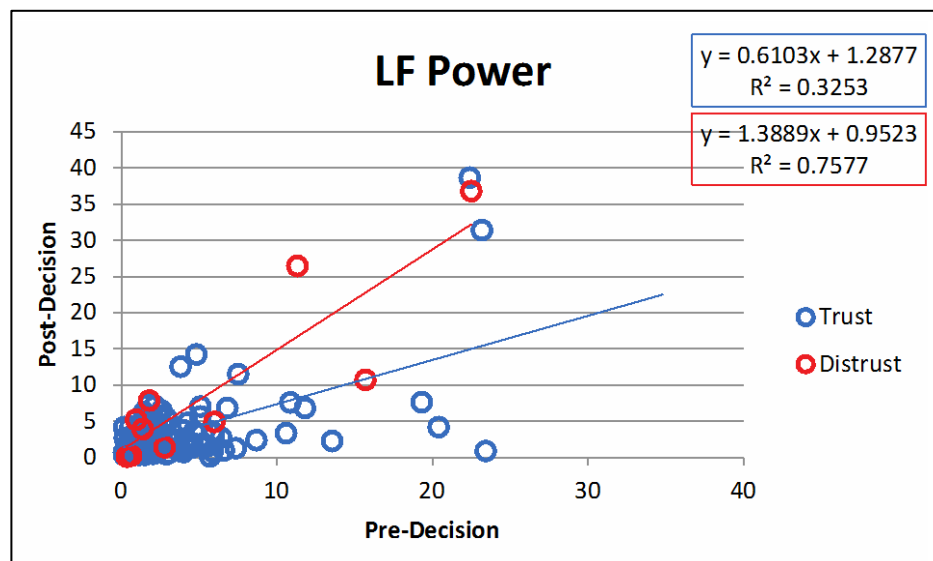
Values for pre-decision and post-decision epochs are displayed in the x-axis and y-axis.

The equation and R2 value for the linear trendline is displayed for trust and distrust interactions in blue and red box.

Figure 34. Scatter plot for LF power (raw signal).
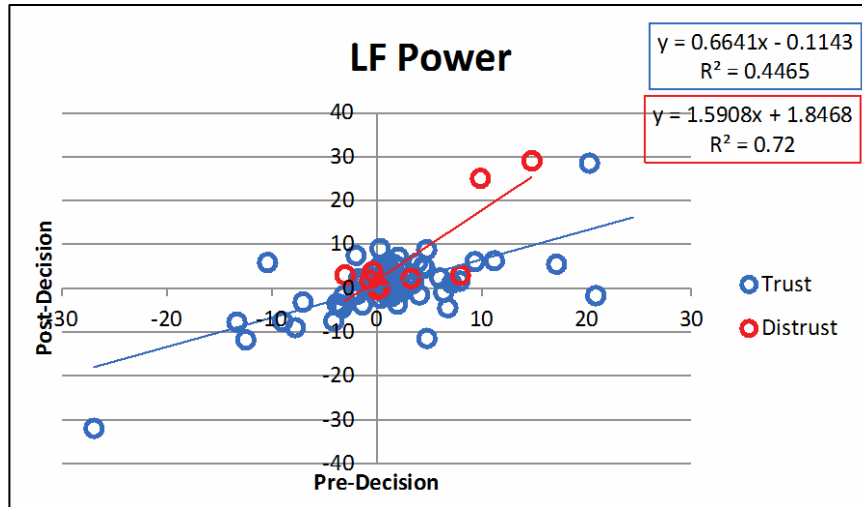
Values for pre-decision and post-decision epochs are displayed in the x-axis and y-axis.
The equation and R2 value for the linear trendline is displayed for trust and distrust
interactions in blue and red box.

Figure 35. Scatter plot for LF power (signal minus baseline).
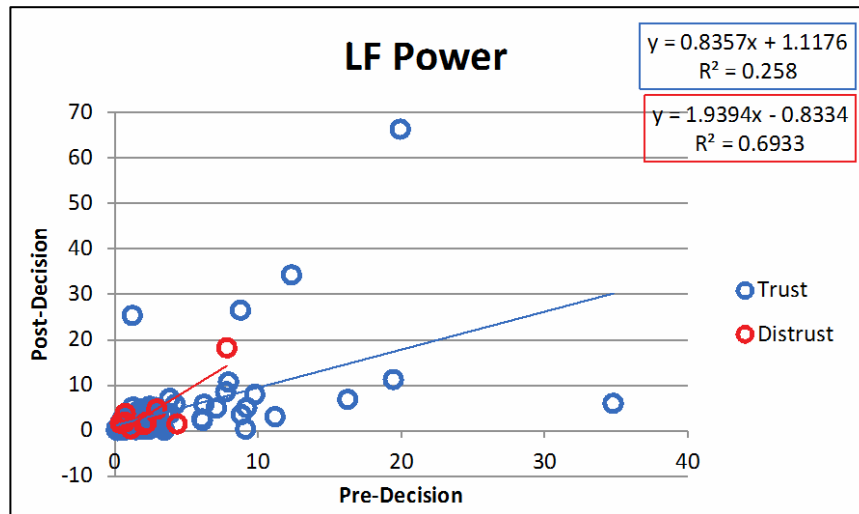
Values for pre-decision and post-decision epochs are displayed in the x-axis and y-axis.
The equation and R2 value for the linear trendline is displayed for trust and distrust
interactions in blue and red box.

Figure 36. Scatter plot for LF power (signal divided by baseline).

3.13 NORMALIZED LOW-FREQUENCY HRV POWER

Table 29 shows all hypotheses and their corresponding statistical tests for Lfnorm.

Table 29. Normalized low-frequency HRV statistical table.

| Specific Hypothesis	Percentage of Decisions that Agree with the Hypothesis	Raw Signal Mean Difference (±SE); p-value	Signal Minus Baseline 95% Confidence Interval for Mean	Signal Divided by Baseline 95% Confidence Interval for Mean
H1d: Low-frequency HRV decreases TRUST: Baseline vs. Pre-decision	33% (44/132)	-0.102 ±0.025 p = 0.000; n.s.*	[0.0741 0.156] n.s.*	[1.249 1.539] n.s.*
H2d: Low-frequency HRV decreases TRUST: Baseline vs. Post-decision	42% (49/118)	-0.041 ±0.025 p = 0.109; n.s.	[0.003 0.108] n.s.*	[1.128 1.543] n.s.*
H3d: Low-frequency HRV increases DISTRUST: Baseline vs. Pre-decision	64% (7/11)	-0.117 ±0.074 p = 0.116; n.s.	[-0.113 0.258] n.s.	[0.896 1.523] n.s.
H4d: Low-frequency HRV increases DISTRUST: Baseline vs. Post-decision	71% (12/17)	-0.135 ±0.069 p = 0.050; *	[0.057 0.118] *	[0.993 1.629] n.s.
H5d: Low-frequency HRV decreases PRE-DECISION: Trust vs. Distrust		0.035 ±0.053 p = 0.514; n.s.	0.042 ±0.081 p = 0.605; n.s.	0.184 ±0.302 p = 0.543; n.s.
H6d: Low-frequency HRV decreases POST-DECISION: Trust vs. Distrust		-0.044 ±0.44 p = 0.320; n.s.	-0.048 ±0.067 p = 0.480; n.s.	0.024 ±0.250 p = 0.923; n.s.

* = significant of the proposed SEM hypothesis
n.s. = not significant
n.s.*   = significant but in the opposite direction of the proposed SEM hypothesis.
dark blue areas   = specific hypothesis trust conditions studied.
light green = the area studied supports SEM (p<0.05; CJ.>95%).
pink = no support for SEM,
red = there was a significant opposite result found to SEM.

The normalized LF analyses produced results were similar to the raw LF HRV signals with three exceptions. The normalized LF signal for trust in the post-decision adjusted values (minus baseline) was significantly different (H2d). Again, the changes were in the opposite direction of the SEM. In a second instance, distrust in the post-decision for signal minus baseline was significant, in support of SEM. Lastly, LF normalized HRV values in the post-decision trust vs. distrust were insignificant.

Collectively, the LF HRV data is more indicative of distrust and bears no relation to SEM related to trust; the data appear to be contradicting the SEM for trust. The LF HRV signal presumably contains components of the sympathetic and parasympathetic nervous system (Malik, 1996).

3.13.1 Average ±S.E.

Figures 37–39 show average ±S.E. for LF normalized power: raw signal, signal minus baseline, and signal divided by baseline. Data details averages for baseline, pre-decision, and post-decision epochs, for trust and distrust interactions. The sub-hypothesis adressed by specific parts of the plot in figures 37–39 are labeled as such.
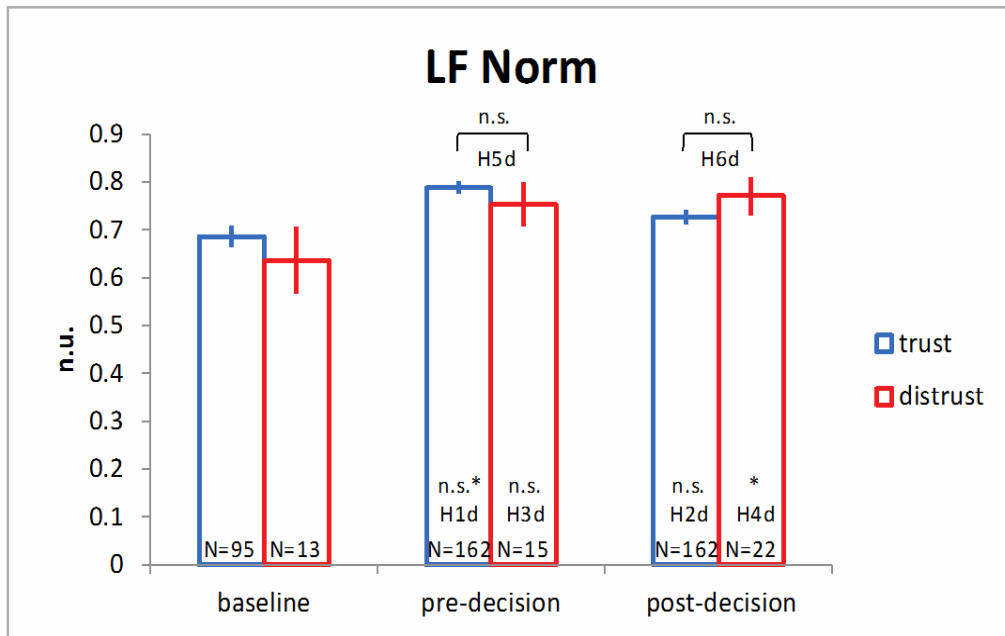
* = significant of the proposed SEM hypothesis

n.s. = not significant

n.s. * = significant but in the opposite direction of the proposed SEM hypothesis

N = the number of values per condition

Figure 37. Average ±S.E. for normalized LF power (raw signal).
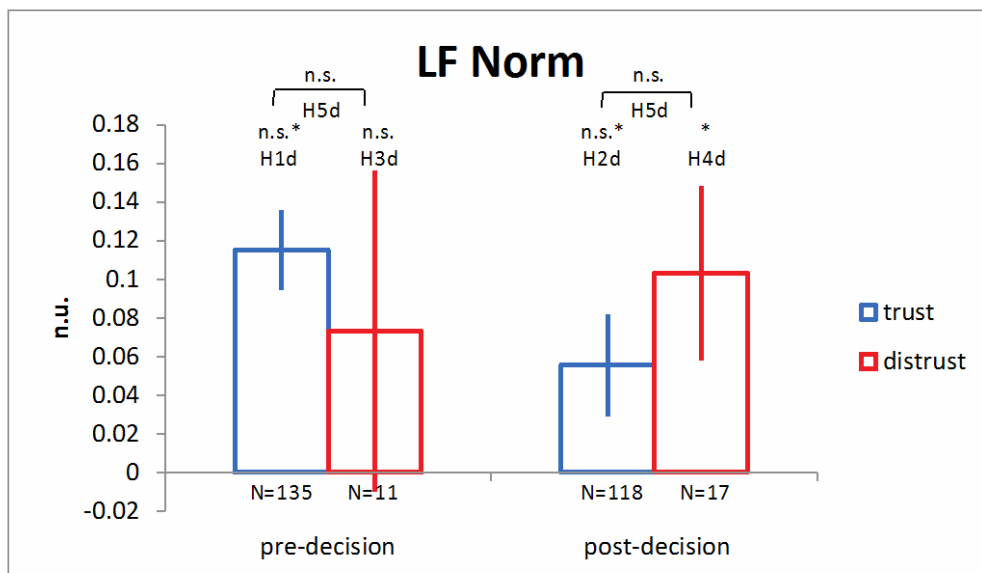
* = significant of the proposed SEM hypothesis

n.s. = not significant

n.s. * = significant but in the opposite direction of the proposed SEM hypothesis

N = the number of values per condition

Figure 38. Average ±S.E. for normalized LF power (signal minus baseline).

LF Norm

* = significant of the proposed SEM hypothesis

n.s. = not significant

n.s. * = significant but in the opposite direction of the proposed SEM hypothesis

N = the number of values per condition

Figure 39. Average ±S.E. for normalized LF power (signal divided by baseline).

3.13.2 Scatter Plots

Figures 40–42 shows scatter plot LF normalized power raw signals: raw signal, signal minus baseline, and signal divided by baseline plots. Values for pre-decision and post-decision epochs are displayed in the x-axis and y-axis. The equation and R^2 value for the linear trendline is displayed for trust and distrust interactions in blue and red box.
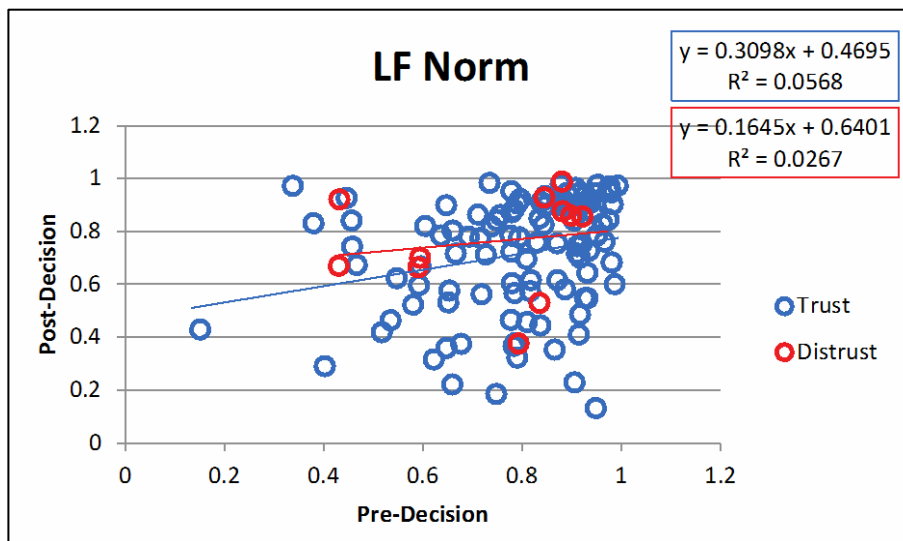
Values for pre-decision and post-decision epochs are displayed in the x-axis and y-axis.

The equation and R2 value for the linear trendline is displayed for trust and distrust interactions in blue and red box.

Figure 40. Scatter plot for normalized LF Power (raw signal).
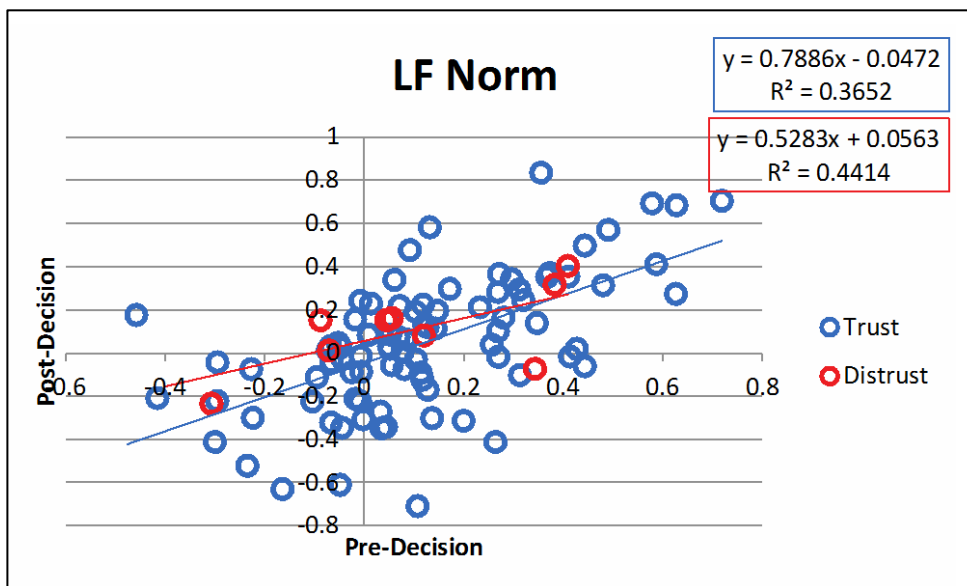
61

Values for pre-decision and post-decision epochs are displayed in the x-axis and y-axis.

The equation and R2 value for the linear trendline is displayed for trust and distrust interactions in blue and red box.

Figure 41. Scatter plot for normalized LF Power (signal minus baseline).
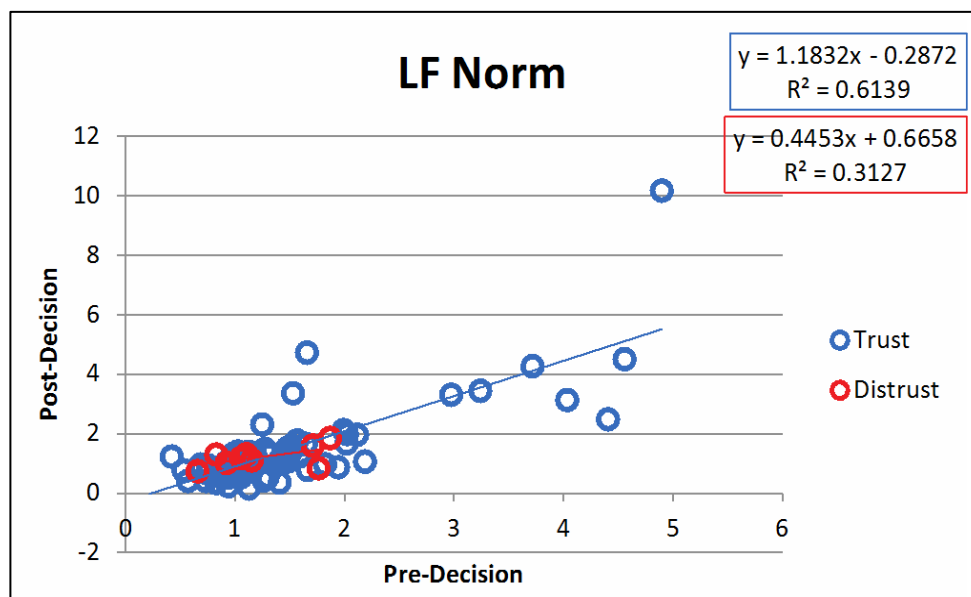
Values for pre-decision and post-decision epochs are displayed in the x-axis and y-axis.

The equation and R2 value for the linear trendline is displayed for trust and distrust interactions in blue and red box.

Figure 42. Scatter plot for normalized LF Power (signal divided by baseline).

3.14 SKIN CONDUCTANCE LEVELS

Table 30 shows all hypotheses and their corresponding statistical tests for SCL.

Table 30. Skin conductance levels statistical table.

Specific Hypothesis	Percentage of Decisions that Agree with the Hypothesis	Raw Signal Mean Difference [Baseline - Post Decision] (±SE); p-value	Signal Minus Baseline 95% Confidence Interval for Mean	Signal Divided by Baseline 95% Confidence Interval for Mean
H1e: Skin conductance level decreases TRUST: Baseline vs. Pre-decision	15% (37/258)	-1.337 ±0.413 p = 0.001; n.s.*	[1.038 1.391]; n.s.*	[1.316 1.452] n.s.*
H2e: Skin conductance level decreases TRUST: Baseline vs. Post-decision	17% (44/256)	-1.319 ±0.413 p = 0.001; n.s.*	[1.018 1.421] n.s.*	[1.332 1.484] n.s.*
H3e: Skin conductance level increases DISTRUST: Baseline vs. Pre-decision	88% (28/32)	-1.578 ±1.061 p = 0.137; n.s.	[1.335 3.141] *	[1.315 1.706] *
H4e: Skin conductance level increases DISTRUST: Baseline vs. Post-decision	87% (27/31)	-1.298 ±1.067 p = 0.224; n.s.	[1.200 3.050] *	[1.294 1.709] *
H5e: Skin conductance level decreases PRE-DECISION: Trust vs. Distrust		-0.756 ±0.696 p = 0.278; n.s.	-1.202 ±0.314 p = 0.001; *	-0.127 ±0.109 p = 0.248; n.s.
H6e: Skin conductance level decreases POST-DECISION: Trust vs. Distrust		-0.494 ±0.705 p = 0.484; n.s.	-0.905 ±0.318 p = 0.005; *	-0.093 ±0.111 p = 0.402; n.s.

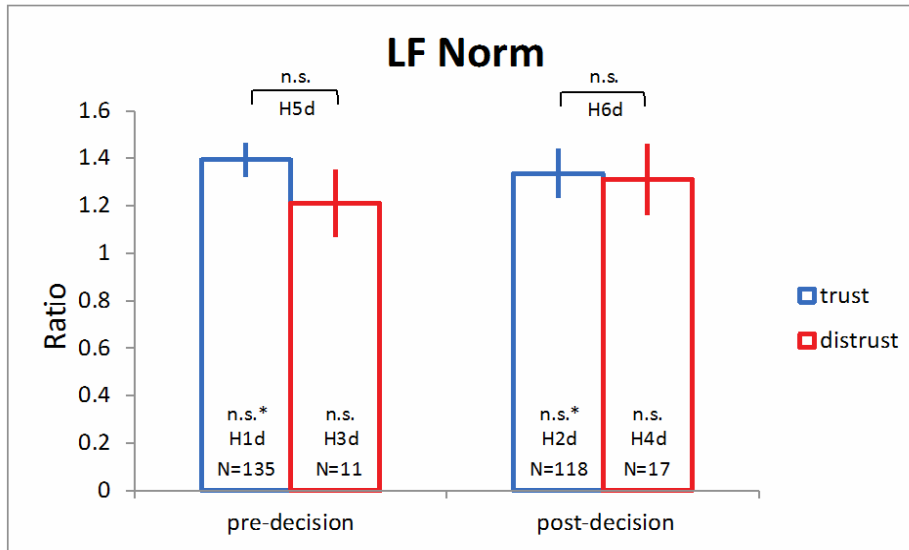 * = significant of the proposed SEM hypothesis

n.s. = not significant

n.s.* = significant but in the opposite direction of the proposed SEM hypothesis.

dark blue areas = specific hypothesis trust conditions studied.

light green = the area studied supports SEM (p<0.05; CJ.>95%).

pink = no support for SEM,

red = there was a significant opposite result found to SEM.

Skin conductance levels (SCL) were significantly different for both pre- and post-decision trust interactions (compared to baseline), but in the direction opposite to that predicted by SEM. There were significant differences in the pre- and post-decision distrust interactions that support the SEM (for binary aggregate and the normalized signals). In other words, SCL went up from baseline regardless of trust or distrust interactions. But importantly, when looking at the signal minus baseline method, a significant difference was present between trust and distrust. Specifically, subjects SCL was significantly higher when they distrusted their partners, which is consistent with SEM.

3.14.1 Average ±S.E.

Figures 43–45 show average ±S.E. for skin conductance levels: raw signal, signal minus baseline, and signal divided by baseline plots. Data details averages for baseline, pre-decision, and post-decision epochs, for trust and distrust interactions. The hypothesis addressed by specific parts of the plot are labeled as such.
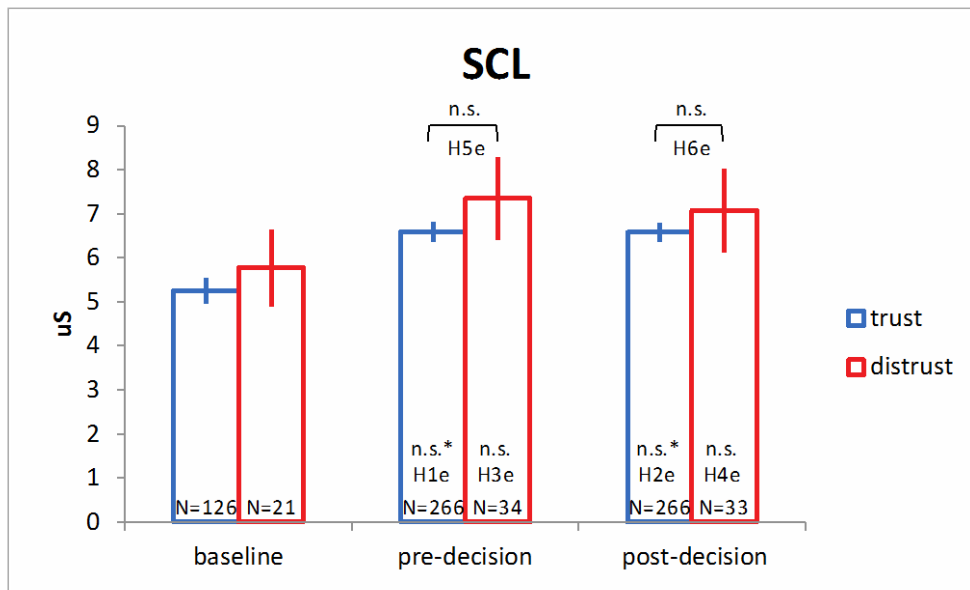
n.s. = not significant
n.s. * = significant but in the opposite direction of the proposed SEM hypothesis
N = the number of values per condition

Figure 43. Average ±S.E. for skin conductance level (raw signal).

* = significant of the proposed SEM hypothesis
n.s. * = significant but in the opposite direction of the proposed SEM hypothesis
N = the number of values per condition

Figure 44. Average ±S.E. for skin conductance level (signal minus baseline).

64

* = significant of the proposed SEM hypothesis

n.s. = not significant

n.s. * = significant but in the opposite direction of the proposed SEM hypothesis

N = the number of values per condition

Figure 45. Average ±S.E. for skin conductance level (signal divided by baseline).

3.14.2 Scatter Plots

Figures 46–48 shows scatter plot for skin conductance levels: raw signal, signal minus baseline, and signal divided by baseline plots.
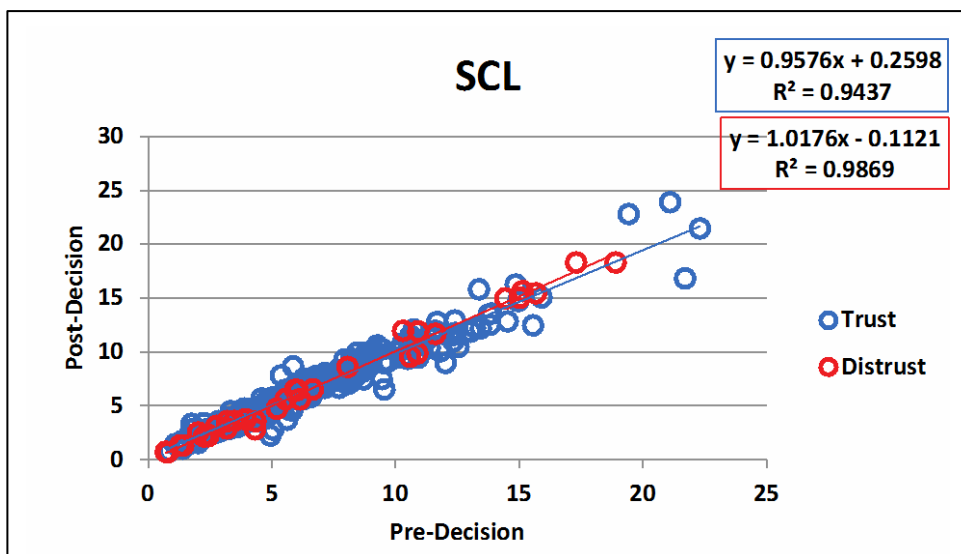
Values for pre-decision and post-decision epochs are displayed in the x-axis and y-axis.

The equation and R2 value for the linear trendline is displayed for trust and distrust interactions in blue and red box.

Figure 46. Scatter plot for skin conductance level (raw signal).
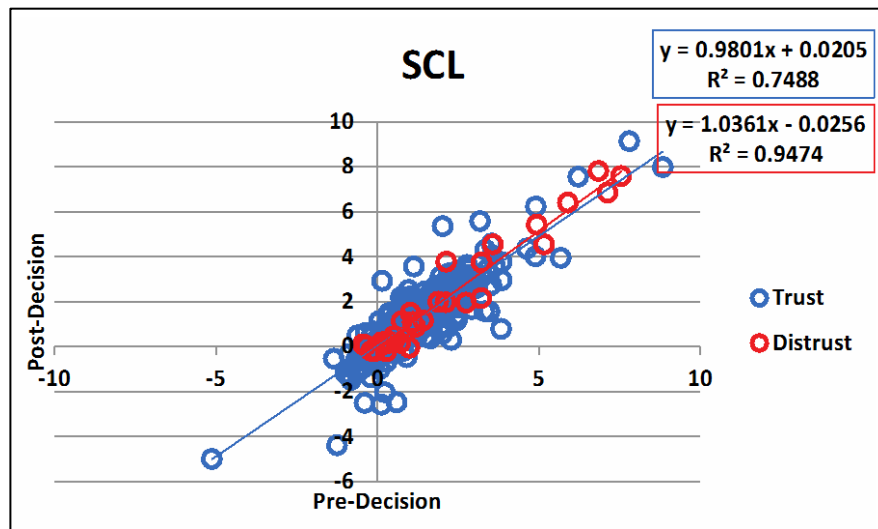
SCL

y = 0.9801x + 0.0205
R² = 0.7488

y = 1.0361x - 0.0256
R² = 0.9474

Values for pre-decision and post-decision epochs are displayed in the x-axis and y-axis.
The equation and R2 value for the linear trendline is displayed for trust and distrust interactions in blue and red box.

Figure 47. Scatter plot for skin conductance level (signal minus baseline).
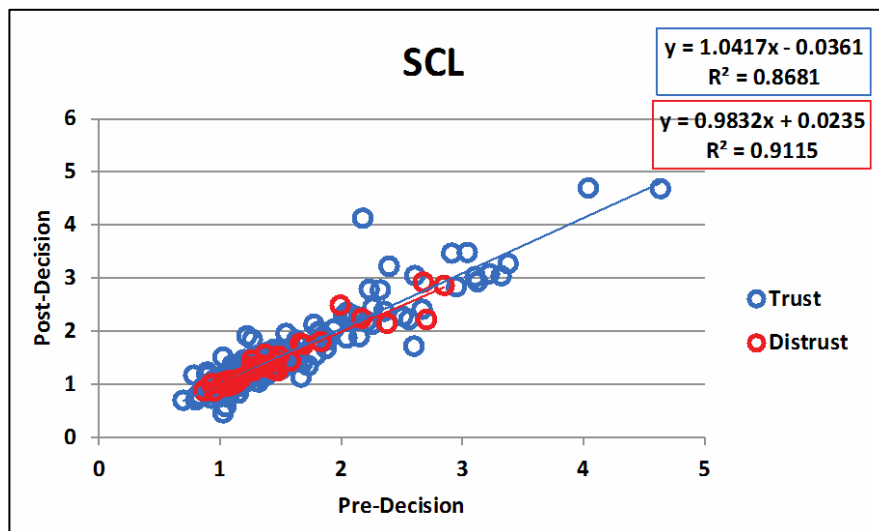
SCL

y = 1.0417x - 0.0361
R² = 0.8681

y = 0.9832x + 0.0235
R² = 0.9115

Values for pre-decision and post-decision epochs are displayed in the x-axis and y-axis.
The equation and R2 value for the linear trendline is displayed for trust and distrust interactions in blue and red box.

Figure 48. Scatter plot for skin conductance level (signal divided by baseline).

3.15 SKIN CONDUCTANCE RESPONSE

Table 31 shows all hypotheses and their corresponding statistical tests for SCR.

Table 31. Skin conductance response statistical table.

Specific Hypothesis	Percentage of Decisions that Agree with the Hypothesis	Raw Signal	Signal Minus Baseline	Signal Divided by Baseline
		Mean Difference (±SE); *p*-value	95% Confidence Interval for Mean	95% Confidence Interval for Mean
H1e: Skin conductance level decreases TRUST: Baseline vs. Pre-decision	31% (74/242)	-5.612 ±1.510 p = 0.000; n.s.*	[3.683 6.809]; n.s.*	[3.864 7.530] n.s.*
H2e: Skin conductance level decreases TRUST: Baseline vs. Post-decision	30% (73/241)	-6.223 ±1.508 p = 0.000; n.s.*	[3.491 7.093] n.s.*	[4.165 9.516] n.s.*
H3e: Skin conductance level increases DISTRUST: Baseline vs. Pre-decision	81% (22/27)	-1.432 ±4.098 p = 0.727; n.s.	[1.45 3 10.652], * *	[1.110 17.283] *
H4e: Skin conductance level increases DISTRUST: Baseline vs. Post-decision	85% (22/26)	-2.147 ±4.124 p = 0.603; n.s.	[2.121 11.784] *	[-0.542 24.951] n.s.
H5e: Skin conductance level decreases PRE-DECISION: Trust vs. Distrust		-0.057 ±2.65 p = 0.983; n.s.	-0.806 ±2.670 p = 0.763; n.s.	-3.500 ±3.865 p = 0.366; n.s.
H6e: Skin conductance level decreases POST-DECISION: Trust vs. Distrust		-0.160 ±2.692 p = 0.953; n.s.	-1.660 ±2.717 p = 0.541; n.s.	-5.364 ±3.912 p = 0.173; n.s.

* = significant of the proposed SEM hypothesis
n.s. = not significant
n.s.* = significant but in the opposite direction of the proposed SEM hypothesis.
dark blue areas   = specific hypothesis trust conditions studied.
light green = the area studied supports SEM (p<0.05; CJ.>95%).
pink = no support for SEM,
red = there was a significant opposite result found to SEM.

Skin Conductance Response (SCR) had similar results to SCL. Specifically, SCR was significantly different for both pre- and post-decision trust interactions (compared to baseline), but in the direction opposite to that predicted by SEM. Also, there were significant differences in the pre- and post-decision distrust interactions that support the SEM (for binary aggregate and the normalized signals). Therefore, like SCL, SCR went up from baseline regardless of trust or distrust interactions. Unlike SCL, no significant differences were present between trust and distrust. Therefore, subject SCL levels were not dependent on whether they trusted or distrusted their partners.

3.15.1 Average ±S.E.

Figures 49–51 show average ±S.E. for skin conductance reponse: raw signal, signal minus baseline, and signal divided by baseline plots. Data details averages for baseline, pre-decision, and post-decision epochs, for trust and distrust interactions. The hypothesis addressed by specific parts of the plot are labeled as such.
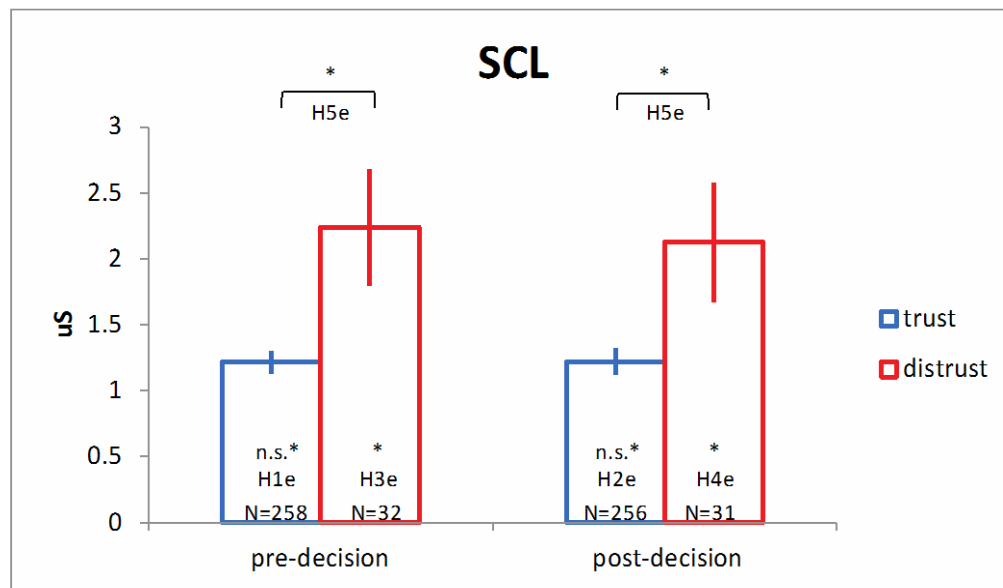
SCR
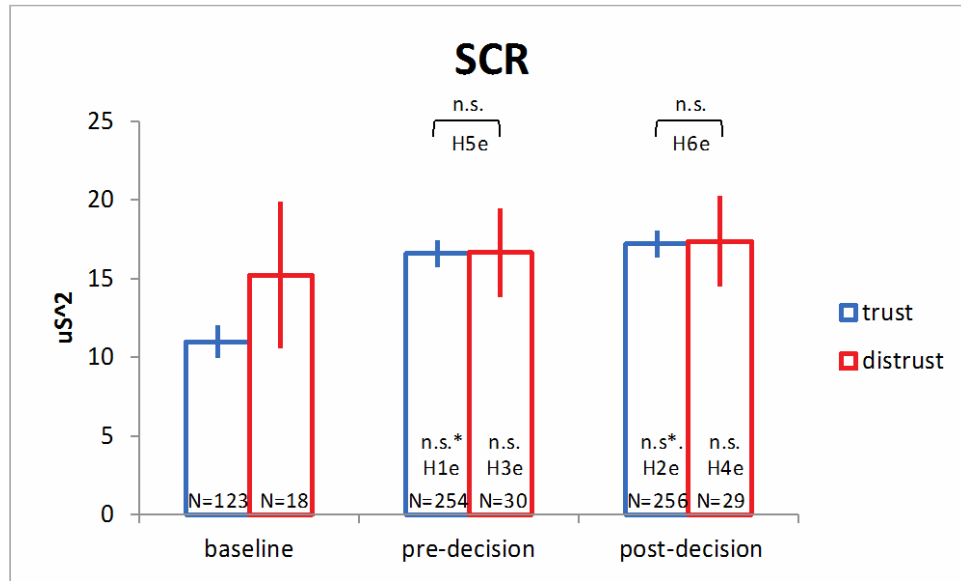
* = significant of the proposed SEM hypothesis

n.s. = not significant

n.s. * = significant but in the opposite direction of the proposed SEM hypothesis

N = the number of values per condition

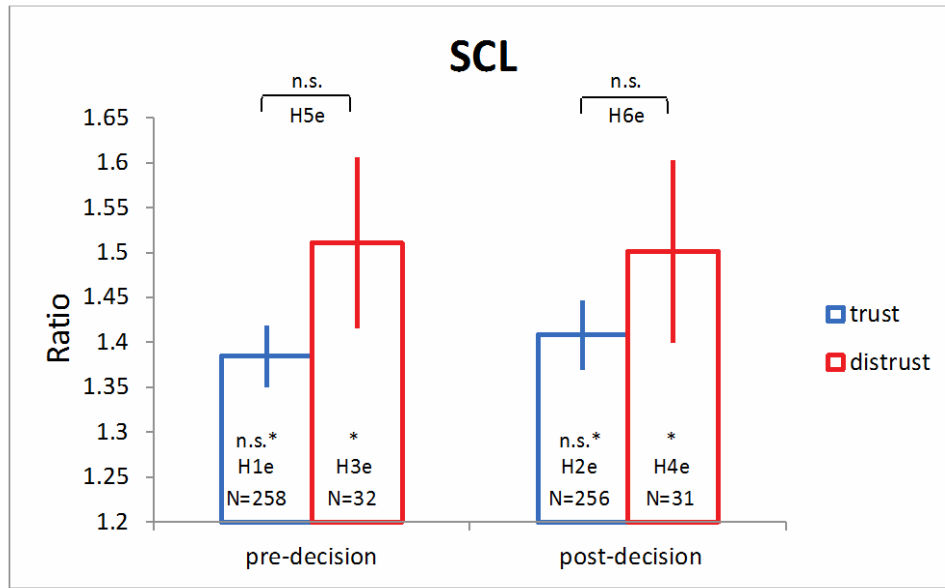Figure 49. Average ±S.E. for skin conductance reponse (raw signal).

SCR

* = significant of the proposed SEM hypothesis

n.s. = not significant

n.s. * = significant but in the opposite direction of the proposed SEM hypothesis

N = the number of values per condition

Figure 50. Average ±S.E. for skin conductance reponse (signal minus baseline).
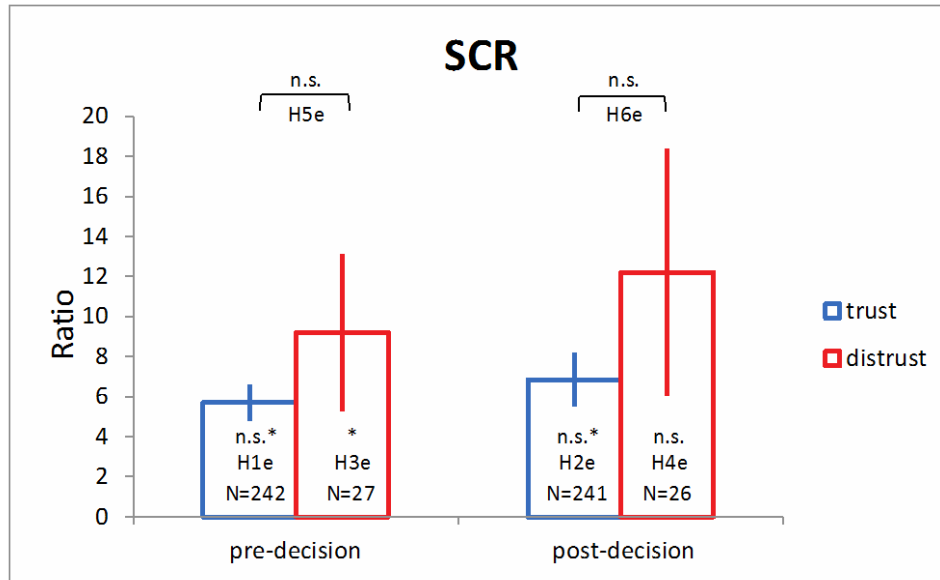
68

Figure 51. Average ±S.E. for skin conductance reponse (signal divided by baseline).

3.15.2 Scatter Plots

Figures 52–54 show scatter plots for skin conductance response: raw signal, signal minus baseline, and signal divided by baseline plots.
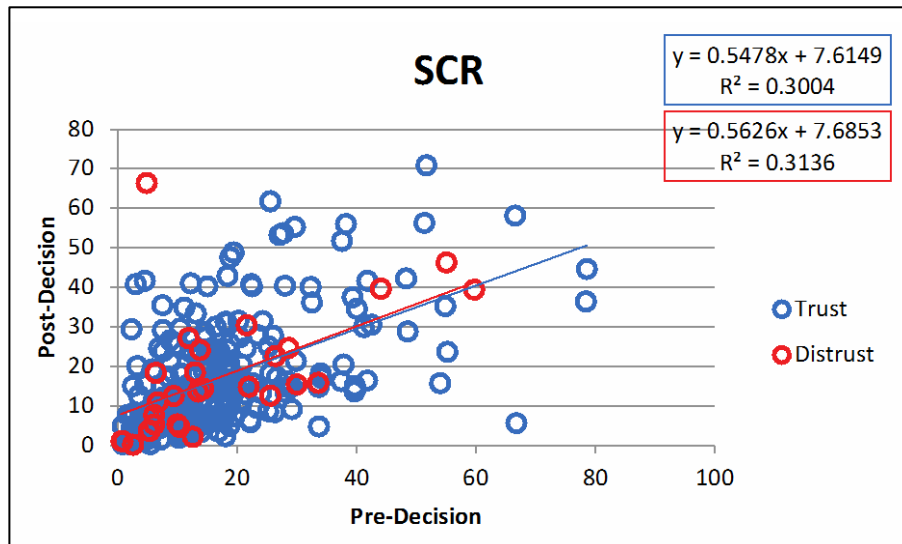
Values for pre-decision and post-decision epochs are displayed in the x-axis and y-axis.

The equation and R2 value for the linear trendline is displayed for trust and distrust interactions in blue and red box.

Figure 52. Scatter plot for skin conductance response (raw signal).
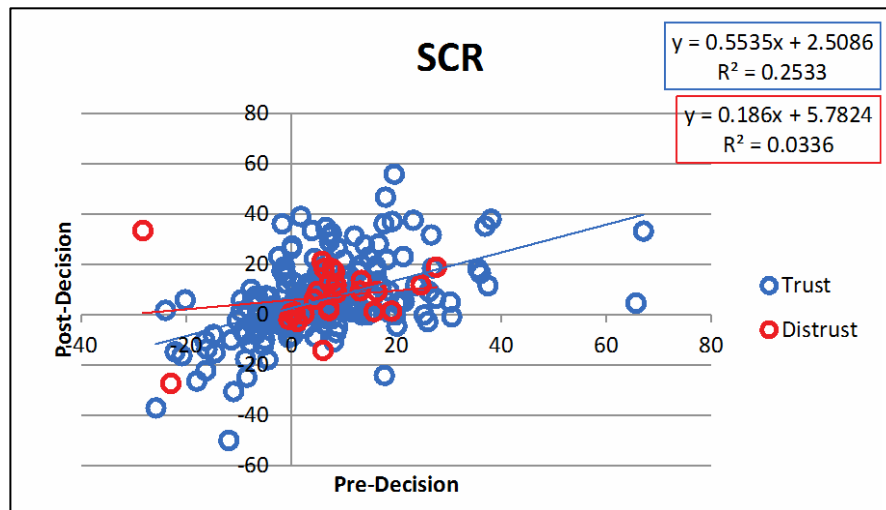
Values for pre-decision and post-decision epochs are displayed in the x-axis and y-axis.

The equation and R2 value for the linear trendline is displayed for trust and distrust interactions in blue and red box.

Figure 53. Scatter plot for skin conductance response (signal minus baseline).
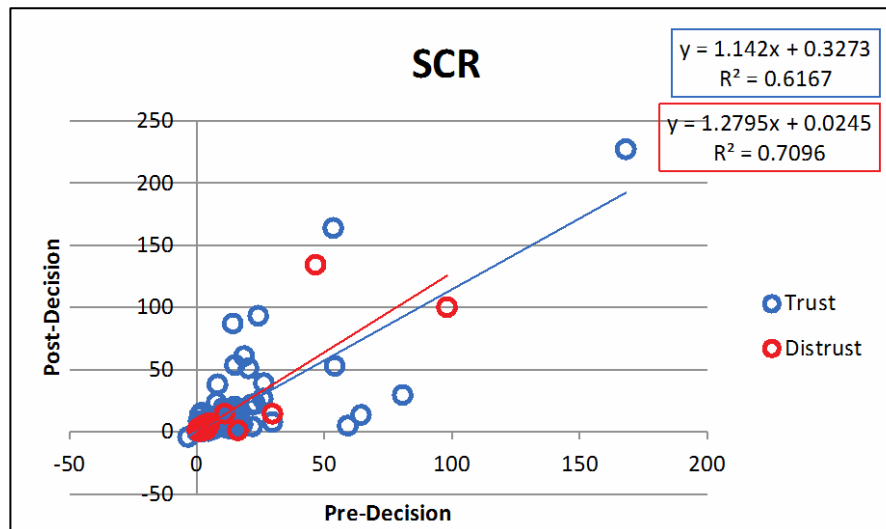
Values for pre-decision and post-decision epochs are displayed in the x-axis and y-axis.

The equation and R2 value for the linear trendline is displayed for trust and distrust interactions in blue and red box.

Figure 54. Scatter plot for skin conductance response (signal divided by baseline).

3.16 OXYTOCIN

Table 32 shows all hypotheses and their corresponding statistical tests for oxytocin.

Table 32. Oxytocin statistical table.

Specific Hypothesis	Percentage of Decisions that Agree with the Hypothesis	Raw Signal Mean Difference (±SE); *p*-value	Signal Minus Baseline 95% Confidence Interval for Mean	Signal Divided by Baseline 95% Confidence Interval for Mean
H1f: Oxytocin concentration increases TRUST: Baseline vs. Pre-decision	50% (106/211)	0.119 ±0.528 p = 0.821; n.s.	[-0.280 0.072] n.s.	[1.051 1.202] *
H2f: Oxytocin concentration increases TRUST: Baseline vs. Post-decision	53% (114/216)	-0.708 ±0.524 p = 0.177; n.s.	[-0.265 0.138] n.s.	[1.017 1.107] *
H3f: Oxytocin concentration decreases DISTRUST: Baseline vs. Pre-decision	56% (15/27)	0.172 ±1.357 p = 0.899; n.s.	[-0.372 0.686] n.s.	[0.866 1.108] n.s.
H4f: Oxytocin concentration decreases DISTRUST: Baseline vs. Post-decision	50% (14/28)	0.635 ±1.348 p = 0.638; n.s.	[-0.891 0.291] n.s.	[0.886 1.166] n.s.
H5f: Oxytocin concentration increases PRE-DECISION: Trust vs. Distrust		-0.296 ±0.911 p = 0.746; n.s.	-0.261 ±0.288 p = 0.365; n.s.	0.139 ±0.111 p = 0.212; n.s.
H6f: Oxytocin concentration increases POST-DECISION: Trust vs. Distrust		0.995 ±0.894 p = 0.266; n.s.	0.237 ±0.283 p = 0.403; n.s.	0.0674 ±0.110 p = 0.539; n.s.

* = significant of the proposed SEM hypothesis
n.s. = not significant
dark blue areas = specific hypothesis trust conditions studied.
light green = the area studied supports SEM (p<0.05; CJ.>95%).
pink = no support for SEM,
red = there was a significant opposite result found to SEM.

None of the raw values or signal minus baseline comparisons were statistically significant. When oxytocin was divided by the baseline, both the pre- and post-decision OT levels were significant for the trust interactions. The trust interactions were interpreted as being consistent with the SEM model (i.e., an increase in the OT with trust). It is difficult to rationalize this finding because neither of the direct comparisons between trust vs. distrust (H5f and H6f) were significant.

3.16.1 Average ±S.E

Figures 55–57 show average ±S.E. for oxytocin: raw signal, signal minus baseline, and signal divided by baseline plots. Data details averages for baseline, pre-decision, and post-decision epochs, for trust and distrust interactions. The hypothesis addressed by specific parts of the plot are labeled as such.
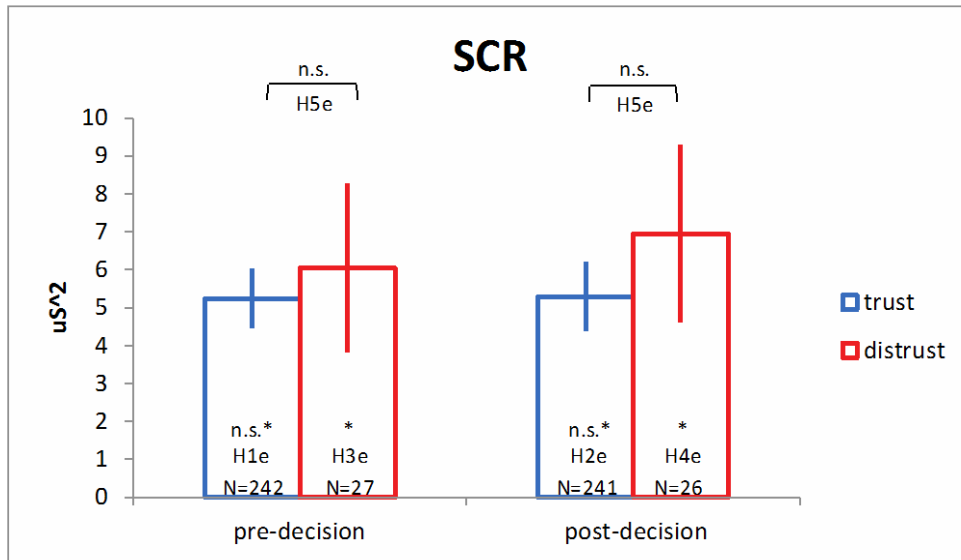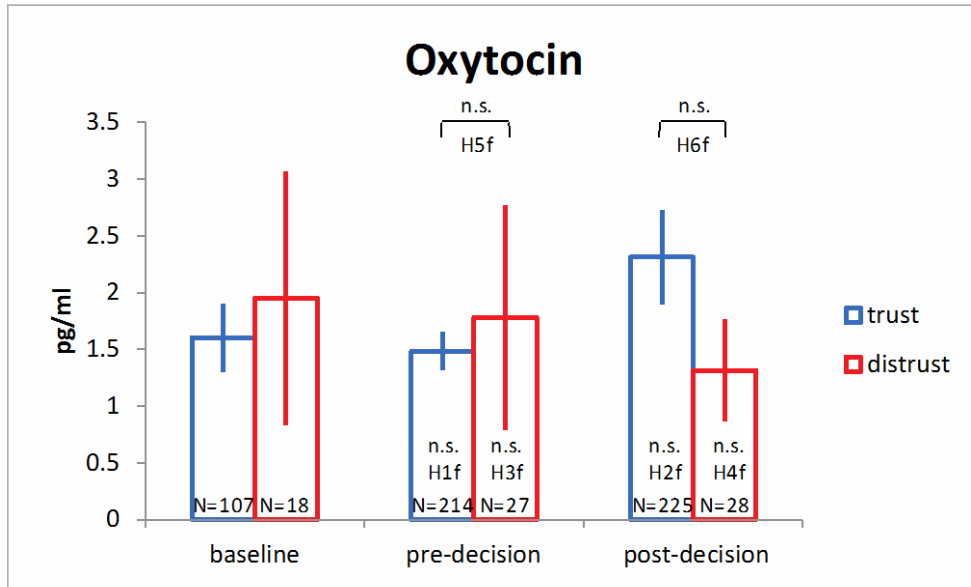
n.s. = not significant
N = the number of values per condition

Figure 55. Average ±S.E. for oxytocin (raw signal).

n.s. = not significant
N = the number of values per condition

Figure 56. Average ±S.E. for oxytocin (signal minus baseline).

Figure 57. Average ±S.E. for oxytocin (signal divided by baseline).

* = significant of the proposed SEM hypothesis

n.s. = not significant

N = the number of values per condition

3.16.2 Scatter Plots

Figures 58–60 show scatter plots for oxytocin: raw signal, signal minus baseline, and signal divided by baseline plots.
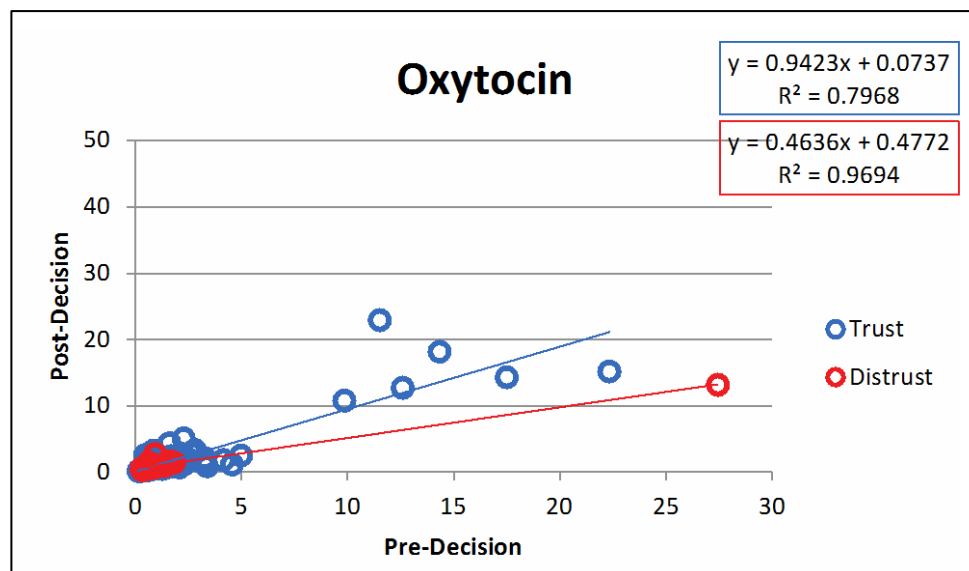
Values for pre-decision and post-decision epochs are displayed in the x-axis and y-axis.

The equation and R2 value for the linear trendline is displayed for trust and distrust interactions in blue and red box.

Figure 58. Scatter plot for oxytocin (raw signal).
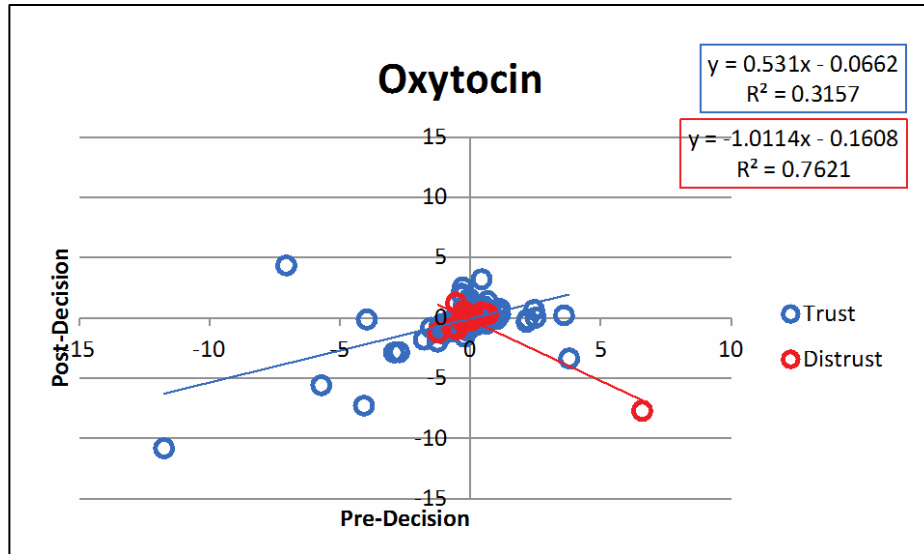
Values for pre-decision and post-decision epochs are displayed in the x-axis and y-axis.

The equation and R2 value for the linear trendline is displayed for trust and distrust interactions in blue and red box.

Figure 59. Scatter plot for oxytocin (signal minus baseline).
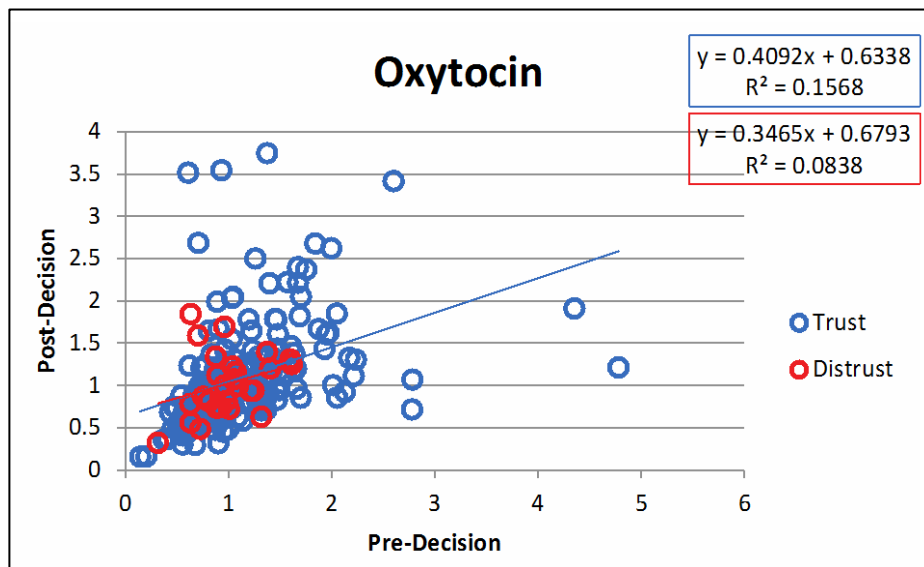
Values for pre-decision and post-decision epochs are displayed in the x-axis and y-axis.

The equation and R2 value for the linear trendline is displayed for trust and distrust interactions in blue and red box.

Figure 60. Scatter plot for oxytocin (signal divided by baseline).

74

3.17 CORTISOL

Table 33 shows all hypotheses and their corresponding statistical tests for cortisol.

Table 33. Cortisol statistical table.

Specific Hypothesis	Percentage of Decisions that Agree with the Hypothesis	Raw Signal — Mean Difference [Baseline - Post Decision] (±SE); p-value	Signal Minus Baseline — 95% Confidence Interval for Mean	Signal Divided by Baseline — 95% Confidence Interval for Mean
H1g: Cortisol concentration decreases TRUST: Baseline vs. Pre-decision	75% (171/227)	1.645 ±0.518 p = 0.002; *	[-1.864 -0.937] *	[0.856 0.962] *
H2g: Cortisol concentration decreases TRUST: Baseline vs. Post-decision	82% (187/227)	2.244 ±0.517 p = 0.000; *	[-2.526 -1.631] *	[0.799 0.903] *
H3g: Cortisol concentration increases DISTRUST: Baseline vs. Pre-decision	35% (9/26)	-0.138 ±1.387 p = 0.921; n.s.	[-2.552 0.232] n.s.	[0.809 1.204] n.s.
H4g: Cortisol concentration increases DISTRUST: Baseline vs. Post-decision	30% (8/27)	0.257 ±1.377 p = 0.852; n.s.	[-3.248 -0.332] n.s.*	[0.766 1.106] n.s.
H5g: Cortisol concentration decreases PRE-DECISION: Trust vs. Distrust		-0.733 ±0.936 p = 0.434; n.s.	-0.240 ±0.723 p = 0.740; n.s.	-0.098 ±0.085 p = 0.248; n.s.
H6g: Cortisol concentration decreases POST-DECISION: Trust vs. Distrust		-0.937 ±0.920 p = 0.309; n.s.	-0.288 ±0.711 p = 0.685; n .s.	-0.085 ±0.083 p = 0.309; n.s.

 * = significant of the proposed SEM hypothesis
n.s. = not significant
n.s.* = significant but in the opposite direction of the proposed SEM hypothesis.
dark blue areas = specific hypothesis trust conditions studied.
light green = the area studied supports SEM (p<0.05; CJ.>95%).
pink = no support for SEM,
red = there was a significant opposite result found to SEM.

The pre-decision and post-decision cortisol levels were significantly reduced when compared to the baseline during trust interactions for both the pre and post-decision epochs. This was true regardless of baseline adjustments. This finding is consistent with the predicted change for the SEM model indicating that cortisol would decrease with trust decisions. The significant change noted in hypothesis H4g is in the opposite direction of the SEM model and would argue against the interpretation above.
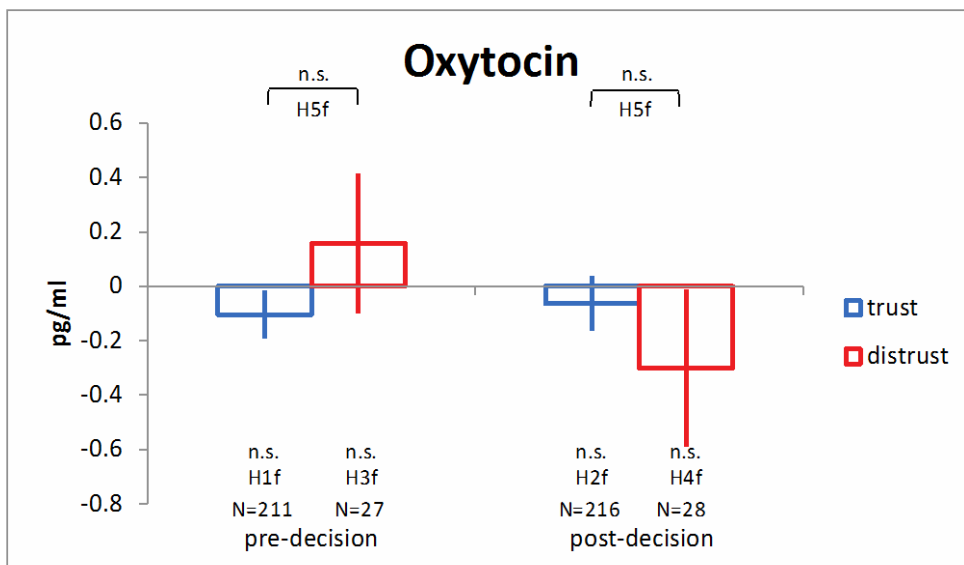
3.17.1 Average ±S.E.

Figures 61–63 show average ±S.E. for cortisol: raw signal, signal minus baseline, and signal divided by baseline plots. Data details averages for baseline, pre-decision, and post-decision epochs, for trust and distrust interactions. The hypothesis addressed by specific parts of the plot are labeled as such..
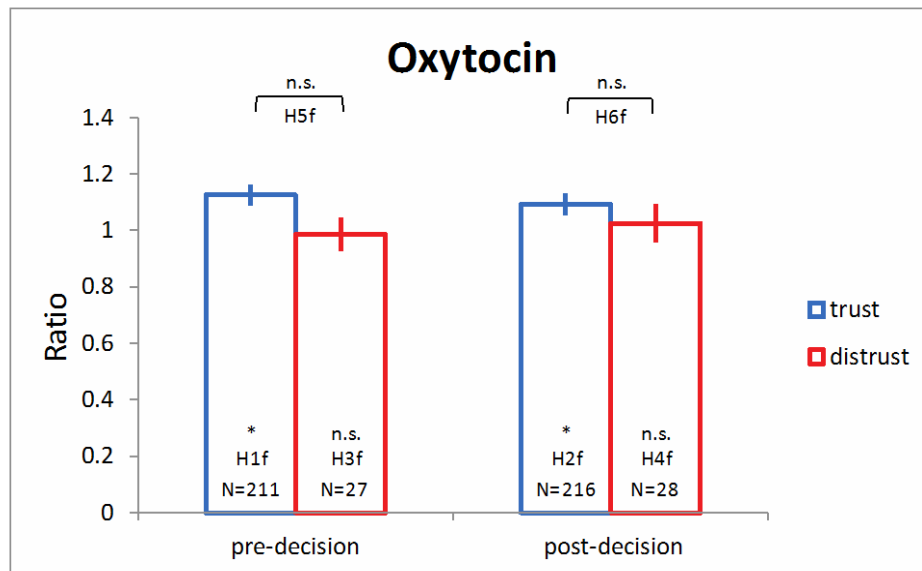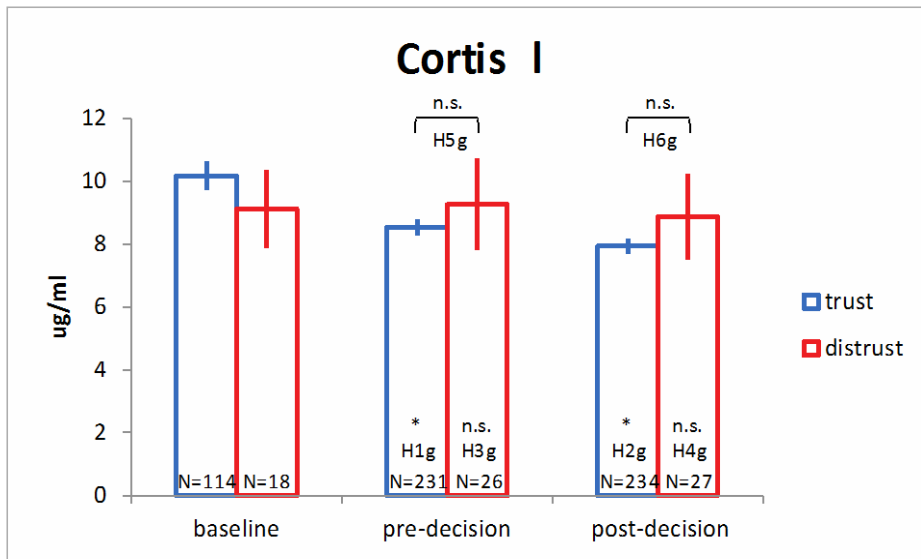
* = significant of the proposed SEM hypothesis

n.s. = not significant

N = the number of values per condition

Figure 61. Average ±S.E. for cortisol (raw signal).


* = significant of the proposed SEM hypothesis

n.s. = not significant

n.s. * = significant but in the opposite direction of the proposed SEM hypothesis

N = the number of values per condition

Figure 62. Average ±S.E. for cortisol (signal minus baseline).
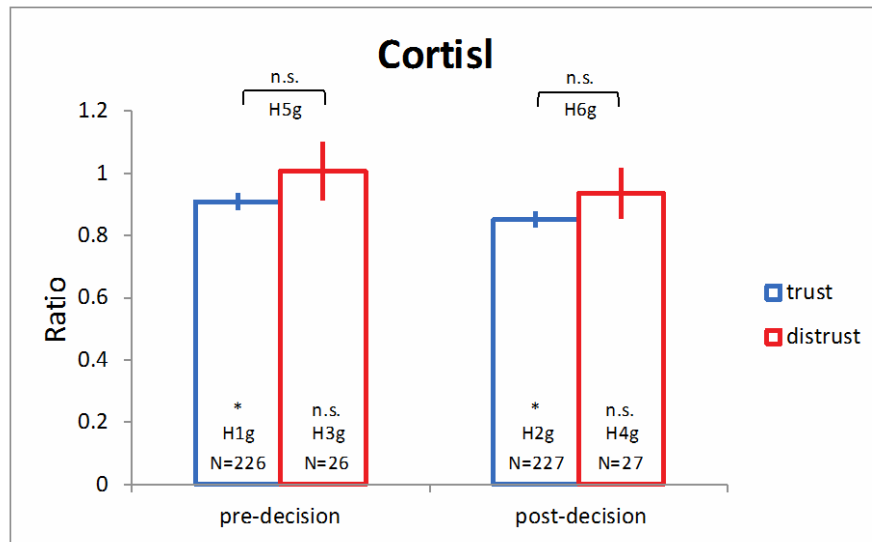
Figure 63. Average ±S.E. for cortisol (signal divided by baseline).

* = significant of the proposed SEM hypothesis

n.s. = not significant

N = the number of values per condition

3.17.2 Scatter Plots

Figures 64–66.show scatter plots for cortisol: raw signal, signal minus baseline, and signal divided by baseline plots.
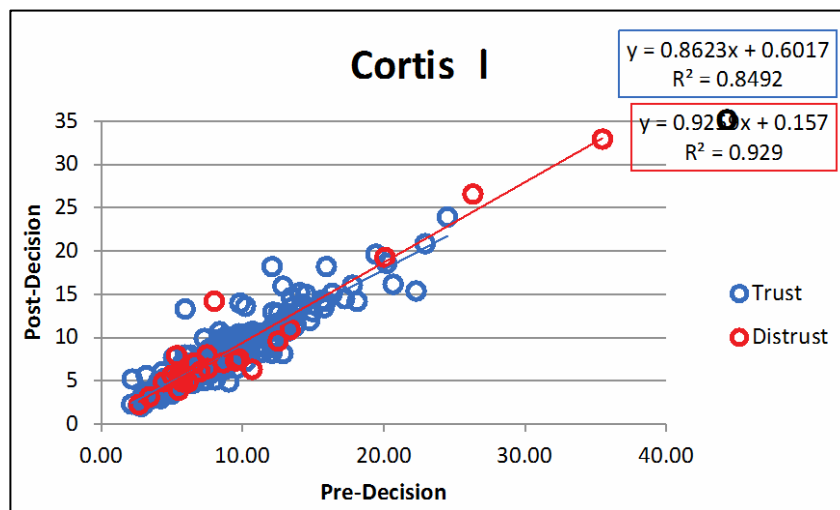
Values for pre-decision and post-decision epochs are displayed in the x-axis and y-axis.

The equation and R2 value for the linear trendline is displayed for trust and distrust interactions in blue and red box.

Figure 64. Scatter plot for cortisol (raw signal).
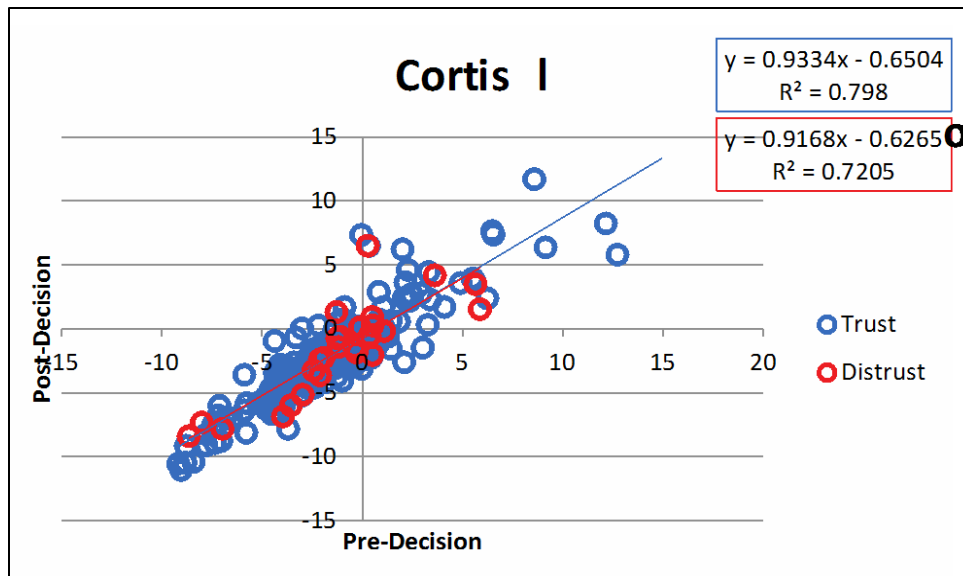
Cortis I

y = 0.9334x - 0.6504
R² = 0.798

y = 0.9168x - 0.6265
R² = 0.7205

Values for pre-decision and post-decision epochs are displayed in the x-axis and y-axis.

The equation and R2 value for the linear trendline is displayed for trust and distrust interactions in blue and red box.

Figure 65. Scatter plot for cortisol (signal minus baseline).
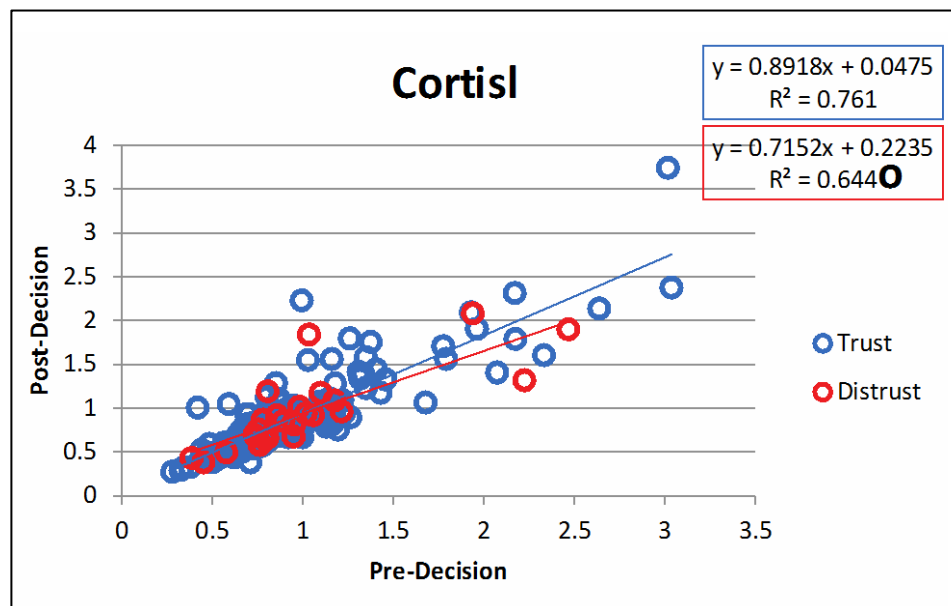
Cortisl

y = 0.8918x + 0.0475
R² = 0.761

y = 0.7152x + 0.2235
R² = 0.644

Values for pre-decision and post-decision epochs are displayed in the x-axis and y-axis.

The equation and R2 value for the linear trendline is displayed for trust and distrust interactions in blue and red box.

Figure 66. Scatter plot for cortisol (signal divided by baseline).

78

3.18 MAYER-ABI

Table 34 shows all hypotheses and their corresponding statistical tests for Mayer-ABI.

Table 34. Mayer-ABI statistical table.

Specific Hypothesis	Percentage of Decisions that Agree with the Hypothesis	Raw Signal Mean Difference (±SE); *p*-value	Signal Minus Baseline 95% Confidence Interval for Mean	Signal Divided by Baseline 95% Confidence Interval for Mean
H5h: Mayer score increases PRE-DECISION: Trust vs. Distrust		A: 0.82 ±0.130 p = 0.000; *	---- no baseline measure ----	---- no baseline measure ----
		B: 0.788 ±0.146 p = 0.000; *	---- no baseline measure ----	---- no baseline measure ----
		I: 0.627 ±0.120 p = 0.000; *	---- no baseline measure ----	---- no baseline measure ----
H6h: Mayer score increases POST-DECISION: Trust vs. Distrust		A: 0.778 ±0.134 p = 0.000; *	---- no baseline measure ----	---- no baseline measure ----
		B: 0.783 ±0.153 p = 0.000; *	---- no baseline measure ----	---- no baseline measure ----
		I: 0.620 ±0.126 p = 0.000; *	---- no baseline measure ----	---- no baseline measure ----

 * = significant of the proposed SEM hypothesis

dark blue areas = specific hypothesis trust conditions studied.

light green = the area studied supports SEM (p<0.05; CJ.>95%).

pink = no support for SEM,

red = there was a significant opposite result found to SEM.

Trust vs. distrust comparisons were significantly different for the Mayer A, B, and I scores for both the pre-decision and post-decision events. This suggests that during trust interactions, subjects thought that their partners had greater ability, benevolence, and integrity compared to subjects that did not trust their partners.

Note that no baseline measure of Mayer-ABI was available for analysis because subjects assessment of their partners trustworthiness could only be measured after they were introduced. Therefore, H1–4h could not be assessed.

3.18.1 Average ±S.E.

Figures 67–69 show average ±S.E. for Mayer A, B: raw signal, signal minus baseline, and signal divided by baseline plots. Data details averages for baseline, pre-decision, and post-decision epochs, for trust and distrust interactions. The hypothesis addressed by specific parts of the plot are labeled as such.
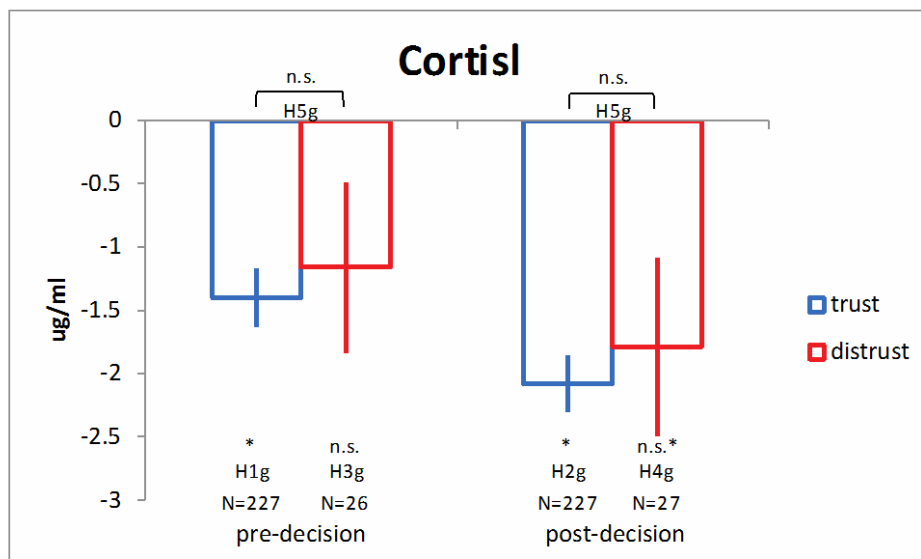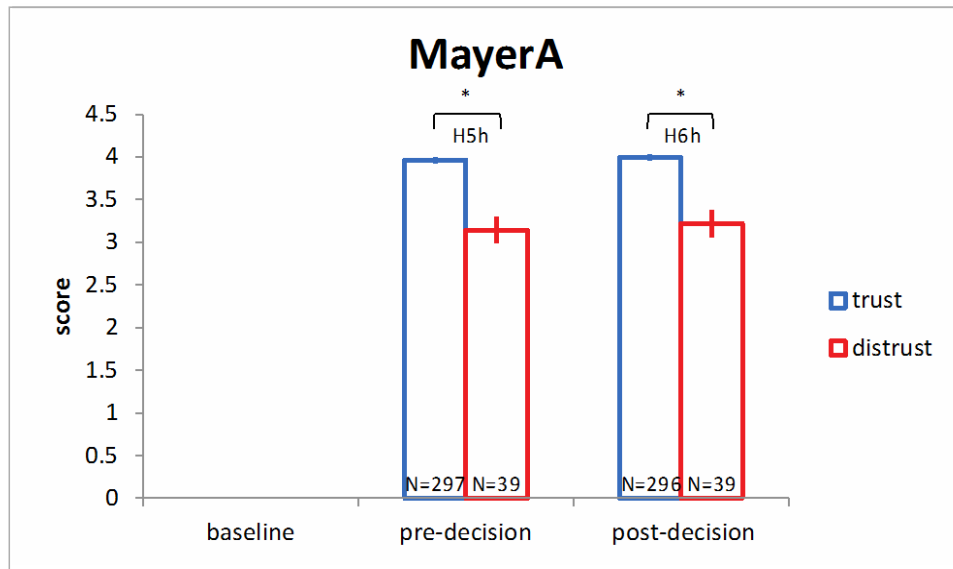
* = significant of the proposed SEM hypothesis
N = the number of values per condition

Figure 67. Average ±S.E. for Mayer A, B, and I (raw signal).

* = significant of the proposed SEM hypothesis

Figure 68. Average ±S.E. for Mayer A, B, and I (signal minus baseline).
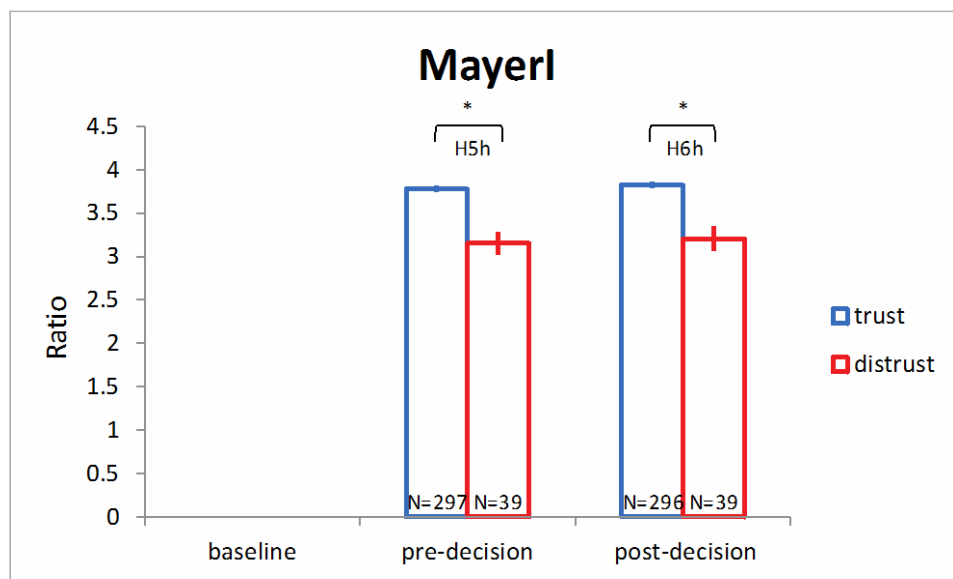
Figure 69. Average ±S.E. for Mayer A, B, and I (signal divided by baseline).

* = significant of the proposed SEM hypothesis
N = the number of values per condition

3.18.2 Scatter Plots

Figures 70–72 show scatter plots for alpha asymmetry: raw signal, signal minus baseline, and signal divided by baseline plots.
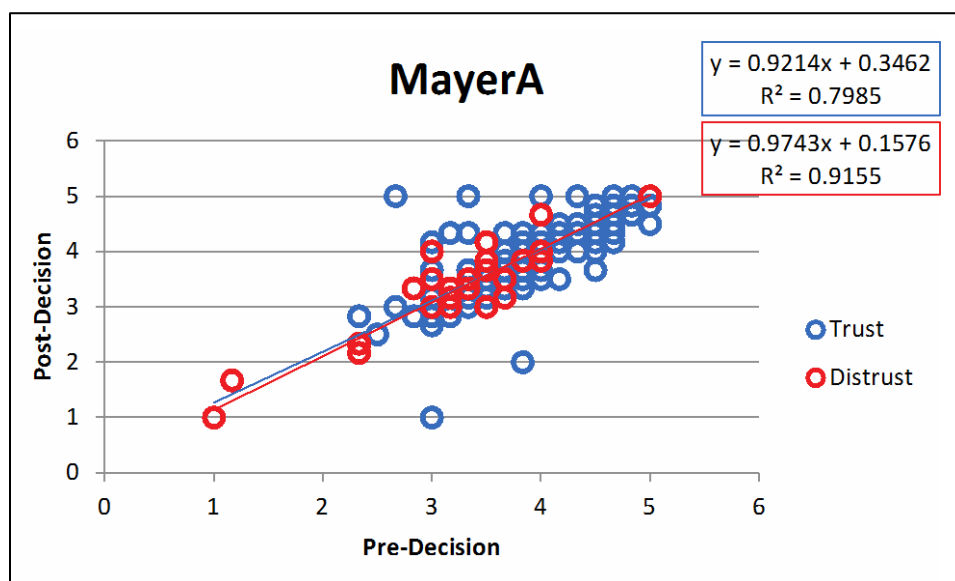
Values for pre-decision and post-decision epochs are displayed in the x-axis and y-axis.

The equation and R2 value for the linear trendline is displayed for trust and distrust interactions in blue and red box.

Figure 70. Scatter plot for alpha asymmetry (raw signal).
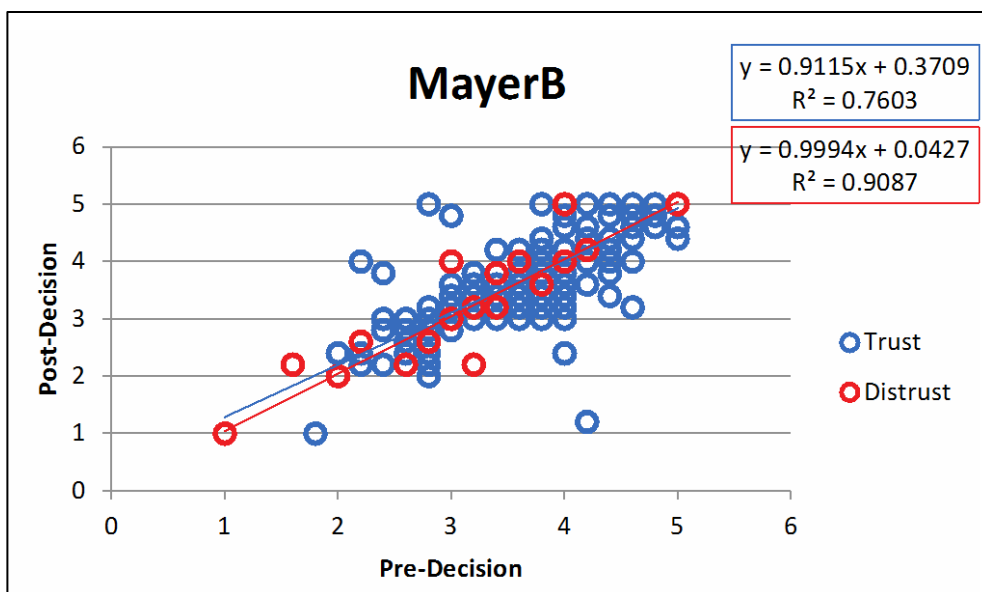
Values for pre-decision and post-decision epochs are displayed in the x-axis and y-axis.

The equation and R2 value for the linear trendline is displayed for trust and distrust interactions in blue and red box.

Figure 71. Scatter plot for alpha asymmetry (signal minus baseline).
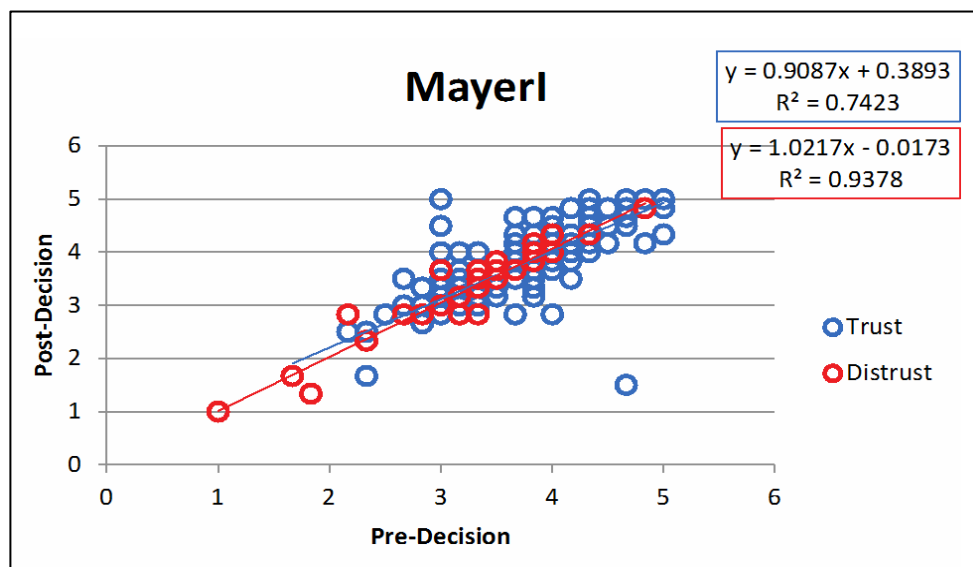
Values for pre-decision and post-decision epochs are displayed in the x-axis and y-axis.

The equation and R2 value for the linear trendline is displayed for trust and distrust interactions in blue and red box.

Figure 72. Scatter plot for alpha asymmetry (signal divided by baseline).

3.19 STAI-S

Table 35 shows all hypotheses and their corresponding statistical tests for STAI-S.

Table 35. STAI-S statistical table.

Specific Hypothesis	Percentage of Decisions that Agree with the Hypothesis	Raw Signal Mean Difference (±SE); p-value	Signal Minus Baseline 95% Confidence Interval for Mean	Signal Divided by Baseline 95% Confidence Interval for Mean
H1i: STAI score decreases TRUST: Baseline vs. Pre-decision	41% (122/297)	0.658 ±0.893 p = 0.461; n.s.	[-1.30 -0.11] *	[0.97 1.01] n.s.
H2i: STAI score decreases TRUST: Baseline vs. Post-decision	44% (130/296)	0.961 ±0.893 p = 0.282; n.s.	[-1.69 -0.35] *	[0.96 1.00] n.s.
H3i: STAI score increases DISTRUST: Baseline vs. Pre-decision	44% (17/39)	0.593 ±2.281 p = 0.795; n.s.	[-3.79 2.56] n.s.	[0.93 1.08] n.s.
H4i: STAI score increases DISTRUST: Baseline vs. Post-decision	41% (16/39)	1.285 ±2.281 p = 0.573; n.s.	[-4.74 2.13] n.s.	[0.92 1.08] n.s.
H5i: STAI score decreases PRE-DECISION: Trust vs. Distrust		-1.676 ±1.497 p = 0.263; n.s.	-0.088 ±1.066 p = 0.934; n.s.	-0.018 ±0.030 p = 0.541; n.s.
H6i: STAI score decreases POST-DECISION: Trust vs. Distrust		-1.287 ±1.498 p = 0.390; n.s.	0.291 ±1.066 p = 0.785; n.s.	-0.019 ±0.030 p = 0.529; n.s.

 * = significant of the proposed SEM hypothesis

n.s. = not significant

dark blue areas = specific hypothesis trust conditions studied.

light green = the area studied supports SEM (p<0.05; CJ.>95%).

pink = no support for SEM,

red = there was a significant opposite result found to SEM.

For the State-Trait Anxiety Inventory (STAI), none of the raw signal or signal divided by baseline comparisons was statistically significant. When STAI scores were baseline subtracted, the 95% confidence intervals of both the pre- and post-decision scores were significantly greater than 0.0. These data could be interpreted as being consistent the SEM model (i.e., a decrease in the STAI scores with trust). Specifically, subjects who trusted their partner exhibited a lower level of anxiety (relative to baseline levels) both prior to and after their decision. The fact that neither of the distrust interactions (relative to baseline) or the direct comparisons between trust vs. distrust (H5i and H6i) were significant makes the interpretation of these results difficult.
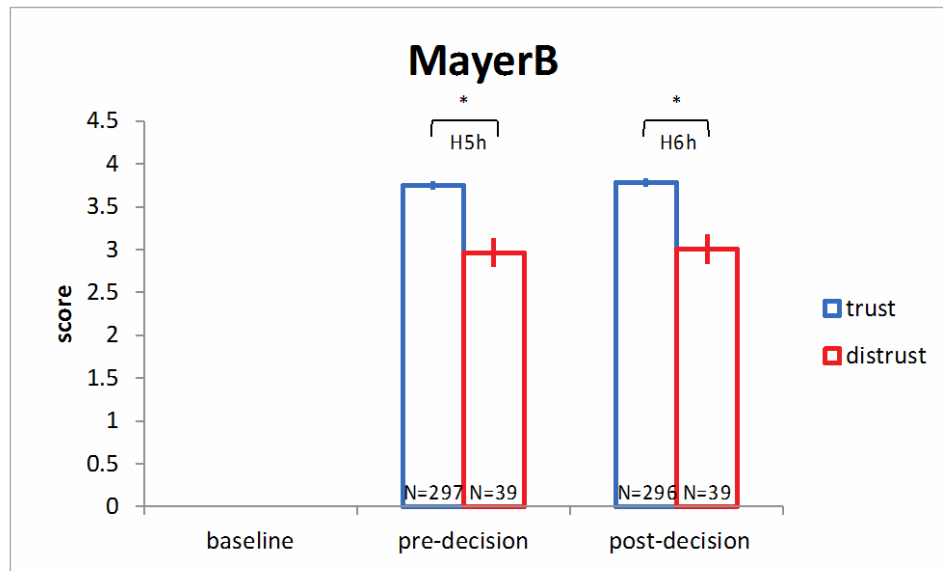
3.19.1 Average ±S.E.

Figures 73–75 show average ±S.E: raw signal, signal minus baseline, and signal divided by baseline plots. Data details averages for baseline, pre-decision, and post-decision epochs, for trust and distrust interactions. The hypothesis addressed by specific parts of the plot are labeled as such.
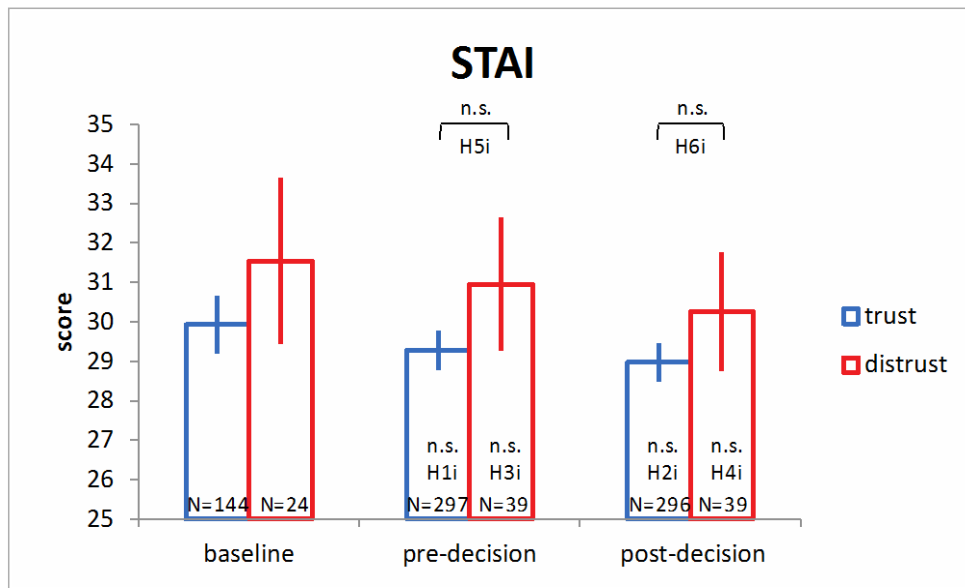
* = significant of the proposed SEM hypothesis

n.s. = not significant

N = the number of values per condition

Figure 73. Average ±S.E. for STAI (raw signal).

* = significant of the proposed SEM hypothesis

n.s. = not significant

N = the number of values per condition

Figure 74. Average ±S.E. for STAI (signal minus baseline).

Figure 75. Average ±S.E. for STAI (signal divided by baseline).

* = significant of the proposed SEM hypothesis

n.s. = not significant

N = the number of values per condition

3.19.2 Scatter Plots

Figures 76–78 show scatter plots for STAI score: raw signal, signal minus baseline, and signal divided by baseline plots.
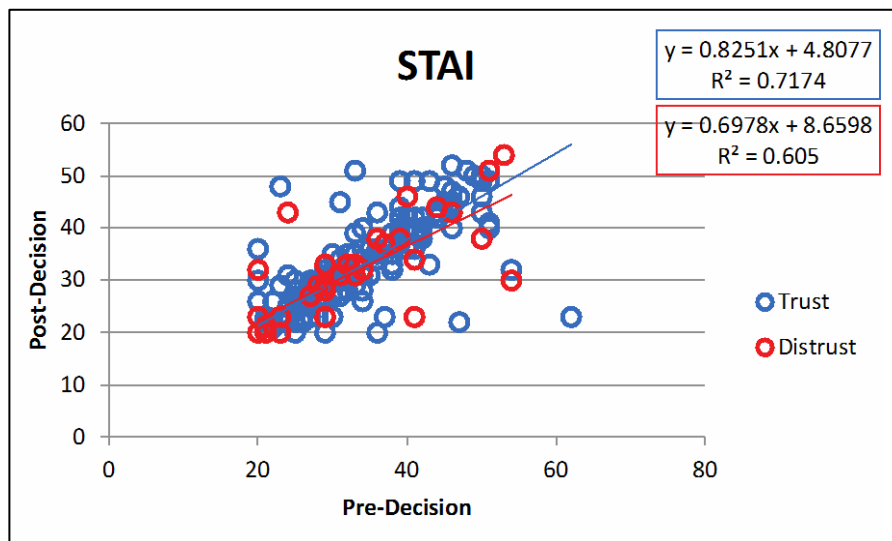
Values for pre-decision and post-decision epochs are displayed in the x-axis and y-axis.

The equation and R2 value for the linear trendline is displayed for trust and distrust interactions in blue and red box.

Figure 76. Scatter plot for STAI score (raw signal).
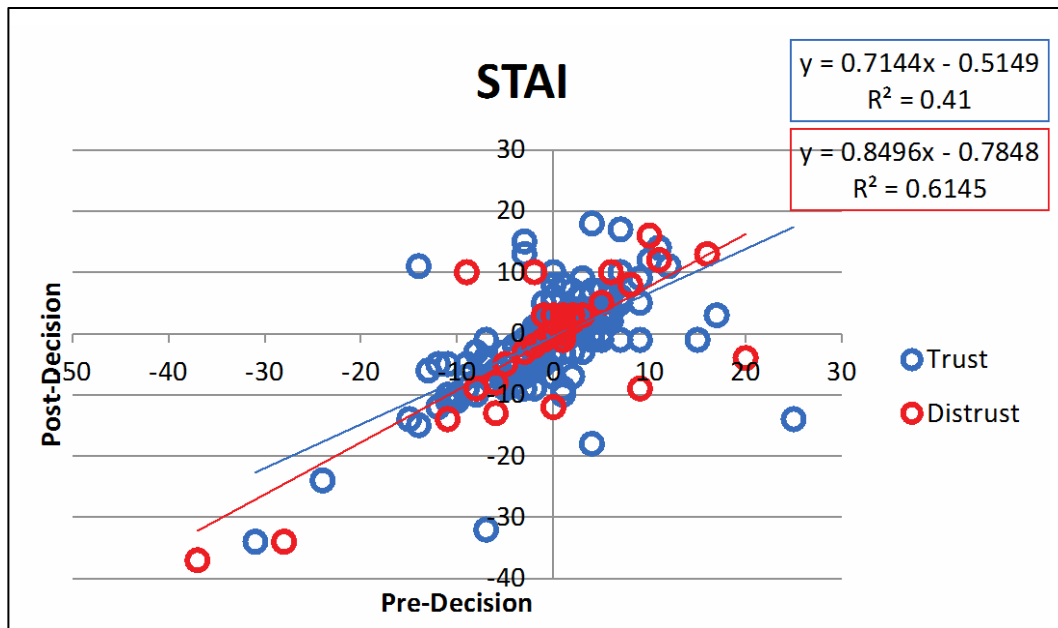
Values for pre-decision and post-decision epochs are displayed in the x-axis and y-axis.

The equation and R2 value for the linear trendline is displayed for trust and distrust interactions in blue and red box.

Figure 77. Scatter plot for STAI score (signal minus baseline).
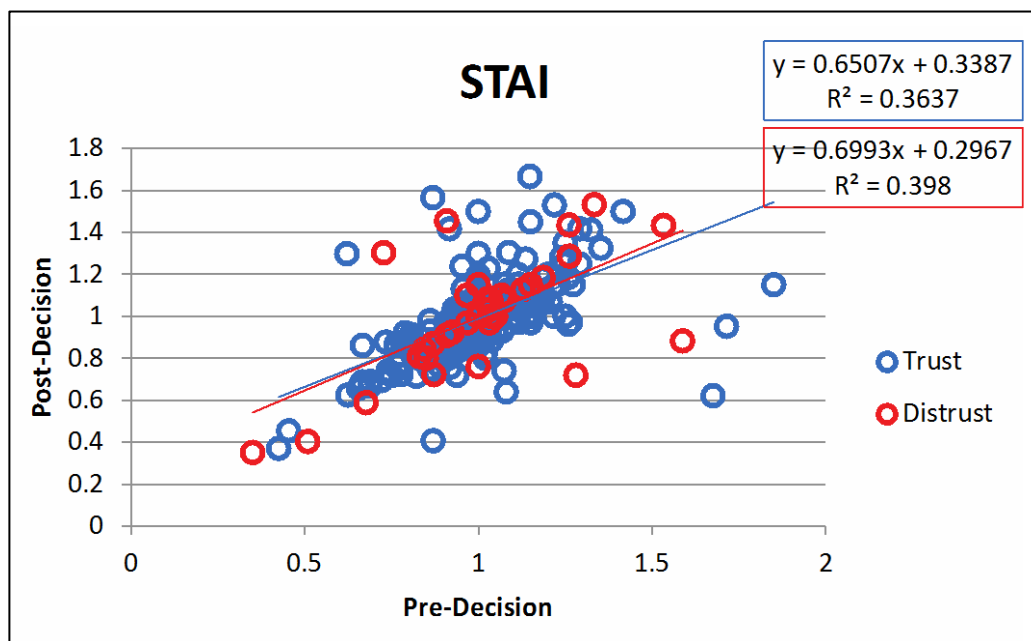
Values for pre-decision and post-decision epochs are displayed in the x-axis and y-axis.

The equation and R2 value for the linear trendline is displayed for trust and distrust interactions in blue and red box.

Figure 78. Scatter plot for STAI score (signal divided by baseline).

3.20 SAS

Table 36 shows all hypotheses and their corresponding statistical tests for SAS.

Table 36. SAS statistical table.

Specific Hypothesis	Percentage of Decisions that Agree with the Hypothesis	Raw Signal	Signal Minus Baseline	Signal Divided by Baseline
		Mean Difference (±SE); p-value	95% Confidence Intrval for Mean	95% Confidence Intrval for Mean
H1j: SAS score decreases TRUST: Baseline vs. Pre-decision	68% (199/294)	0.174 ±0.060 p = 0.004; *	[-0.232 -0.170] *	[0.898 0.942] *
H2j: SAS score decreases TRUST: Baseline vs. Post-decision	----------------	no post-decision measure		----------------
H3j: SAS score increases DISTRUST: Baseline vs. Pre-decision	39% (15/38)	0.222 ±0.167 p = 0.109; n.s.	[-0.224 -0.054] n.s.*	[0.906 1.045] n.s.
H4j: SAS score increases DISTRUST: Baseline vs. Post-decision	----------------	no post-decision measure		----------------
H5j: SAS score decreases PRE-DECISION: Trust vs. Distrust		-0.049 ±0.100 p = 0.629; n.s.	-0.062 ±0.091 p = 0.493; n.s.	-0.055 ±0.067 p = 0.405; n.s.
H6j: SAS score decreases POST-DECISION: Trust vs. Distrust	----------------	no post-decision measure		----------------

 * = significant of the proposed SEM hypothesis

n.s. = not significant

n.s.* = significant but in the opposite direction of the proposed SEM hypothesis.

dark blue areas   = specific hypothesis trust conditions studied.

light green = the area studied supports SEM (p<0.05; CJ.>95%).

pink = no support for SEM,

red = there was a significant opposite result found to SEM.

For the Stress Appraisal Scale (SAS), pre-decision scores were significantly reduced when compared to the baseline during trust interactions. Further, statistical significance was present in the raw signal, and when adjusting for the baseline (subtracting or dividing by baseline). This finding is consistent with the prediction of the SEM model (i.e., SAS scores decrease with trust), indicating that subjects that trusted their partners were less stressed (relative to baseline) prior to making a trust decision. A significant change present when subjects distrusted their partner (H4j; signal minus baseline) is in the opposite direction of the SEM model and would argue against the interpretation above.

Note that there was no post-decision measure for SAS and therefore H2j, H4j, and H6j were not addressed.

3.20.1 Average ±S.E.

Figures 79–81 show average ±S.E. for SAS score: raw signal, signal minus baseline, and signal divided by baseline plots. Data details averages for baseline, pre-decision, and post-decision epochs, for trust and distrust interactions. The hypothesis addressed by specific parts of the plot are labeled as such.
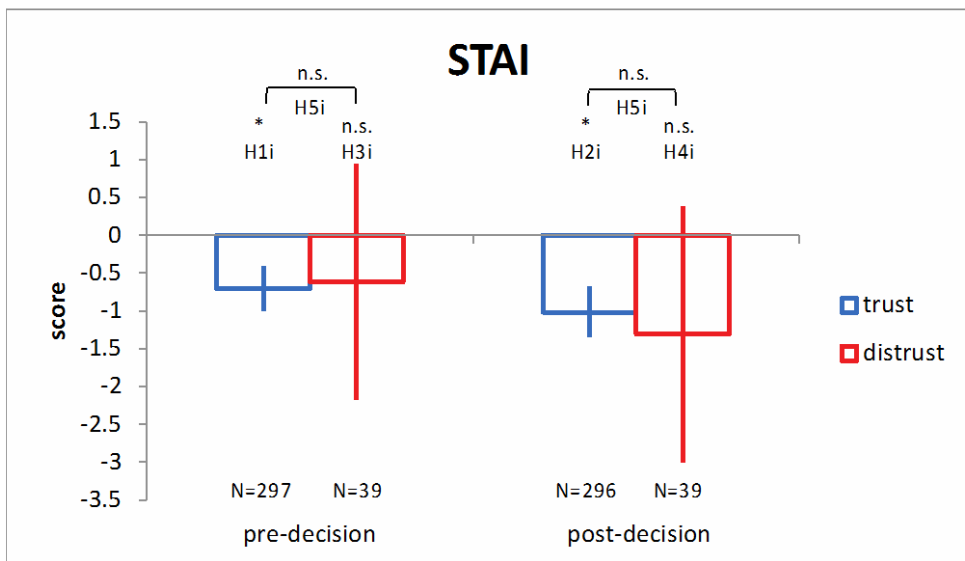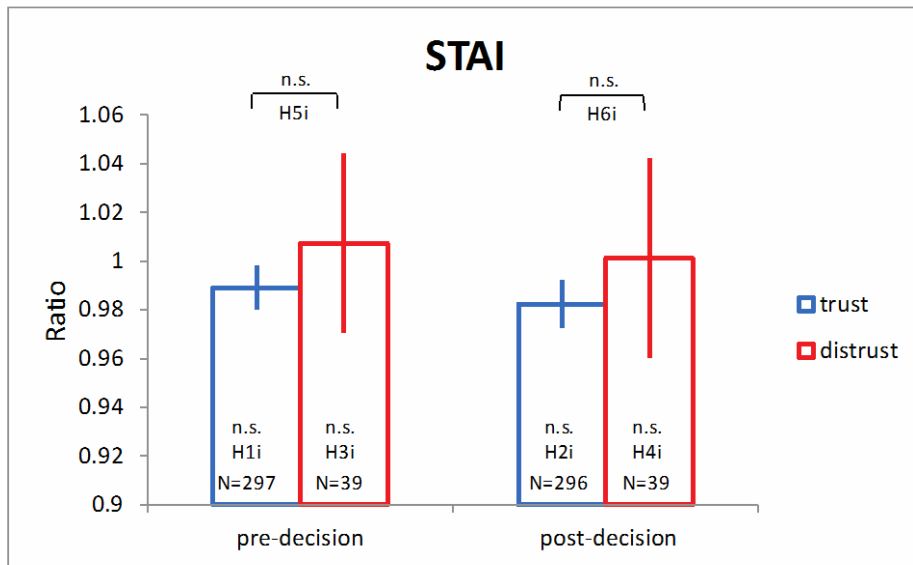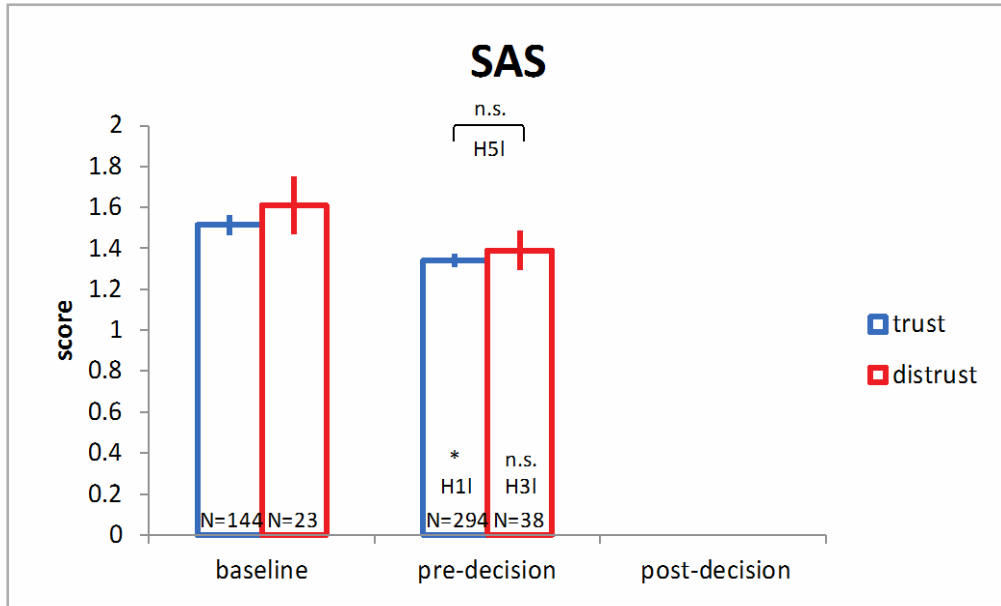
* = significant of the proposed SEM hypothesis

n.s. = not significant

N = the number of values per condition

Figure 79. Average ±S.E. for SAS score (raw signal).
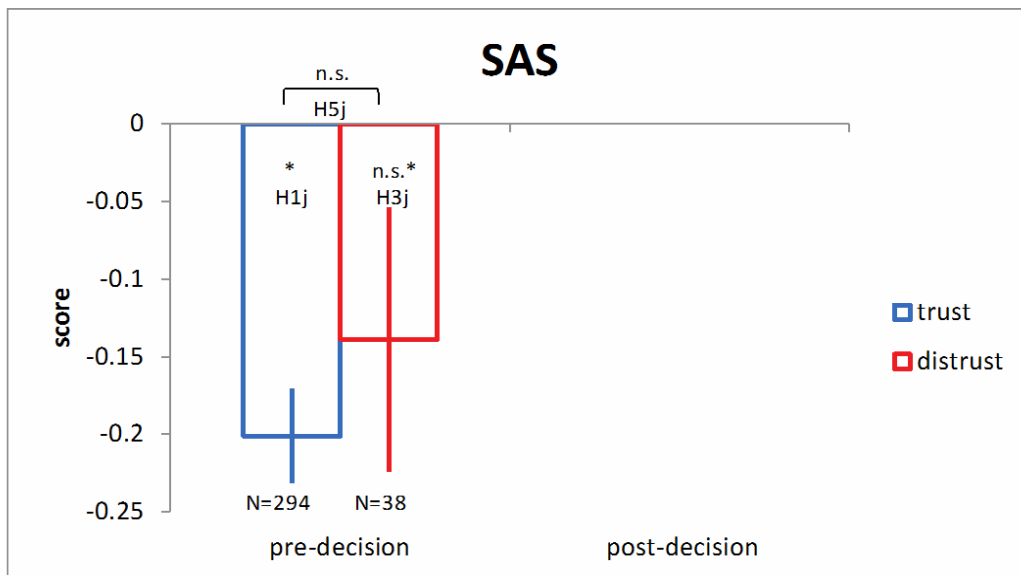

* = significant of the proposed SEM hypothesis

n.s. = not significant

n.s. * = significant but in the opposite direction of the proposed SEM hypothesis

N = the number of values per condition

Figure 80. Average ±S.E. for SAS score (signal minus baseline).
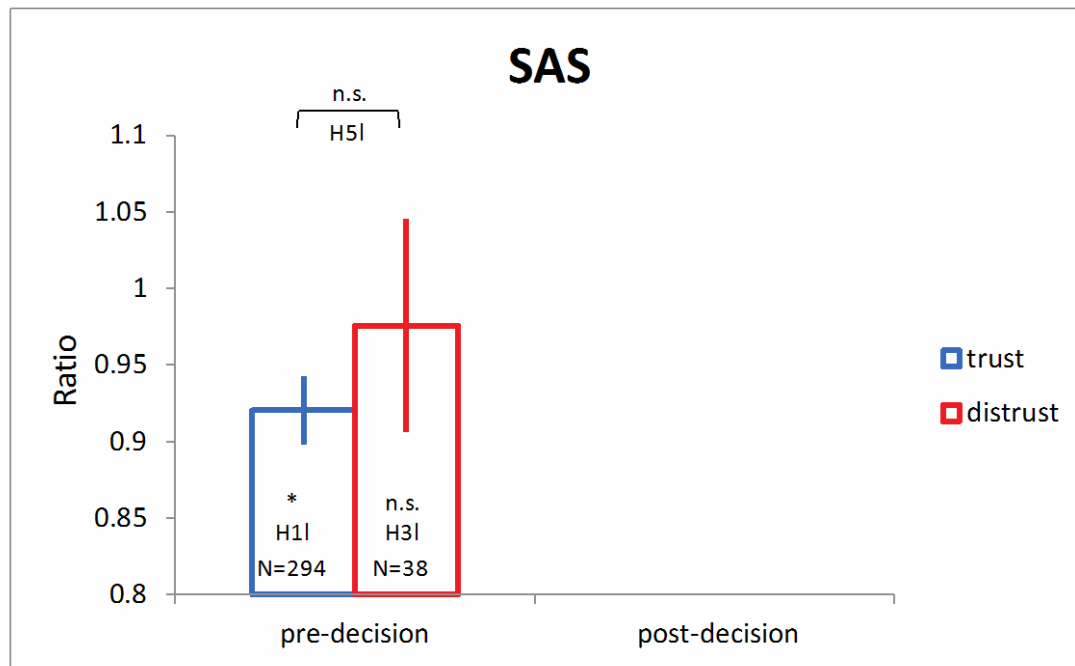
Figure 81. Average ±S.E. for SAS score (signal divided by baseline).

3.21 ALL ANALYSES, HYPOTHESES, AND MEASURES

This section contains a summary of all statistical analyses performed for the project. Tables 37–39 show which variables held significance in each of the hypotheses. For each table, the left table focuses on pre-decision hypotheses. The right table focuses on post-decision hypotheses. Table 37 centers on trust interactions. Table 38 focuses on distrust interactions and Table 39 addresses trust vs. distrust.

Table 37. All analyses, hypotheses and measures, trust interactions.

PRE-DECISION HYPOTHESES

Specific Hypothesis for Trust Condition	Percentage of Decisions that Agree with the Hypothesis	Raw Values — Mean Difference [Baseline - Post Decision] (±SE); p-value	Signal Minus Baseline — 95% Confidence Interval for Mean	Signal Divided by Baseline — 95% Confidence Interval for Mean
H1a: [F4 – F3] alpha asymmetry increases	54% (150/280)	-0.030 ±0.212 p = 0.889; n.s.	[-0.236 0.183] n.s.	[-2.771 1.646] n.s.
H1b: RR interval increases	26% (34/131)	22.378 ±14.285 p= 0.146; n.s.	[-50.218 -24.667] n.s.*	[0.948 0.976] n.s.*
H1c: High-frequency HRV increases	HF: 38% (51/133)	HF: -0.357 ±0.430 p = 0.407; n.s.	HF: [-0.165 1.202] n.s.	HF: [1.335 4.007] *
	HFnorm: 33% (44/135)	HFnorm: 0.102 ±0.025 p = 0.000; n.s.*	HFnorm: [-0.156 -0.074]; n.s.*	HFnorm: [0.835 1.304] n.s.
H1d: Low-frequency HRV decreases	LF: 33% (44/135)	LF: -1.552 ±0.680, p = 0.023; n.s.*	LF: [0.421 2.629] n.s.*	LF: [2.754 4.517] n.s.*
	LFnorm: 33% (44/132)	LFnorm: -0.102 ±0.025 p = 0.000; n.s.*	LFnorm: [0.0741 0.156]; n.s.*	LFnorm: [1.249 1.539] n.s.*
H1e: Skin conductance level decreases	SCL: 15% (37/258)	SCL: -1.337 ±0.413 p = 0.001; n.s.*	SCL: [1.038 1.391]; n.s.*	SCL: [1.316 1.452] n.s.*
	SCR: 31% (74/242)	SCR: -5.612 ± 1.510 p = 0.000; n.s.*	SCR: [3.683 6.809]; n.s.*	SCR: [3.864 7.530] n.s.*
H1f: Oxytocin concentration increases	50% (106/211)	0.119 ±0.528 p = 0.821; n.s.	[-0.280 0.072] *	[1.051 1.202] *
H1g: Cortisol concentration decreases	75% (171/227)	1.645 ±0.518 p = 0.002; *	[-1.864 -0.937] *	[0.856 0.962] *
H1i: STAI score decreases	41% (122/297)	0.658 ±0.893 p = 0.461; n.s.	[-1.30 -0.11] *	[0.97 1.01] n.s.
H1j: SAS score decreases	68% (199/294)	0.174 ±0.060 p = 0.004; *	[-0.232 -0.170] *	[0.898 0.942] *

POST-DECISION HYPOTHESES

Specific Hypothesis for Trust Condition	Percentage of Decisions that Agree with the Hypothesis	Raw Values — Mean Difference [Baseline - Post Decision] (±SE); p-value	Signal Minus Baseline — 95% Confidence Interval for Mean	Signal Divided by Baseline — 95% Confidence Interval for Mean
H2a: [F4 – F3] alpha asymmetry increases	56% (155/277)	-0.099 ±0.213 p = 0.643; n.s.	[-0.182 0.220] n.s.	[-6.337 1.032] n.s.
H2b: RR interval increases	46% (52/114)	12.224 ±15.402 p = 0.428; n.s.	[-25.709 -1.084] n.s.*	[0.973 1.002] n.s.
H2c: High-frequency HRV increases	HF: 51% (59/115)	HF: -0.143 ±0.431 p = 0.740; n.s.	HF: [-0.226 0.830] n.s.	HF: [1.649 3.366] *
	HFnorm: 42% (49/118)	HFnorm: 0.041 ±0.025 p = 0.109; n.s.	HFnorm: [-0.108 -0.003] n.s.*	HFnorm: [1.114 1.984] *
H2d: Low-frequency HRV decreases	LF: 39% (45/114)	LF: -0.855 ±0.681 p = 0.210; n.s.	LF: [-0.233 1.802] n.s.	LF: [2.300 5.169] n.s.*
	LFnorm: 42% (49/118)	LFnorm: -0.041 ±0.025 p = 0.109; n.s.	LFnorm: [0.003 0.108] n.s.*	LFnorm: [1.128 1.543] n.s.*
H2e: Skin conductance level decreases	SCL: 17% (44/256)	SCL: -1.319 ±0.413 p = 0.001; n.s.*	SCL: [1.018 1.421] n.s.*	SCL: [1.332 1.484] n.s.*
	SCR: 30% (73/241)	SCR: -6.223 ±1.508 p = 0.000; n.s.*	SCR: [3.491 7.093] n.s.*	SCR: [4.165 9.516] n.s.*
H2f: Oxytocin concentration increases	53% (114/216)	-0.708 ±0.524 p = 0.177; n.s.	[-0.265 0.138] n.s.	[1.017 1.107] *
H2g: Cortisol concentration decreases	82% (187/227)	2.244 ±0.517 p = 0.000; *	[-2.526 -1.631] *	[0.799 0.903] *
H2i: STAI score decreases	44% (130/296)	0.961 ±0.893 p = 0.282; n.s.	[-1.69 -0.35] *	[0.96 1.00] n.s.
H2j: SAS score decreases	-------------------------- no post-decision measure --------------------------			

* = significant of the proposed SEM hypothesis

n.s. = not significant

N = the number of values per condition

dark blue areas = specific hypothesis trust conditions studied.

light green = the area studied supports SEM (p<0.05; CJ.>95%).

pink = no support for SEM,

Table 38. All analyses, hypotheses and measures, distrust interactions.

PRE-DECISION HYPOTHESES

Specific Hypothesis for Trust Condition	Percentage of Decisions that Agree with the Hypothesis	Raw Values — Mean Difference [Baseline - Post Decision] (±SE); p-value	Signal Minus Baseline — 95% Confidence Interval for Mean	Signal Divided by Baseline — 95% Confidence Interval for Mean
H3a: [F4 – F3] alpha asymmetry decreases	46% (7/38)	0.232 ±0.535 p = 0.664, n.s.	[-0.112 0.355] n.s.	[-0.017 2.449] n.s.
H3b: RR interval decreases	91% (10/11)	68.677 ±44.658 p = 0.125; n.s.	[-122.219 -24.943] *	[0.871 0.971] *
H3c: High-frequency HRV decreases	HF: 78% (7/9)	HF: -0.153 ±1.280 p = 0.905; n.s.	HF: [-2.249 1.265] n.s.	HF: [0.347 1.140] n.s.
	HFnorm: 64% (7/11)	HFnorm: 0.117 ±0.074 p = 0.116; n.s.	HFnorm: [-0.258 0.113] n.s.	HFnorm: [-0.022 3.528] n.s.
H3d: Low-frequency HRV increases	LF: 73% (8/11)	LF: -2.901 ±2.008 p = 0.149; n.s.	LF: [-0.538 6.779] n.s.	LF: [0.928 3.824] n.s.
	LFnorm: 64% (7/11)	LFnorm: -0.117 ±0.074 p = 0.116; n.s.	LFnorm: [-0.113 0.258] n.s.	LFnorm: [0.896 1.523] n.s.
H3e: Skin conductance level increases	SCL: 88% (28/32)	SCL: -1.578 ±1.061 p = 0.137; n.s.	SCL: [1.335 3.141] *	SCL: [1.315 1.706] *
	SCR: 81% (22/27)	SCR: -1.432 ±4.098 p = 0.727; n.s.	SCR: [1.45 3 10.652], * *	SCR: [1.110 17.283] *
H3f: Oxytocin concentration decreases	56% (15/27)	0.172 ±1.357 p = 0.899; n.s.	[-0.372 0.686] n.s.	[0.866 1.108] n.s.
H3g: Cortisol concentration increases	35% (9/26)	-0.138 ±1.387 p = 0.921; n.s.	[-2.552 0.232] n.s.	[0.809 1.204] n.s.
H3i: STAI score increases	44% (17/39)	0.593 ±2.281 p = 0.795; n.s.	[-3.79 2.56] n.s.	[0.93 1.08] n.s.
H3j: SAS score increases	39% (15/38)	0.222 ±0.167 p = 0.109; n.s.	[-0.224 -0.054] n.s.*	[0.906 1.045] n.s.

POST-DECISION HYPOTHESES

Specific Hypothesis for Trust Condition	Percentage of Decisions that Agree with the Hypothesis	Raw Values — Mean Difference [Baseline - Post Decision] (±SE); p-value	Signal Minus Baseline — 95% Confidence Interval for Mean	Signal Divided by Baseline — 95% Confidence Interval for Mean
H4a: [F4 – F3] alpha asymmetry decreases	39% (14/36)	0.137 ±0.538 p = 0.799; n.s.	[-0.040 0.442] n.s.	[0.090 2.290] n.s.
H4b: RR interval decreases	76% (13/17)	40.493 ±41.227 p = 0.327; n.s.	[-101.998 -7.922] *	[0.889 0.992] *
H4c: High-frequency HRV decreases	HF: 47% (8/17)	HF: -0.095 ±1.173 p = 0.935; n.s.	HF: [-0.526 0.950] n.s.	HF: [0.760 2.356] n.s.
	HFnorm: 71% (12/17)	HFnorm: 0.135 ±0.069 p = 0.050; *	HFnorm: [-0.199 -0.008] *	HFnorm: [0.461 1.615] n.s.
H4d: Low-frequency HRV increases	LF: 82% (14/17)	LF: -4.885 ± 1.839 p = 0.008; *	LF: [-0.319 8.682] n.s.	LF: [0.908 5.387] n.s.
	LFnorm: 71% (12/17)	LFnorm: -0.135 ±0.069 p = 0.050; *	LFnorm: [0.057 0.118] n.s.	LFnorm: [0.993 1.629] n.s.
H4e: Skin conductance level increases	SCL: 87% (27/31)	SCL: -1.298 ±1.067 p = 0.224; n.s.	SCL: [1.200 3.050] *	SCL: [1.294 1.709] *
	SCR: 85% (22/26)	SCR: -2.147 ±4.124 p = 0.603; n.s.	SCR: [2.121 11.784] *	SCR: [-0.542 24.951] n.s.
H4f: Oxytocin concentration decreases	50% (14/28)	0.635 ±1.348 p = 0.638; n.s.	[-0.891 0.291] n.s.	[0.886 1.166] n.s.
H4g: Cortisol concentration increases	30% (8/27)	0.257 ±1.377 p = 0.852; n.s.	[-3.248 -0.332] n.s.*	[0.766 1.106] n.s.
H4i: STAI score increases	41% (16/39)	1.285 ±2.281 p = 0.573; n.s.	[-4.74 2.13] n.s.	[0.92 1.08] n.s.
H4j: SAS score increases	-------------------------- no post-decision measure --------------------------			

* = significant of the proposed SEM hypothesis

n.s. = not significant

n.s. * = significant but in the opposite direction of the proposed SEM hypothesis

dark blue areas   = specific hypothesis trust conditions studied.

light green = the area studied supports SEM (p<0.05; CJ.>95%).

pink = no support for SEM,

red = there was a significant opposite result found to SEM.

Table 39. All analyses, hypotheses and measures, trust verses distrust.

PRE-DECISION HYPOTHESES

Specific Hypothesis for Trust Condition		Raw Values — Mean Difference [Baseline - Post Decision] (±SE); p-value	Signal Minus Baseline — 95% Confidence Interval for Mean	Signal Divided by Baseline — 95% Confidence Interval for Mean
H5a: [F4 – F3] alpha asymmetry increases		0.339 ±0.356 p = 0.342; n.s.	-0.148 ±0.290 p = 0.610; n.s.	-1.778 ±4.236 p = 0.675; n.s.
H5b: RR interval increases		64.743 ±31.807 p = 0.042; *	36.138 ±22.598 p = 0.111; n.s.	0.041 ±0.025 p = 0.104; n.s.
H5c: High-frequency HRV increases		HF: 0.095 ±0.926 p = 0.919; n.s.	HF: 1.061 ±1.227 p = 0.388; n.s.	HF: 1.928 ±2.149 p = 0.370; n.s.
		HFnorm: -0.035 ±0.053 p = 0.514; n.s.	HFnorm: -0.042 ±0.081 p = 0.605; n.s.	HFnorm: -0.684 ±0.599 p = 0.255; n.s.
H5d: Low-frequency HRV decreases		LF: 0.542 ±1.453 p = 0.709; n.s.	LF: -1.595 ±1.946 p = 0.413; n.s.	LF: 1.259 ±1.961 p = 0.521; n.s.
		LFnorm: 0.035 ±0.053 p = 0.514; n.s.	LFnorm: 0.042 ±0.081 p = 0.605; n.s.	LFnorm: 0.184 ±0.302 p = 0.543; n.s.
H5e: Skin conductance level decreases		SCL: -0.756 ±0.696 p = 0.278; n.s.	SCL: -1.202 ±0.314 p = 0.001; *	SCL: -0.127 ±0.109 p = 0.248; n.s.
		SCR: -0.057 ±2.65 p = 0.983; n.s.	SCR: -0.806 ±2.670 p = 0.763; n.s.	SCR: -3.500 ±3.865 p = 0.366; n.s.
H5f: Oxytocin concentration increases		-0.296 ±0.911 p = 0.746; n.s.	-0.261 ±0.288 p = 0.365; n.s.	0.139 ±0.111 p = 0.212; n.s.
H5g: Cortisol concentration decreases		-0.733 ±0.936 p = 0.434; n.s.	-0.240 ±0.723 p = 0.740; n.s.	-0.098 ±0.085 p = 0.248; n.s.
H5h: Mayer score increases		A: 0.82 ±0.130 p = 0.000; *	----------- no baseline measure -----------	
		B: 0.788 ±0.146 p = 0.000; *	----------- no baseline measure -----------	
		I: 0.627 ±0.120 p = 0.000; *	----------- no baseline measure -----------	
H5i: STAI score decreases		-1.676 ±1.497 p = 0.263; n.s.	-0.088 ±1.066 p = 0.934; n.s.	-0.018 ±0.030 p = 0.541; n.s.
H5j: SAS score decreases		-0.049 ±0.100 p = 0.629; n.s.	-0.062 ±0.091 p = 0.493; n.s.	-0.055 ±0.067 p = 0.405; n.s.

POST-DECISION HYPOTHESES

Specific Hypothesis for Trust Condition		Raw Values — Mean Difference [Baseline - Post Decision] (±SE); p-value	Signal Minus Baseline — 95% Confidence Interval for Mean	Signal Divided by Baseline — 95% Confidence Interval for Mean
H6a: [F4 – F3] alpha asymmetry increases		0.313 ± 0.361 p = 0.386; n.s.	-0.182 ±0.294 p = 0.536; n.s.	-3.842 ±4.290 p = 0.371; n.s.
H6b: RR interval increases		46.713 ±26.788 p = 0.082; n.s.	41.564 ±18.716 p = 0.027; *	0.047 ±0.021 p = 0.026; *
H6c: High-frequency HRV increases		HF: -0.062 ±0.772 p = 0.936; n.s.	HF: 0.090 ±0.926 p = 0.923; n.s.	HF: 0.950 ±1.621 p = 0.558; n.s.
		HFnorm: 0.044 ±0.045 p = 0.320; n.s.	HFnorm: 0.048 ±0.067 p = 0.480; n.s.	HFnorm: 0.511 ±0.495 p = 0.304; n.s.
H6d: Low-frequency HRV decreases		LF: -3.222 ±1.211 p = 0.008; *	LF: -3.408 ± 1.612 p = 0.659; n.s.	LF: 0.587 ±1.624 p = 0.718; n.s.
		LFnorm: -0.044 ±0.44 p = 0.320; n.s.	LFnorm: -0.048 ±0.067 p = 0.480; n.s.	LFnorm: 0.024 ±0.250 p = 0.923; n.s.
H6e: Skin conductance level decreases		SCL: -0.494 ±0.705 p = 0.494; n.s.	SCL: -0.905 ±0.318 p = 0.005; *	SCL: -0.093 ±0.111 p = 0.402; n.s.
		SCR: -0.160 ±2.692 p = 0.953; n.s.	SCR: -1.660 ±2.717 p = 0.541; n.s.	SCR: -5.364 ±3.912 p = 0.173; n.s.
H6f: Oxytocin concentration increases		0.995 ±0.894 p = 0.266; n.s.	0.237 ±0.283 p = 0.403; n.s.	0.0674 ±0.110 p = 0.539; n.s.
H6g: Cortisol concentration decreases		-0.937 ±0.920 p = 0.309; n.s.	-0.288 ±0.711 p = 0.685; n.s.	-0.085 ±0.083 p = 0.309; n.s.
H6h: Mayer score increases		A: 0.778 ±0.134 p = 0.000; *	----------- no baseline measure -----------	
		B: 0.783 ±0.153 p = 0.000; *	----------- no baseline measure -----------	
		I: 0.620 ±0.126 p = 0.000; *	----------- no baseline measure -----------	
H6i: STAI score decreases		-1.287 ±1.498 p = 0.390; n.s.	0.291 ±1.066 p = 0.785; n.s.	-0.019 ±0.030 p = 0.529; n.s.
H6j: SAS score decreases		-------------------------- no post-decision measure --------------------------		

* = significant of the proposed SEM hypothesis

n.s. = not significant

N = the number of values per condition

dark blue areas = specific hypothesis trust conditions studied.

light green = the area studied supports SEM (p<0.05; CJ.>95%).

pink = no support for SEM,

red = there was a significant opposite result found to SEM.

3.22 ADDITIONAL ANALYSES

In addition to the variables described above in the SEM model, we measured other related variables during experimentation. These included the following:

- F3 alpha
- F4 alpha
- Pz alpha
- Fz theta
- LF/HF ratio
- Heart rate

The same tests were performed as the variables explicitly stated in the scientific approach (Analyses 2 and 3), and plots are labeled in a similar fashion (i.e., the significance of each test is displayed).

3.23 F3 ALPHA

3.23.1 Average ±S.E.

Figures 82–84 show average ±S.E. for F3 alpha: raw signal, signal minus baseline, and signal divided by baseline plots. Data details averages for baseline, pre-decision, and post-decision epochs, for trust and distrust interactions. See Section 2.6 for specifics on statistical tests.

* = significant of the proposed SEM hypothesis

n.s. = not significant

N = the number of values per condition

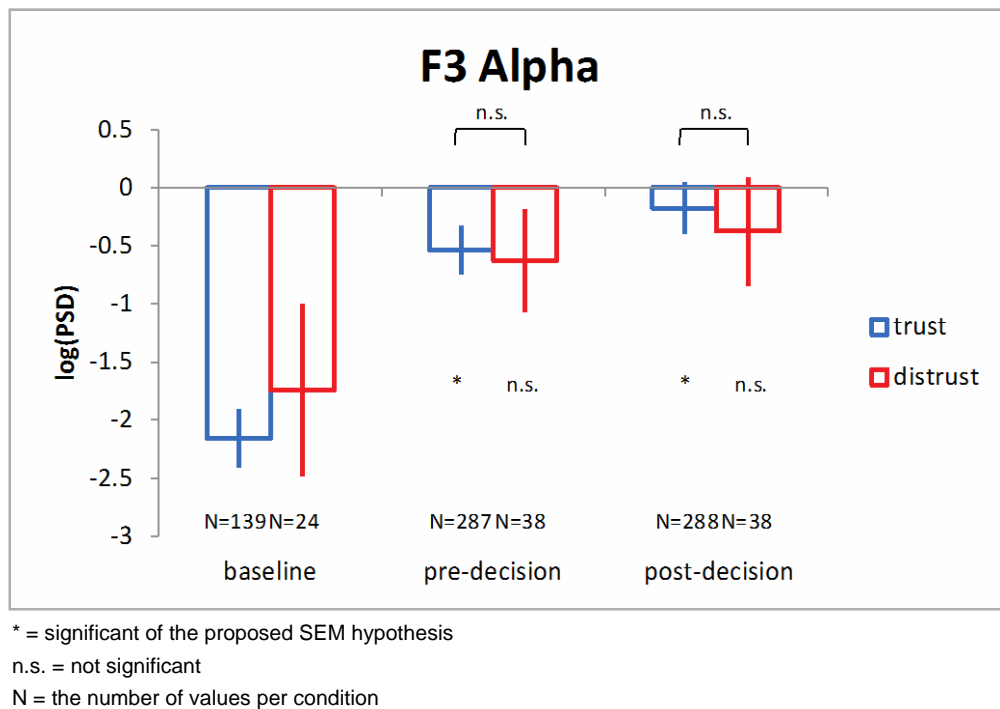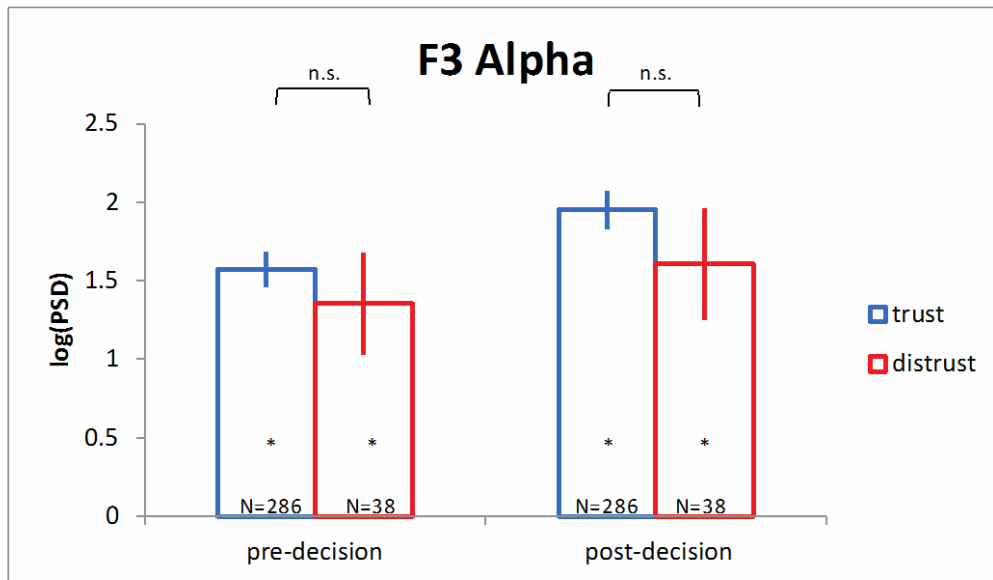Figure 82. Average ±S.E. for F3 alpha (raw signal).

* = significant of the proposed SEM hypothesis

n.s. = not significant

N = the number of values per condition

Figure 83. Average ±S.E. for F3 alpha (signal minus baseline).

* = significant of the proposed SEM hypothesis

n.s. = not significant

N = the number of values per condition

Figure 84. Average ±S.E. for F3 alpha (signal divided by baseline).

3.23.2 Scatter Plots

Figures 85–87 show scatter plots for F3 alpha: raw signal, signal minus baseline, and signal divided by baseline plots.
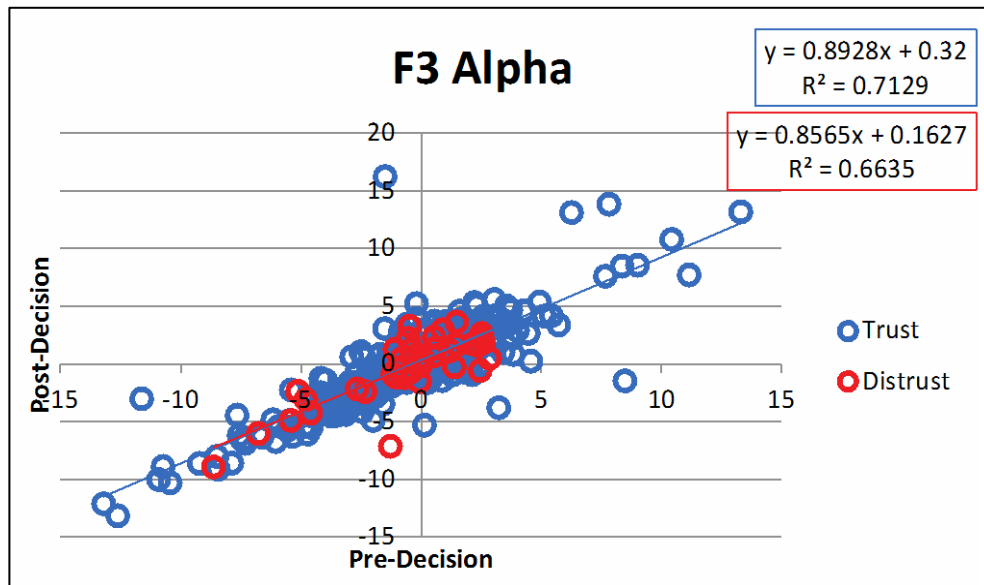
Values for pre-decision and post-decision epochs are displayed in the x-axis and y-axis.

The equation and R2 value for the linear trendline is displayed for trust and distrust interactions in blue and red box.

Figure 85. Scatter plot for F3 alpha (raw signal).

Values for pre-decision and post-decision epochs are displayed in the x-axis and y-axis.

The equation and R2 value for the linear trendline is displayed for trust and distrust interactions in blue and red box.

Figure 86. Scatter plot for F3 alpha (signal minus baseline).

Values for pre-decision and post-decision epochs are displayed in the x-axis and y-axis.

The equation and R2 value for the linear trendline is displayed for trust and distrust interactions in blue and red box.

Figure 87. Scatter plot for F3 alpha (signal divided by baseline).

3.24 F4 ALPHA

3.24.1 Average ±S.E.

Figures 88–90 show average ±S.E. for F4 alpha: raw signal, signal minus baseline, and signal divided by baseline plots. Data details averages for baseline, pre-decision, and post-decision epochs, for trust and distrust interactions.
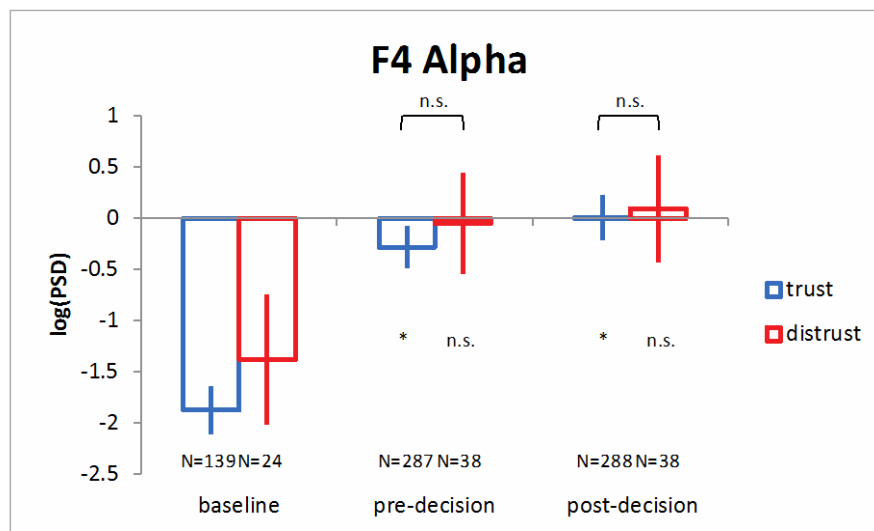
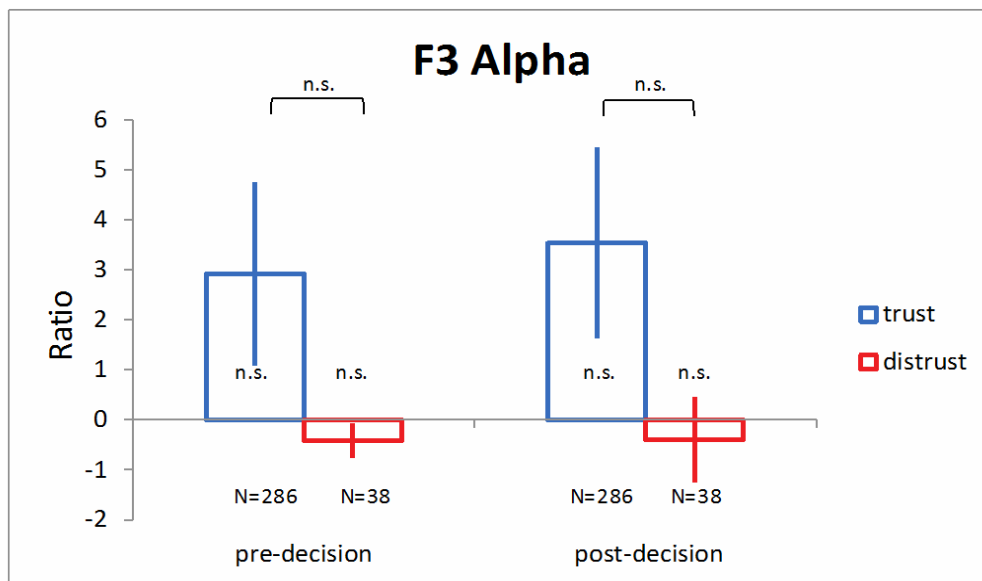* = significant of the proposed SEM hypothesis

n.s. = not significant

N = the number of values per condition

Figure 88. Average ±S.E. for F4 alpha (raw signal).

96

* = significant of the proposed SEM hypothesis

n.s. = not significant

N = the number of values per condition

Figure 89. Average ±S.E. for F4 alpha (signal minus baseline).


* = significant of the proposed SEM hypothesis

n.s. = not significant

N = the number of values per condition

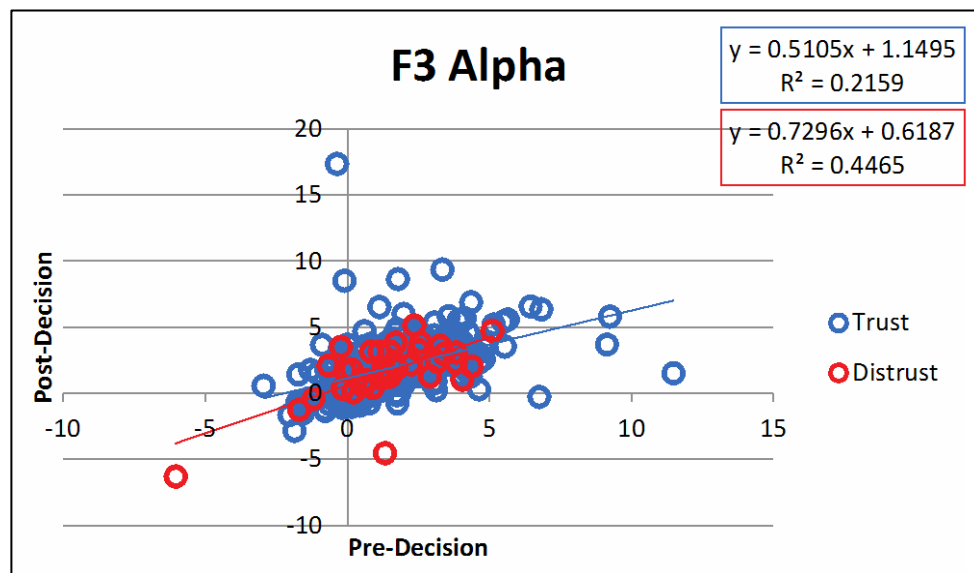Figure 90. Average ±S.E. for F4 alpha (signal divided by baseline).

3.24.2 Scatter Plots

Figures 91–93 show scatter plots for F4 alpha: raw signal, signal minus baseline, and signal divided by baseline plots. Data details averages for baseline, pre-decision, and post-decision epochs, for trust and distrust interactions. See Section 2.6 for specifics on statistical tests.
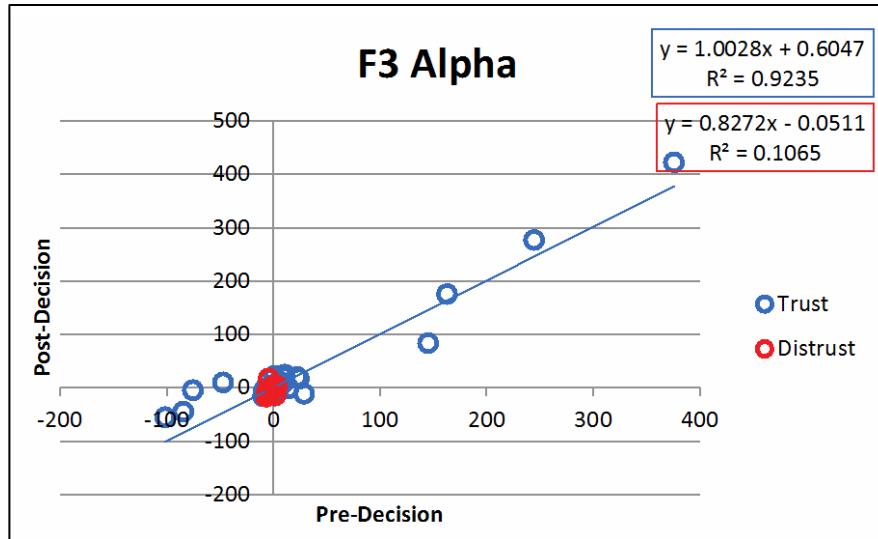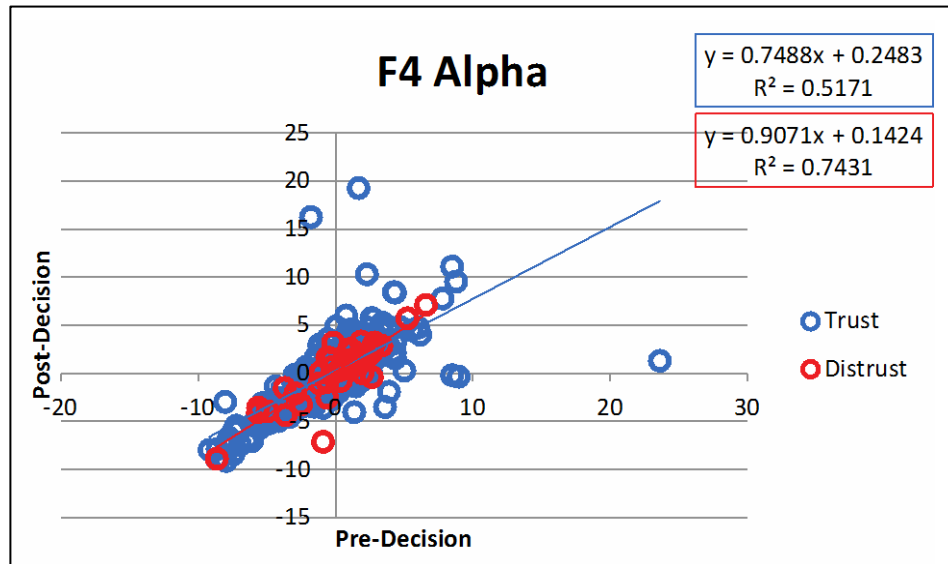

Values for pre-decision and post-decision epochs are displayed in the x-axis and y-axis.

The equation and R2 value for the linear trendline is displayed for trust and distrust interactions in blue and red box.

Figure 91. Scatter plot for F4 alpha (raw signal).
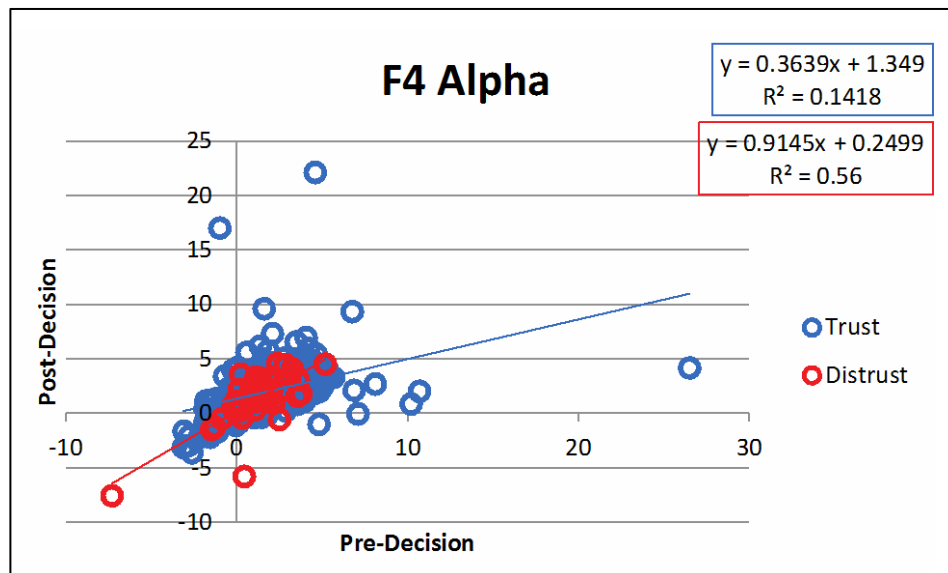
Values for pre-decision and post-decision epochs are displayed in the x-axis and y-axis.

The equation and R2 value for the linear trend line is displayed for trust and distrust interactions in blue and red box.

Figure 92. Scatter plot for F4 alpha (signal minus baseline).

98

Values for pre-decision and post-decision epochs are displayed in the x-axis and y-axis.

The equation and R2 value for the linear trend line is displayed for trust and distrust interactions in blue and red box.

Figure 93. Scatter plot for F4 alpha (signal divided by baseline).

3.25 FZ THETA

3.25.1 Average ±S.E.

Figures 94–96 show average ±S.E. Fz theta for: raw signal, signal minus baseline, and signal divided by baseline plots. Data details averages for baseline, pre-decision, and post-decision epochs, for trust and distrust interactions.
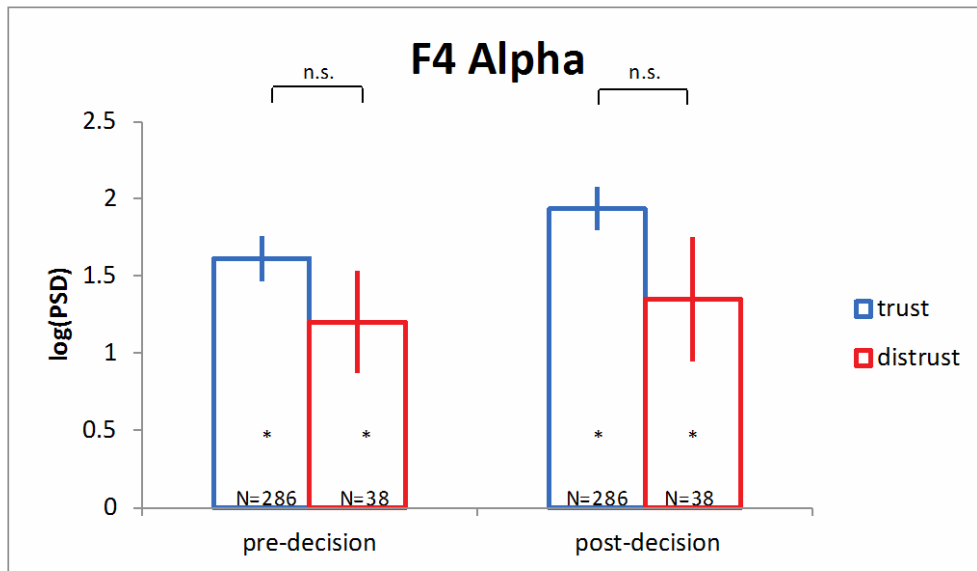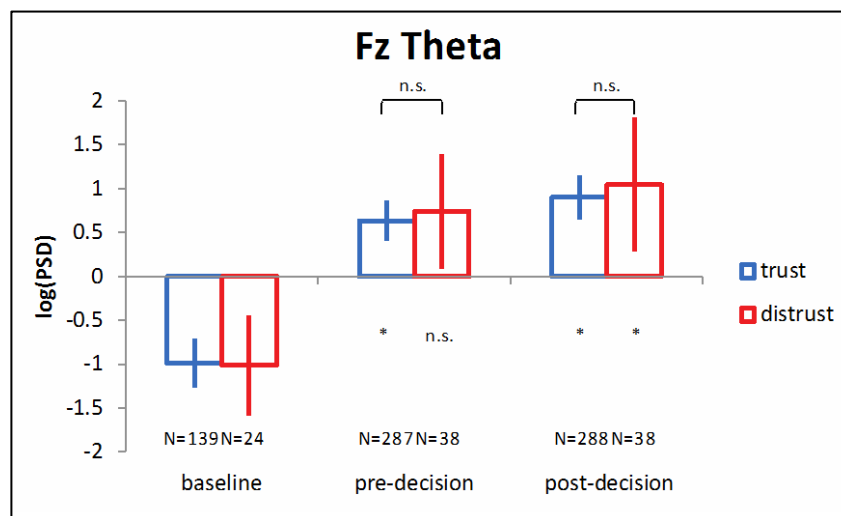

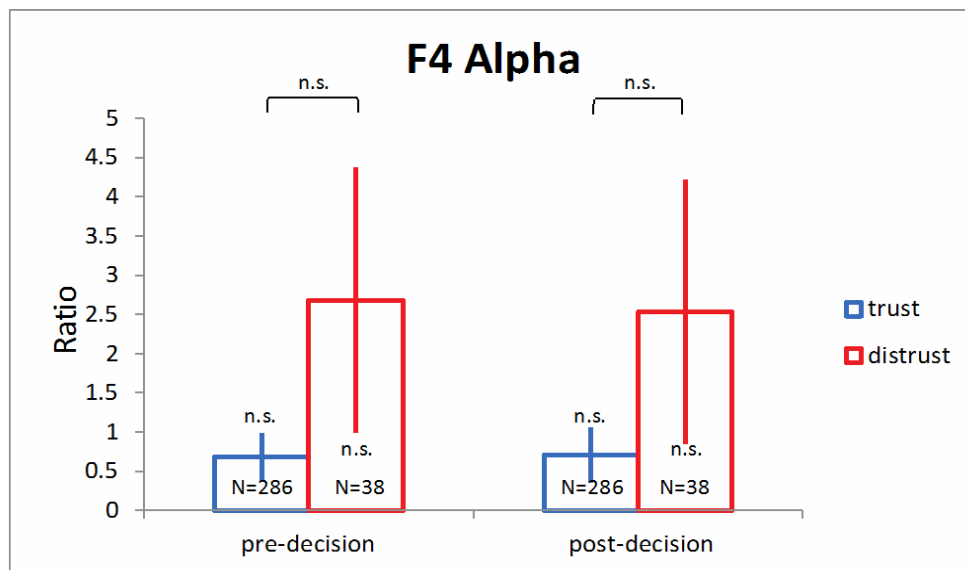* = significant of the proposed SEM hypothesis

n.s. = not significant

N = the number of values per condition

Figure 94. Average ±S.E. for Fz theta (raw signal).

99

* = significant of the proposed SEM hypothesis
n.s. = not significant
N = the number of values per condition

Figure 95. Average ±S.E. for Fz theta (signal minus baseline).


* = significant of the proposed SEM hypothesis
n.s. = not significant
N = the number of values per condition

Figure 96. Average ±S.E. for Fz theta (signal divided by baseline).

3.25.2 Scatter Plots

Figures 97–99 show scatter plots for Fz theta: raw signal, signal minus baseline, and signal divided by baseline plots.
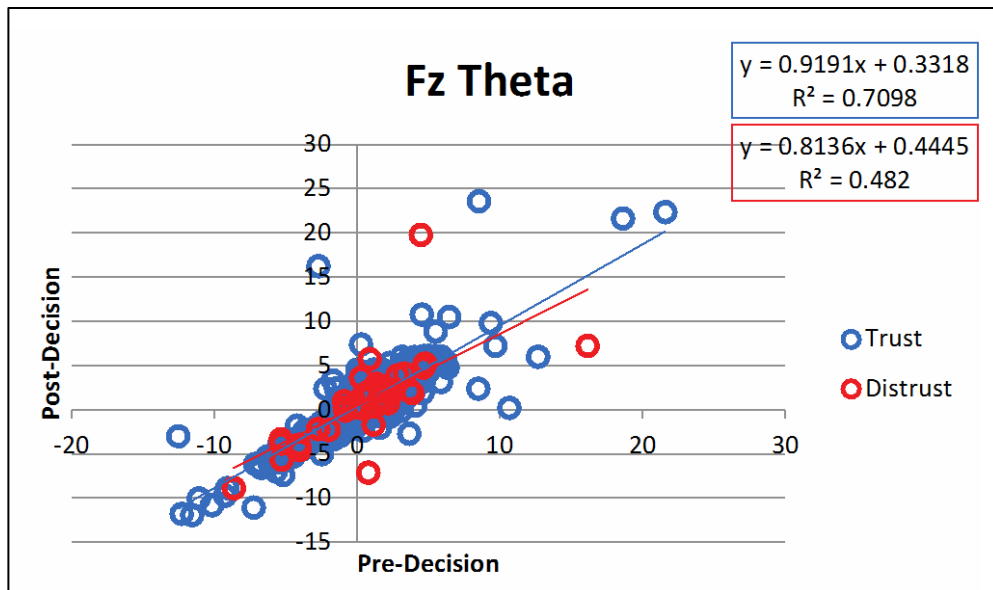
Figure 97. Scatter plot for Fz theta (raw signal).

Values for pre-decision and post-decision epochs are displayed in the x-axis and y-axis.

The equation and R2 value for the linear trend line is displayed for trust and distrust interactions in blue and red box.

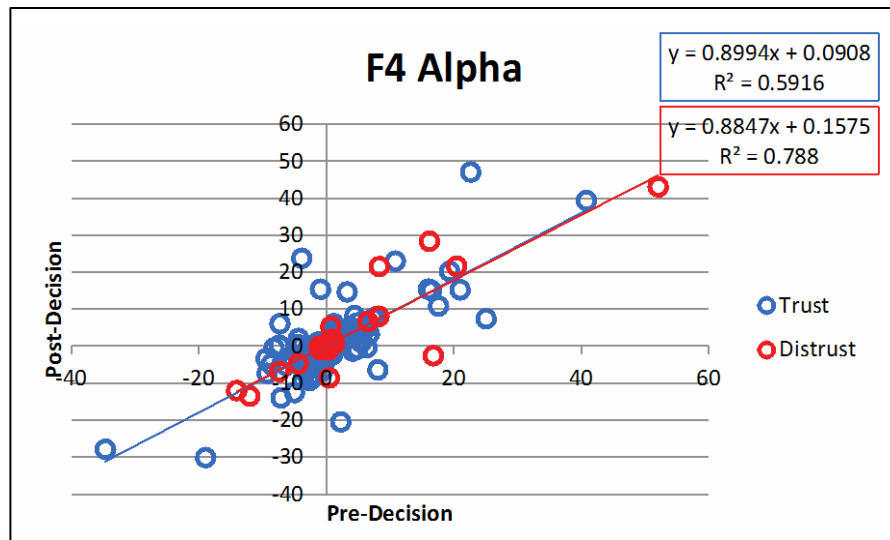Figure 98. Scatter plot for Fz theta (signal minus baseline).

Values for pre-decision and post-decision epochs are displayed in the x-axis and y-axis.

The equation and R2 value for the linear trendline is displayed for trust and distrust interactions in blue and red box.

101

Fz Theta

y = 0.9325x + 0.2872
R² = 0.5704

y = 0.945x + 3.3224
R² = 0.546

Values for pre-decision and post-decision epochs are displayed in the x-axis and y-axis.

The equation and R2 value for the linear trendline is displayed for trust and distrust interactions in blue and red box.

Figure 99. Scatter plot for Fz theta (signal divided by baseline).

3.26 PZ ALPHA

3.26.1 Average ±S.E.

Figures 100–103 show average ±S.E. for Pz alpha: raw signal, signal minus baseline, and signal divided by baseline plots. Data details averages for baseline, pre-decision, and post-decision epochs, for trust and distrust interactions.. See Section 2.6 for specifics on statistical tests.
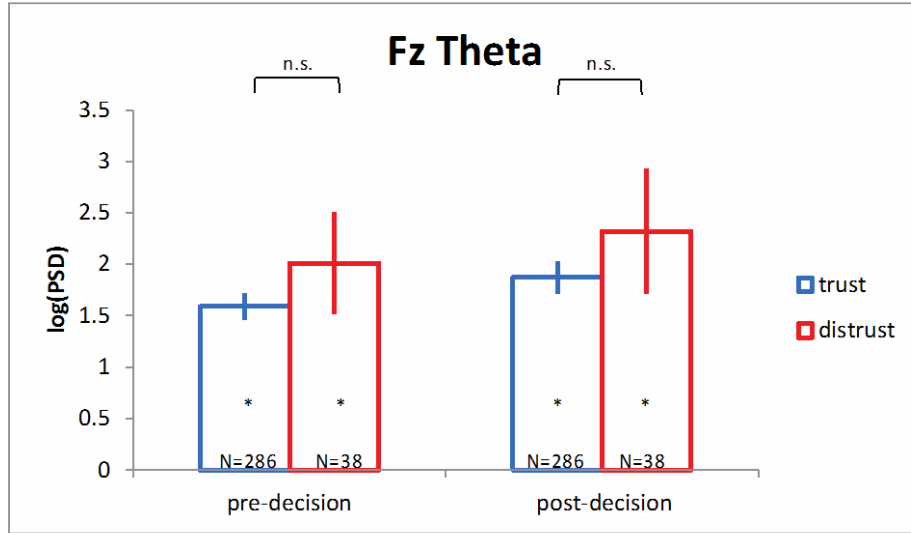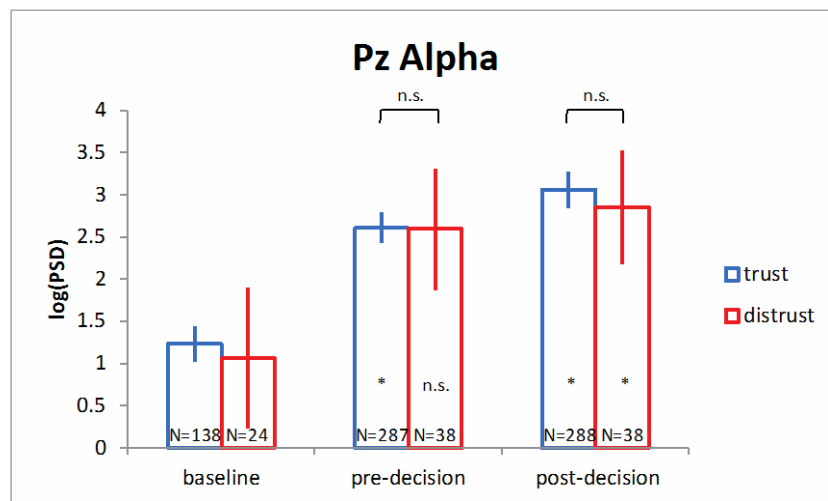

* = significant of the proposed SEM hypothesis

n.s. = not significant

N = the number of values per condition

Figure 100. Average ±S.E. for Pz alpha (raw signal).

* = significant of the proposed SEM hypothesis
n.s. = not significant
N = the number of values per condition

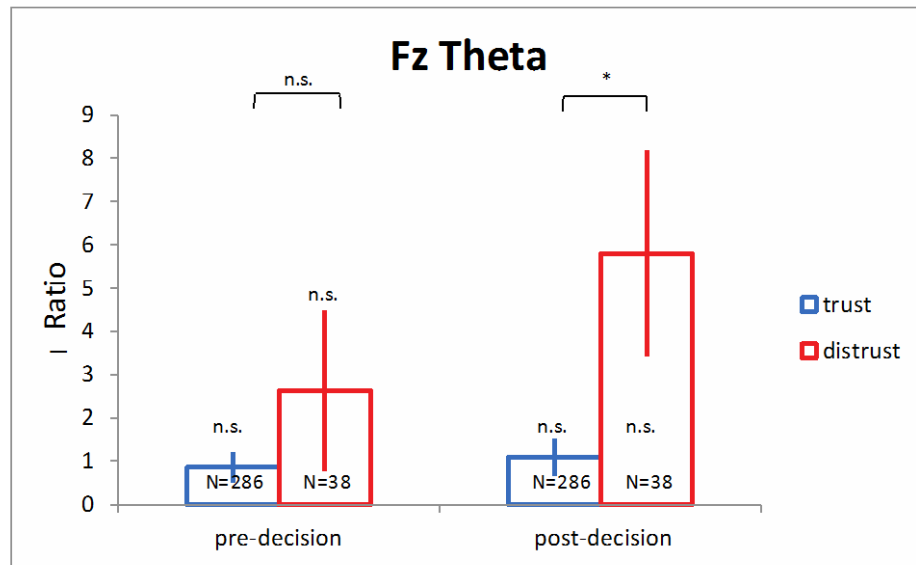Figure 101. Average ±S.E. for Pz alpha (signal minus baseline).

* = significant of the proposed SEM hypothesis
n.s. = not significant
N = the number of values per condition

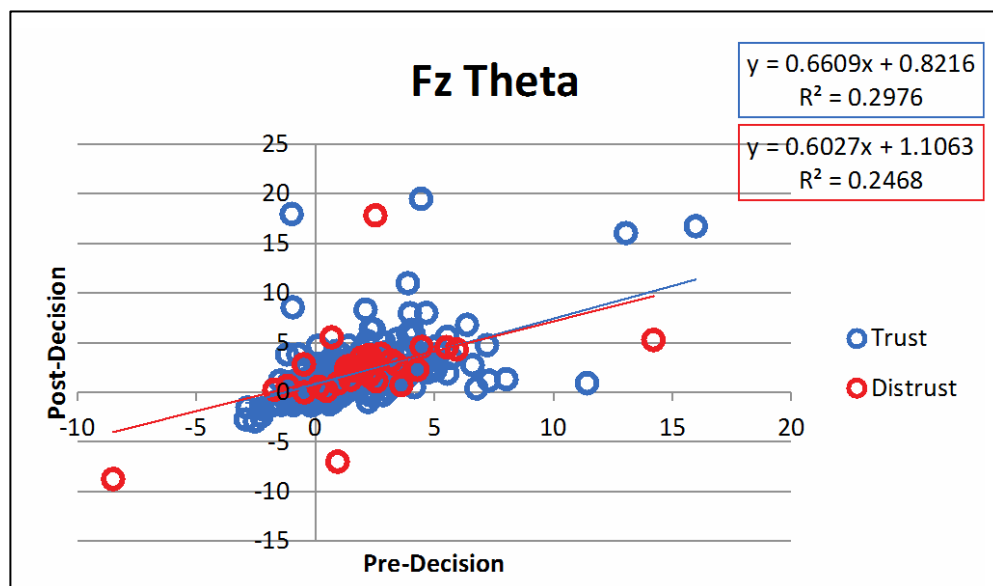Figure 102. Average ±S.E. for Pz alpha, (signal divided by baseline).

3.26.2 Scatter Plots

Figures 103–105 show scatter plots for Pz alpha: raw signal, signal minus baseline, and signal divided by baseline plots.
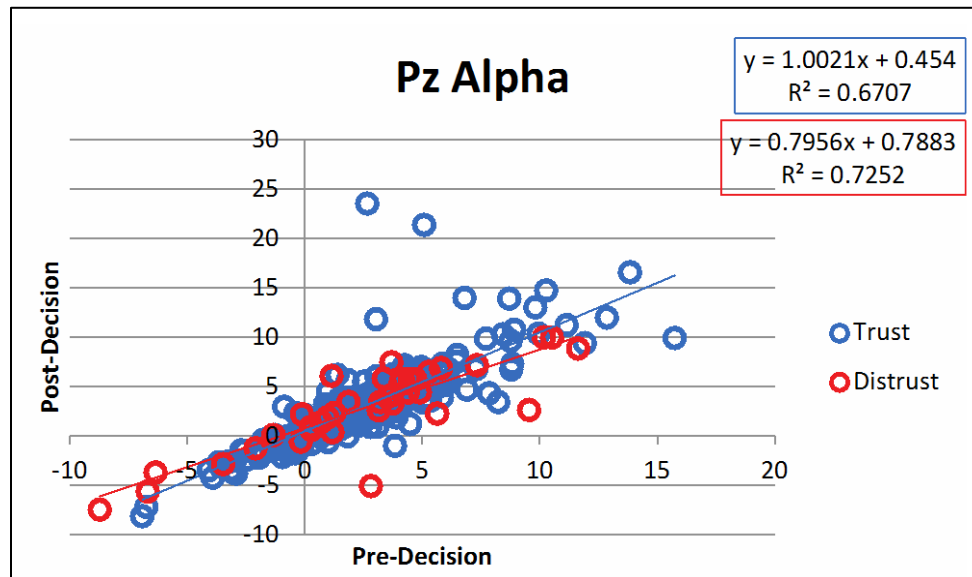
Values for pre-decision and post-decision epochs are displayed in the x-axis and y-axis.

The equation and R2 value for the linear trendline is displayed for trust and distrust interactions in blue and red box.

Figure 103. Scatter plot for Pz alpha (raw signal).

Values for pre-decision and post-decision epochs are displayed in the x-axis and y-axis.

The equation and R2 value for the linear trendline is displayed for trust and distrust interactions in blue and red box.

Figure 104. Scatter plot for Pz alpha (signal minus baseline).

104

Values for pre-decision and post-decision epochs are displayed in the x-axis and y-axis.

The equation and R2 value for the linear trendline is displayed for trust and distrust interactions in blue and red box.
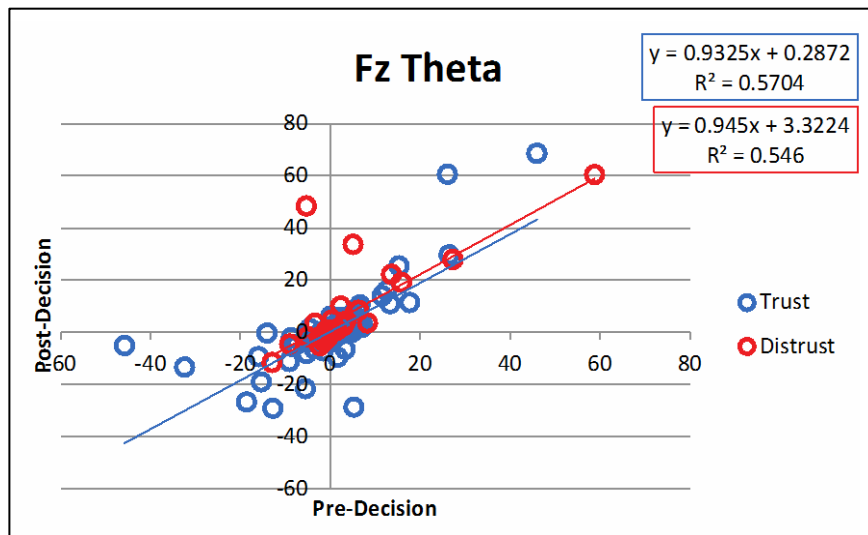
Figure 105. Scatter plot for Pz alpha (signal divided by baseline).

3.27 HEART RATE

Figures 106–108 show average ±S.E. for heart rate: raw signal, signal minus baseline, and signal divided by baseline plots. Data details averages for baseline, pre-decision, and post-decision epochs, for trust and distrust interactions.

3.27.1 Average ±S.E.
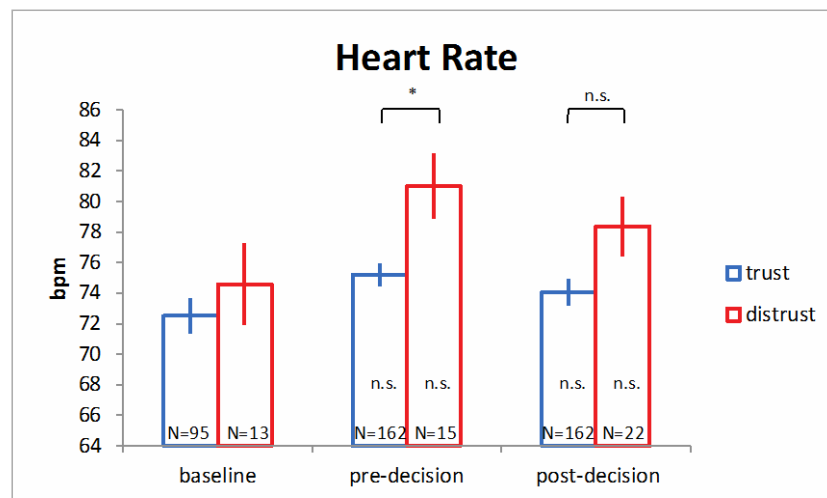
* = significant of the proposed SEM hypothesis

n.s. = not significant

N = the number of values per condition

Figure 106. Average ±S.E. for heart rate (raw signal).
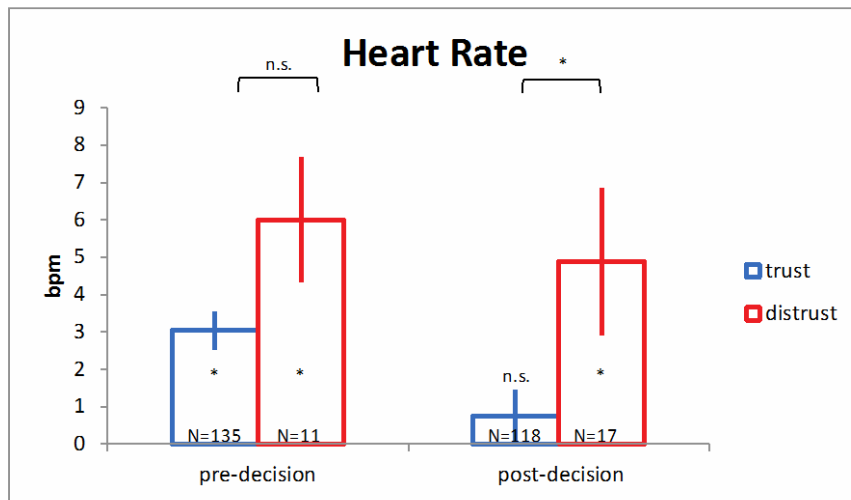
* = significant of the proposed SEM hypothesis

n.s. = not significant

N = the number of values per condition

Figure 107. Average ±S.E. for heart rate (signal minus baseline).
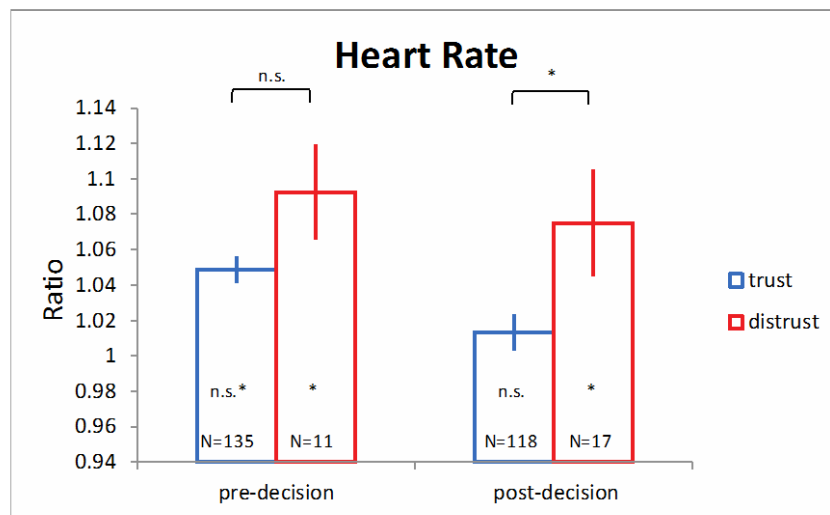
* = significant of the proposed SEM hypothesis

n.s. = not significant

N = the number of values per condition

Figure 108. Average ±S.E. for heart rate (signal divided by baseline).

3.27.2 Scatter Plots

Figures 109–111 show scatter plots for heart rate: raw signal, signal minus baseline, and signal divided by baseline plots.
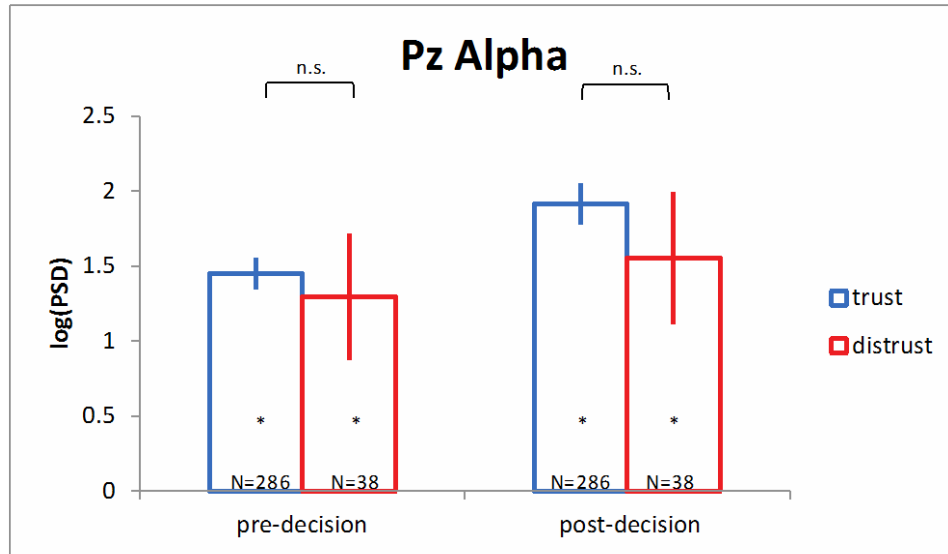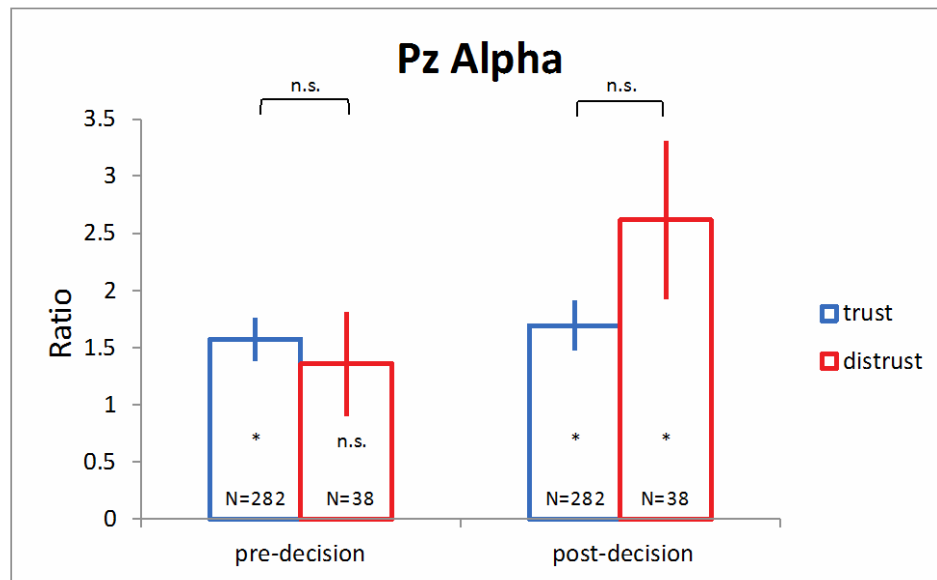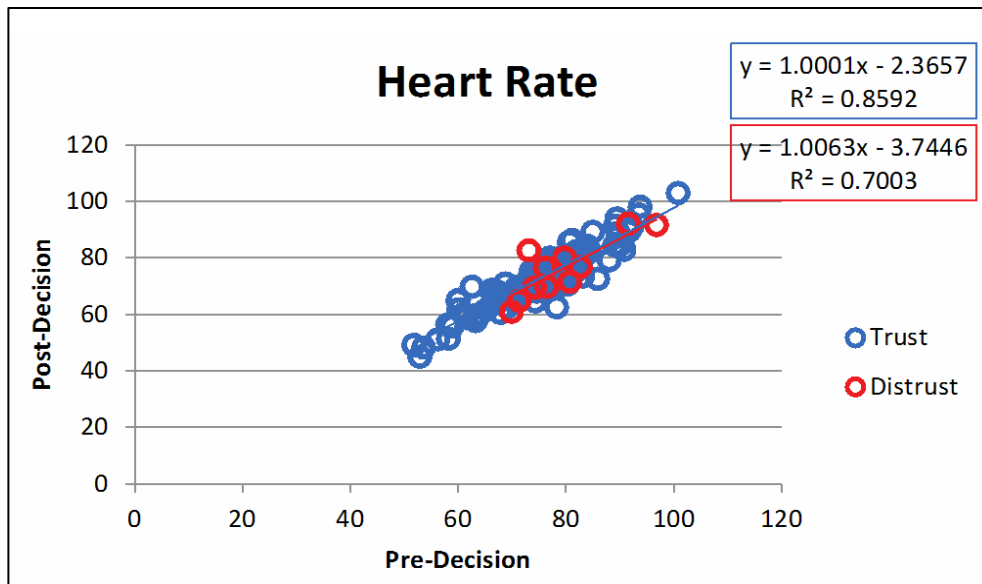
Values for pre-decision and post-decision epochs are displayed in the x-axis and y-axis.

The equation and R2 value for the linear trendline is displayed for trust and distrust interactions in blue and red box.

Figure 109. Scatter plot for heart rate (raw signal).
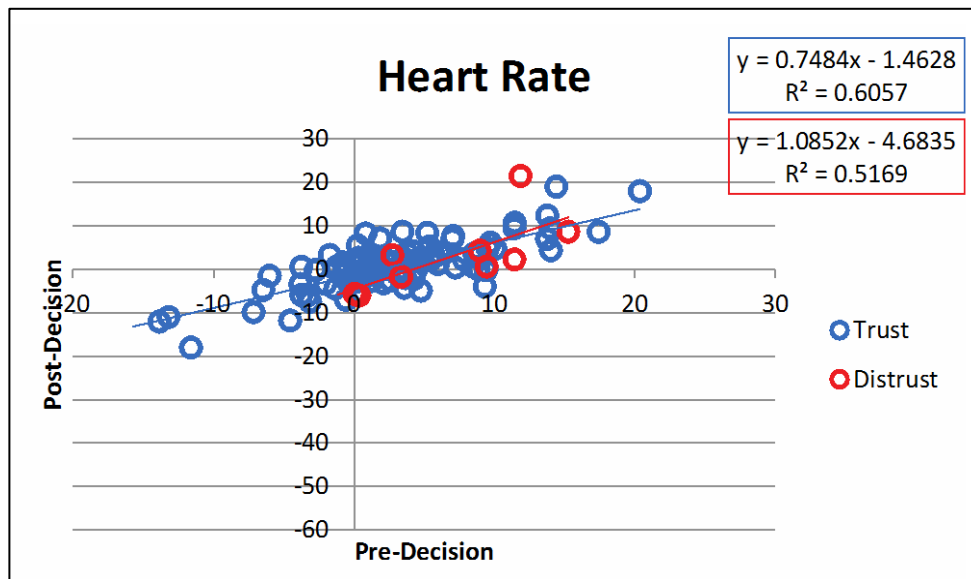
Values for pre-decision and post-decision epochs are displayed in the x-axis and y-axis.

The equation and R2 value for the linear trendline is displayed for trust and distrust interactions in blue and red box.

Figure 110. Scatter plot for heart rate (signal minus baseline).
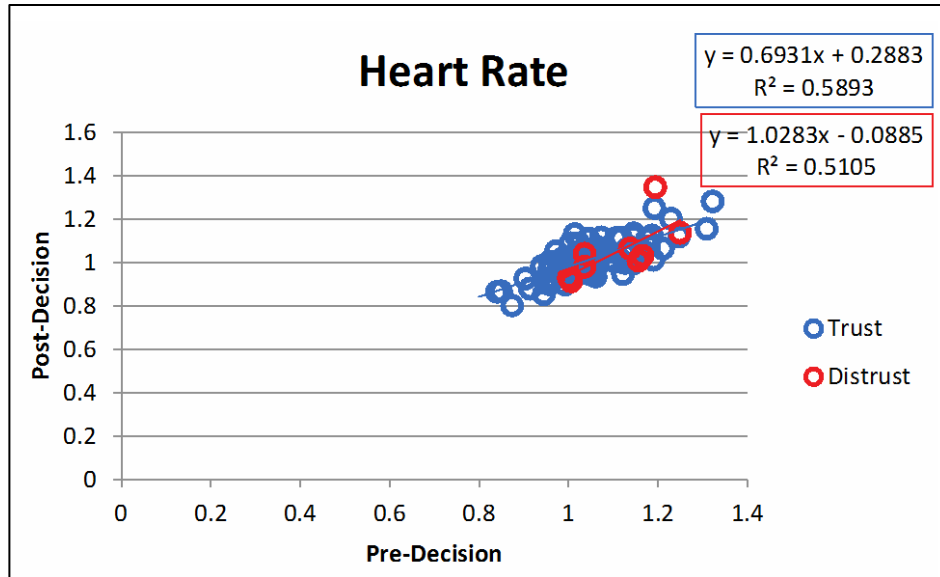
Values for pre-decision and post-decision epochs are displayed in the x-axis and y-axis.

The equation and R2 value for the linear trendline is displayed for trust and distrust interactions in blue and red box.

Figure 111. Scatter plot for heart rate (signal divided by baseline).

3.28 LF/HF RATIO

3.28.1 Average ±S.E.

Figures 112–114 show average ±S.E. for LF/HF: raw signal, signal minus baseline, and signal divided by baseline plots. Data details averages for baseline, pre-decision, and post-decision epochs, for trust and distrust interactions.
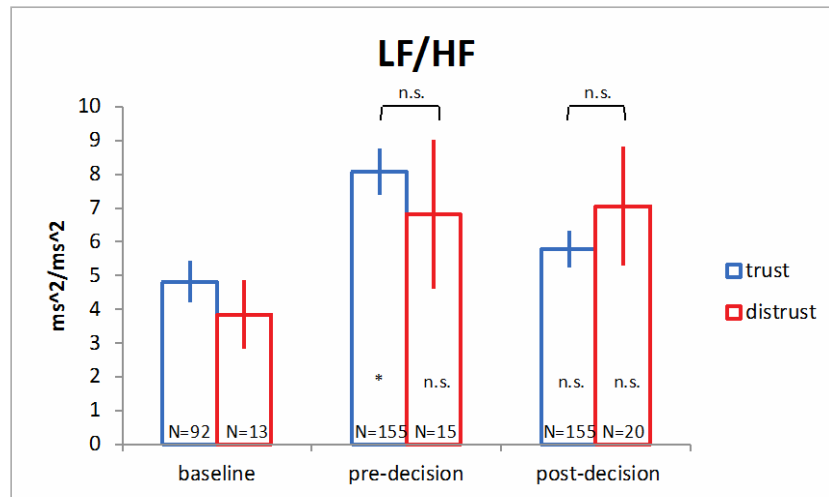
* = significant of the proposed SEM hypothesis

n.s. = not significant

N = the number of values per condition

Figure 112. Average ±S.E. for LF/HF (raw signal).
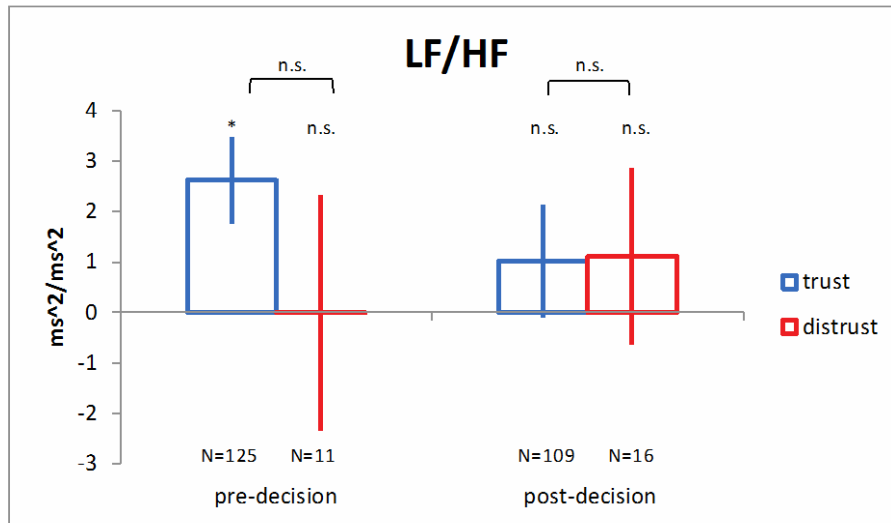
*= significant of the proposed SEM hypothesis

n.s. = not significant

N = the number of values per condition

Figure 113. Average ±S.E. for LF/HF (signal minus baseline).
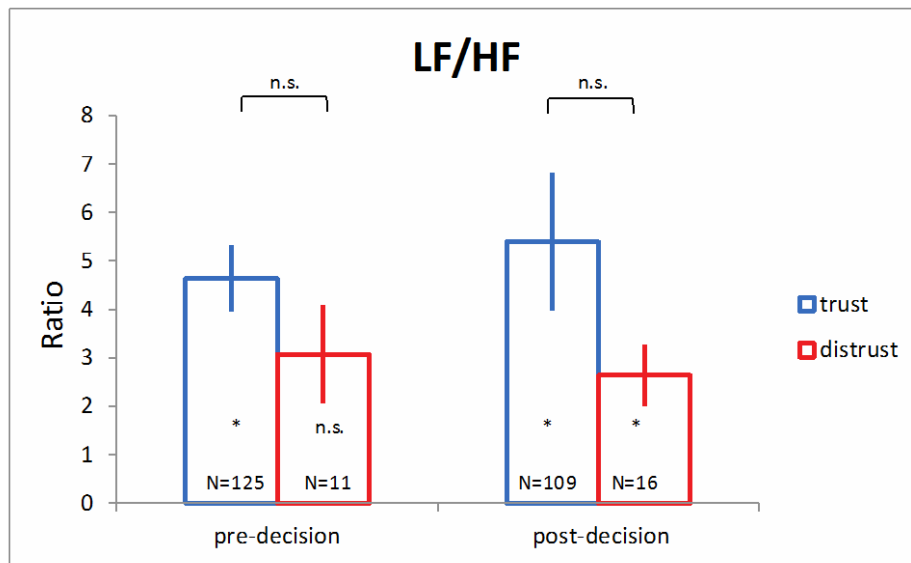

*= significant of the proposed SEM hypothesis

n.s. = not significant

N = the number of values per condition

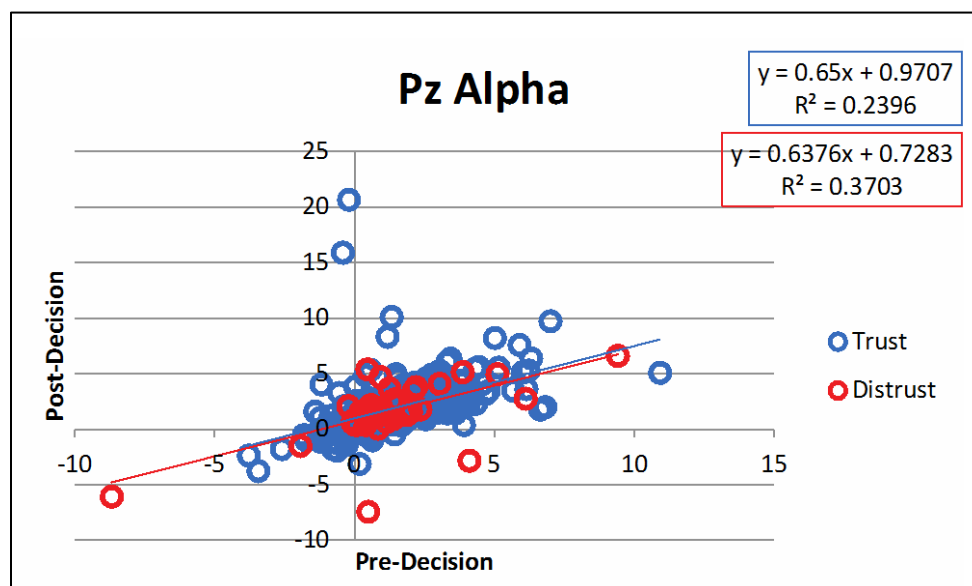Figure 114. Average ±S.E. for LF/HF (signal divided by baseline).

3.28.2 Scatter Plots

Figures 115–117 show scatter plots for LF/HF: raw signal, signal minus baseline, and signal divided by baseline plots.
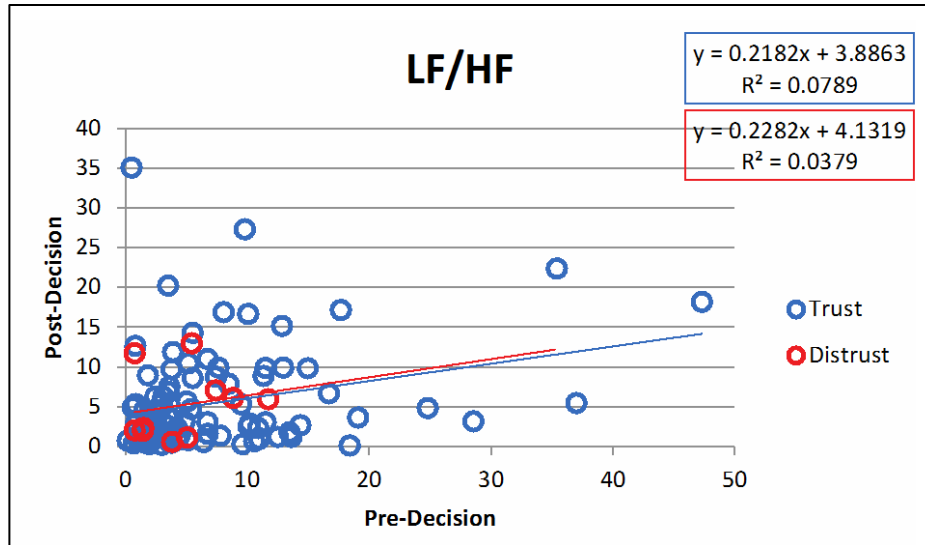
Values for pre-decision and post-decision epochs are displayed in the x-axis and y-axis.

The equation and R2 value for the linear trendline is displayed for trust and distrust interactions in blue and red box.
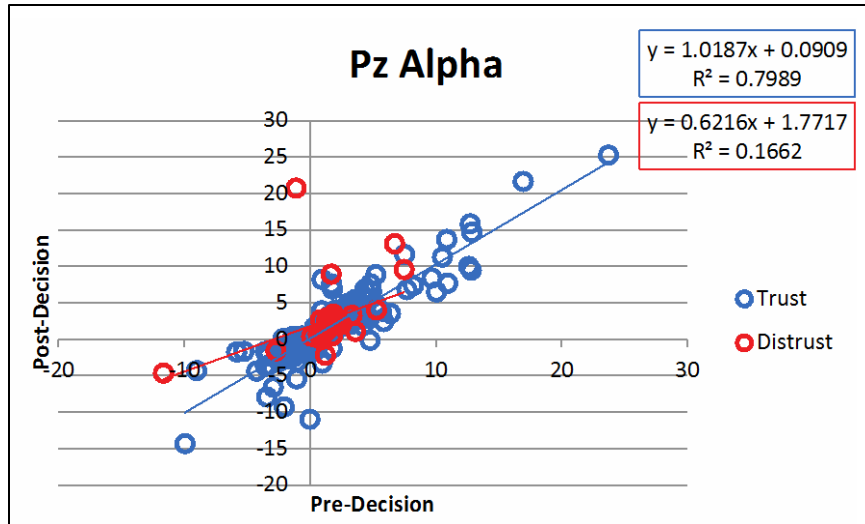
Figure 115. Scatter plot for LF/HF (raw signal).
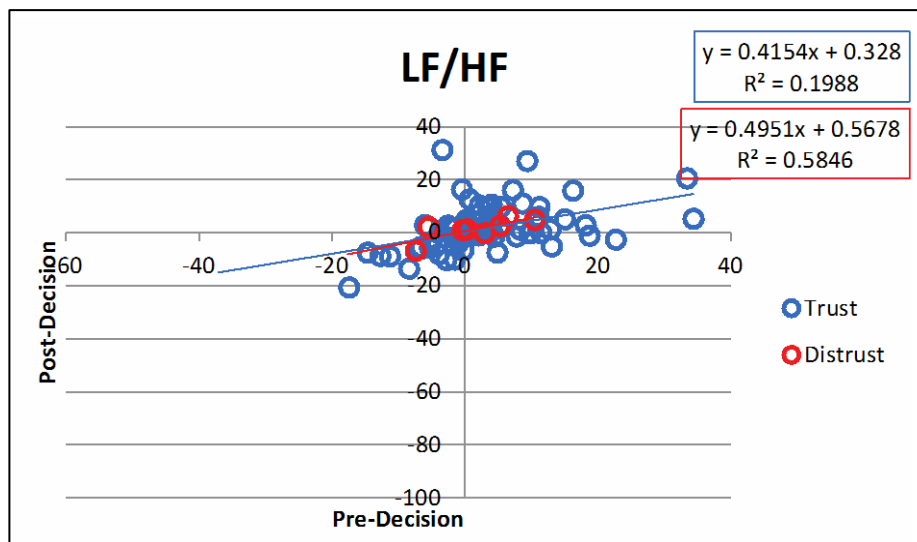
Values for pre-decision and post-decision epochs are displayed in the x-axis and y-axis.

The equation and R2 value for the linear trendline is displayed for trust and distrust interactions in blue and red box.

Figure 116. Scatter plot for LF/HF (signal minus baseline).
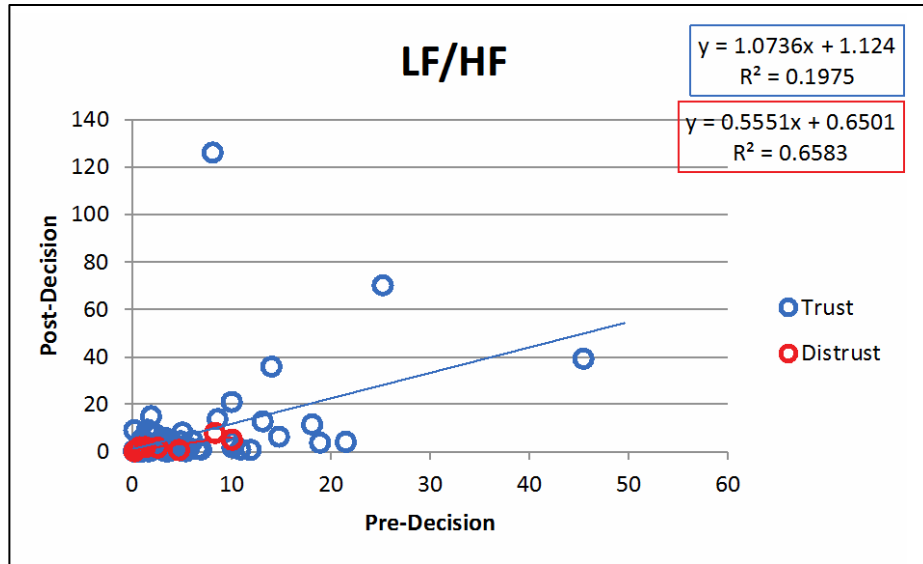
110

Values for pre-decision and post-decision epochs are displayed in the x-axis and y-axis.

The equation and R2 value for the linear trendline is displayed for trust and distrust interactions in blue and red box.

Figure 117. Scatter plot for LF/HF (signal divided by baseline).

3.29 EEG: FRONTAL POWER SPECTRAL DENSITY

Left, middle, and right plots in Figure 118 in show average PSD across all subjects for right (channel F4), left (channel F3) frontal hemisphere signals, and the difference between them (F4–F3) for trust and distrust interactions. For each plot, the average power of the 2-minute window for baseline, pre-decision, and post-decision is shown in Figure 118. Colors for power on the right of the spectral density graphics are shown in decibels.
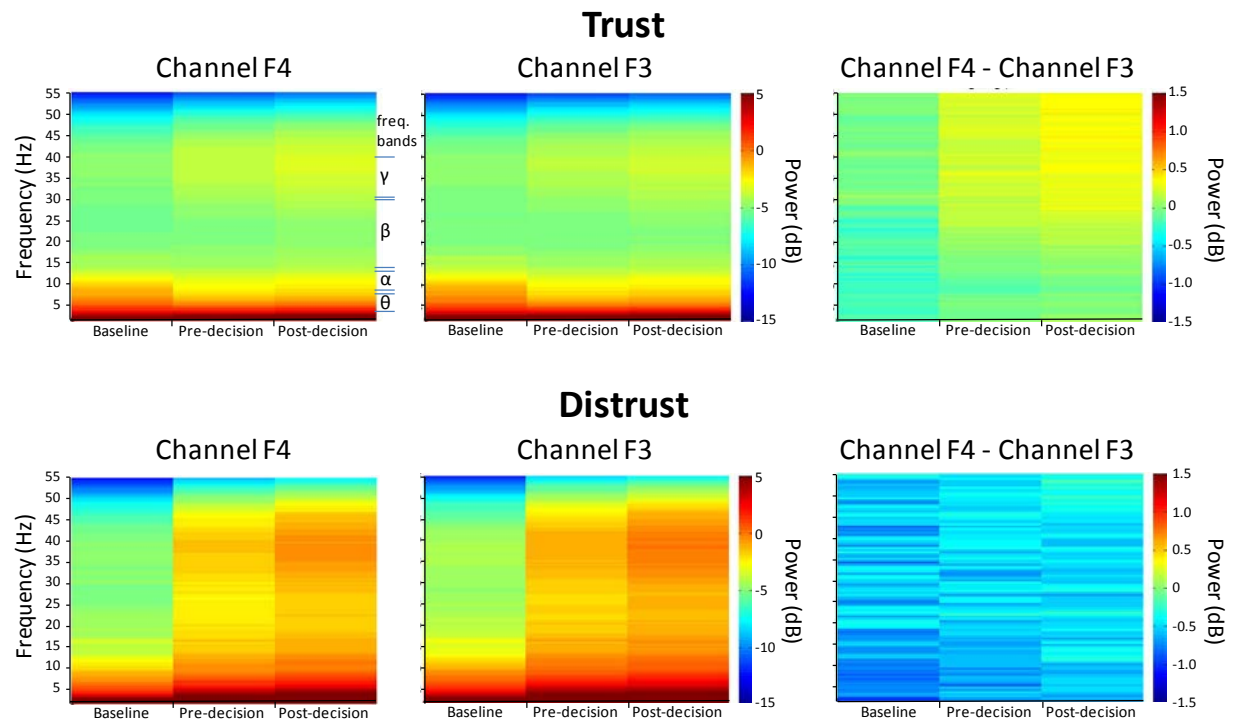
Figure 118. EEG frontal power spectral density plot.

Frequencies are displayed along the y-axis and time/event along the x-axis. The power of each frequency is represented in color, as labeled by the color bar on the right. Overall, the left hemisphere exhibits relatively higher power when subjects are involved in a distrust interaction. This seems particularly true in the higher frequencies (i.e., γ-band). As stated in Section 3.8, there were no significant differences between any of the comparisons specifically for frontal alpha asymmetry.

4. DISCUSSION

4.1 SIGNIFICANCE OF FINDINGS

We performed 252 statistical tests between various interactions and measures. The different methods of analysis (i.e., raw signals, signals minus baseline, and signals divided by baseline) across each hypothesis (1–6) yielded variable results for each measure Section 3. This approach made interpretation of significant findings challenging. An explanation for each measure is given in this report above the statistical table in Sections 0 through 0. An explanation of the significant findings is provided in Sections 4.1.1 through 4.1.11.

4.1.1 Alpha Asymmetry

No significant differences were found for fontal alpha power asymmetry. One reason for this may be that the original hypotheses stems from previous work stating that frontal alpha asymmetry (i.e., greater left frontal activity) is correlated with greater approach (Coan and Allen, 2003). It was hypothesized that a trust behavior is indicative of approach. The correlation of EEG and approach is mainly based on the comparison of questionnaires (i.e., the *propensity* to approach) to *resting state* EEG alpha power, not actual behavior (Coan, Allen, and McKnight, 2006). This discrepancy could be a reason why significant frontal hemispheric differences were not found. As in most studies looking at this measure, differences in processing techniques applied to the data could be manipulating the results for reviews, see Coan Allen, and Nazarian (2004) and Davidson (2004).

Although significant differences were not present in this measure, other aspects of the EEG signal appear to show promising differences between trust and distrust interactions. Figure 118, showing the average power of the frequency bands across a larger spectrum for the frontal channels (F3 and F4), suggests that differences may be present at other frequency bands and/or when looking at individual channels rather than asymmetries across hemispheres. Given that trust has not been explicitly searched for in EEG, looking at the spatial-temporal dynamics of other channels is an important venture and may prove to be fruitful. For example, Cacioppo relates asymmetrical alpha activity over the anterior lobe to feelings and emotion, which could be a viable region of interest for future analyses (Cacioppo, 2004).

4.1.2 RR Interval

Overall, the RR interval changes are somewhat confusing. In the case of distrust, some changes appeared to be consistent with the SEM hypothesis (H3b, H5b). But in those instances related to trust, there was either no change or the change contradicted the SEM. The reversal of the significance patterns when adjusting for the baseline is also confusing and seems to be an artifact due to variable manipulation (i.e., reverse response) as opposed to any experimentally induced changes. Significant RR intervals changes between trust and distrust were present in pre-decision tests. This suggests that RR intervals decreased (compared to baseline) regardless of whether subjects trusted or distrusted. RR interval decrease significantly more during distrust interactions which supports the SEM.

4.1.3 Low- and High-Frequency HRV

Increases in the LF signal relative the HF signal are postulated to indicate activation of the sympathetic nervous system consistent with an increased sympathetic drive in regulating heart rate leading to a decrease in HRV. Recent experimental evidence brings this interpretation into question. (Goldstein, 2010; Goldstein, Bentho, Park, and Sharabi, 2011) provides a compelling argument that the LF HRV signal bears no relation to the autonomic drive of the sympathetic nervous system outflows to the heart, but is an index of the autonomic outflows in response to the baroreflex. The LF HRV signal is independent of normalization or the HF HRV signal. In other words, the LF HRV signals are likely related to blood pressure regulation and not necessarily to heart rate regulation.

Under resting conditions the HF modulation of heart rate variability is related to the parasympathetic nervous system activity in relation to respiratory sinus arrhythmia corresponding to the frequency of breathing. In the current SS experimental paradigm, assessment of HF as an index of parasympathetic activity is probably valid; the LF PSD is related to blood pressure modulation, which was not assessed during the experimental paradigm. Therefore, the increase in HF PSD would indicate a reduction in the parasympathetic drive and a decrease in heart rate when the decision was made to trust (Malik, 1996).

4.1.4 Skin Conductance Levels

SCL went up from baseline regardless of trust or distrust interactions. When subjects were put in a situation to trust or not trust their partner, subjects SCL was significantly higher when they distrusted their partners, which is consistent with SEM. This suggests that the task itself caused an increase in SCL. The degree to which SCL increased was a function of the decision the subjects made. Skin conductance level is a more tonic measure of perspiration response over a longer periods of time, it is a good measure for this type of task in which the actual point at which trust/distrust was attained is unknown and measured over 2-minute epochs.

4.1.5 Skin Conductance Response

Like SCL, SCR went up from baseline regardless of trust or distrust interactions. Unlike SCL, no significant differences were present between trust and distrust. Therefore, subjects' SCL levels were not dependent on whether they trusted or distrusted their partners. Given that SCR is a more phasic measure of skin conductance, typically a response to particular acute events, it is not surprising that the average response over 2-minute epochs with no defined event time revealed no differences between trust vs. distrust interactions.

4.1.6 Oxytocin

The oxytocin results were consistent with the SEM model (i.e., an increase in the OT with trust). Note that direct comparisons between trust vs. distrust were not significant.Table 32 shows that the levels of oxytocin are trending in the directions predicted by SEM. Lack of significance may be because of the number of samples (especially for distrust interactions) was small. This suggests that oxytocin may be associated with a trusting relationship, but more work must be done to determine if this is truly the case.

4.1.7 Cortisol

Cortisol results are consistent with the predicted change for the SEM model (i.e., a decrease in CT with trust). This was true prior to the decision (i.e., pre-decision) and was sustained through the actual decision to trust (i.e., post-decision). This interpretation is also supported by the observation that the pre- vs. post-decision cortisol levels were both significantly reduced compared to baseline. Note that the baseline cortisol may not reflect the true baseline due to the tendency for cortisol levels to decline during the course of the day. Also, the baseline blood collection is taken when the subjects first arrived at the testing center and after the IV catheter was placed into the subject's vein. Either of these circumstances (exposure to new surrounds and/or the stress of the blood draw, could lead to a temporal rise in serum cortisol (Meeran, Hatterersly, Mould, and Bloom, 1993).

4.1.8 Mayer-ABI

Mayer-ABI is the Mayer trust scale for partners ability, benevolence and integrity. As stated in the results, trust vs. distrust comparisons were significantly different for the Mayer A, B, and I scores for both the pre-decision and post-decision events. This suggests that during trust interactions subjects thought that their partners had greater ability, benevolence, and integrity compared to subjects that did not trust their partners.

4.1.9 STAI-S

The STAI-S results show that subjects who trusted their partners exhibited a lower level of anxiety (relative to baseline levels) both prior to and after their decision. No significance differences were present for the distrust interactions (relative to baseline). This suggests that exhibiting a trusting behavior decreases anxiety, but lack of significance between trust vs. distrust makes this interpretation less strong. These inconsistent results may be due to the fact that the unequal samples sizes between groups.

4.1.10 SAS

SAS scores decrease with trust, which is consistent with the SEM hypotheses. SAS scored also decreased with distrust. This suggests subjects were less stressed prior to making a decision, regardless of whether that decision was to trust or not trust, compared to baseline levels.

4.1.11 Simultaneous signal changes

Figure 5 shows the distribution of the percentage of signals that agree with the SEM for each decision. There are only a few instances (~ 3.9%) in which the signals associate each decision to trust/distrust were in complete agreement with the SEM, with the majority of decision lying around 40–60%. If the signals agreed with the SEM for most decisions, these distributions would be shifted to the right (towards 100%). The post-decision distrust distribution is somewhat representative of this shift, which may be a good place to further investigate the SEM. Another point of interest is that there are a non-trivial number of instances in which 0% of the signals agree with the SEM. Given that the probability of this is very small, it may be worth re-evaluating the classification of these decisions as trust interactions.

4.2 ADDITIONAL ANALYSES

Given the complexity and magnitude of this dataset, there are still a number of analyses that could be performed to examine psychophysiological responses to trust.

4.2.1 Measures

In addition to the analyses described in this report, other mythologies the following could be used to examine the data. Although this list is nearly infinite, some relevant analyses include the following:

- Other channels/frequency bands in EEG
- Temporal and spatial correlations between EEG channels
- Examination of the time course of signal responses rather than an average over 2-minute epochs
- Other heart rate variability analyses (e.g., RMSSD, NN50)
- Examination of the last blood draw of the morning and afternoon sessions
- Correlation of baseline questionnaires (i.e., general personality) to behavior
- Cluster/discriminant analysis of SEM measures
- Predictive model of trust/distrust based on SEM measures

4.2.2 Statistical Procedures

For Analyses 2 (raw values) and Analysis 3, data were analyzed using one-way ANOVAs with least-square difference (LSD) to make comparisons of interest between groups separately associated with each hypothesis. Other methods may need to be examined include the following:

- A 3 x 2 multivariate ANOVA, multivariate analysis of variance (MANOVA) to compare all events (baseline, pre-decision, and post-decision) between the interactions (trust and distrust).
- Student-Newman-Keuls (SNK) comparison tests may be a good option for making comparisons. Although LSD is more powerful (in a statistical sense), it does not hold the experiment-wise error rate at ($p < 0.05$). Therefore, a better multiple comparison procedure may be SNK, which does hold the error rate. Both methods do not adequately adjust for the multiple comparison problems, especially true when more than three groups are compared. But SNK may be a good test to run based on the number of experiments (tests) that were actually performed.

4.2.3 Grouping variables

There were numerous variables associated with each subject that could be used to parse the data into different groups. These include the following:

- Acculturation
- Type of interaction (familiar or unfamiliar)
- Type of protocol (1 or 2)
- Age
- Gender

Variables associated with each subject used to parse data into different groups:

- Partner's trust
- Morning or afternoon session
- Partner interaction with similar or different:
- Acculturation
- Gender
- Age

4.2.4 Events

   Although the focus of this report is on the time epochs surrounding the point of the trust decisions, there are additional time periods that might prove interesting to examine. These epochs include the following:

- Partner introductions
- Subject/partner interview
- Subject/partner reveal of interview outcome
- Endowment adjustment
- Hypothetical game (Round 3)

5. CONCLUSIONS

Although we may be able to articulate our personal understanding of trust with ease, quantifying, manipulating, and measuring trust is extremely complex and dynamic. It represents an amalgam of unknowns, including emotional, psychological, behavioral, physiological responses, changing both instantaneously depending on our interactions with our surrounding, and gradually over the course of a lifetime, all based on a myriad of acute and chronic experiences and exposures.

The gestalt of trust is not one that is easily rendered in a scientific setting for controlled experimentation. Despite this, the goal of measuring trust is a worthy endeavor with enormous implications. Not only did this study attempt to understand the holistic neural, psychophysiological, psychological, and behavioral underpinnings of the nature of trust, but more broadly, enhance our understanding of the social dynamic of human interaction vital to the success of everyday life, especially in the defense and intelligence community context.

The purpose of TRUST Phase 1 was to address the feasibility of performing trust research and the applicability of varying novel paradigms, based on classic trust literature, which required research subjects to make a decision on the trustworthiness of another person. Although this undertaking could have been designed and executed in many ways, the Sharing Secrets protocols were designed to measure and require trust context under, and close to, ecological settings, so that the results and findings could be translated to real-world applications, rather than simple laboratory settings like those discovered in previous literature. We found that despite the challenges that are inherent to measuring trust in an ecological rather than a more traditionally controlled laboratory setting, some physiological, psychological, hormonal, and behavioral responses to trusting situations changed significantly depending on subjects assessment of their partners trustworthiness. And, as expected, some did not. The sum of these measures is currently the most complete evaluation of simultaneously recorded multimodal measures to assess trust and trustworthiness.

Accepting that ecologically valid research naturally contains inherent empirical challenges, based on the findings (both statistically and the logistical execution of these complex protocols), there is inconclusive evidence for recommendation of further study, especially without clearer definition of TRUST Phase 2 goals and objectives. If the latter is planned to be the implementation or deployment of the Sharing Secrets protocols with only minor (or no) modification, we conclude that Phase 2 should not be implemented. If Phase 2 should move forward, we recommend major alteration to the paradigm design to reflect the significant recommendations included herein.

6. RECOMMENDATIONS

The idea of an ecological study design is theoretically plausible. It opens the door for multiple extraneous and confounding variables that impede the results and thus the interpretations. If Phase 2 mirrors the Sharing Secrets protocol, we suggest a revised study design that controls more for these variables and creates results that are easily interpretable, so as to establish that these specific measures that were employed are a valid means of measuring trust.

6.1 STUDY DESIGN

We learned many things that we recommend be applied to future studies. Although one of the primary objectives of the study was to test the ecological validity of the Sharing Secrets protocol, the scientific validity of the study is also critical for the interpretation of the findings. In order to ensure scientific validity some aspects of the protocol should be more controlled. Specifically, the exact timing trust is established and how to go about measuring that interaction. Since trust or distrust can be established as soon as one sees another individual, movement should be restricted to prevent unwanted noise in the EEG signal. To prevent this extra noise, subjects should not be able to see their partner until both subjects are sitting still. By knowing the exact moment trust was acquired, psycho/physiological signals related to the event could be definitively interpreted.

During the first screening procedures, questionnaires should be mailed to potential subjects to establish an individual's phenotype in relation to trust/distrust. When examining the payout matrix, make the consequences for trust/distrust much greater. This will create a higher risk scenario. We found unequal sample sizes within groups (trust and distrust) posed statistical problems when analyzing the data. To overcome these problems, we suggest focusing study on individuals who have inherent distrust. Given the design of the study, each decision should be treated as an independent event rather than combining events (i.e., predecision, post-decision).

Considering there are multiple rounds within each session, any decision after the first round cannot stand alone and subsequently influences decisions in rounds two and three. It may be more practical to exclude round's two and three and only use one round per session to reduce the independent variables from being influenced/washed out. Along the same lines rather than combining Protocol 1 and 2 for data analysis, it is important to maintain independency on the basis that the design of each study is different enough to cause invalid results when merging the two data collections. Using only one round per session will greatly shorten the amount of time subjects are asked to be studied and reduce the busyness of the study design. This will enable subjects to comprehend the study in greater detail. Along with a shorter study design, we believe it is important to reduce social interaction (besides partner–partner interaction) with research staff. Also, due to the variability of oxytocin, any prolonged or behavioral interaction (laughing, stand-offish feelings, any behavioral feeling when psychophysiological recording equipment is applied) with research staff can alter oxytocin levels. We believe creating a shorter study design will prevent subject fatigue and disinterest and result in cleaner/uncomplicated results.

6.2 PHYSIOLOGICAL SUGGESTIONS

Physiologically speaking, there are a few things that should be factored in and controlled to create more validity in the study design. One important aspect that should be controlled is food-intake. Specifically, the dietary composition (amount of fat, protein, sugar, etc.) and exact time is highly relevant to the results. Simply eating a meal (particularly an afternoon meal) causes an increase in pulsatile adrenal corticotropic hormore (ACTH) secretion and a surge in cortisol along with insulin. Additionally, the dietary composition of the meal can cause variable biochemical results that may hinder the expected results. Since, cortisol is one of the primary outcome variables and is thought to be inversely related to oxytocin, it is highly important to control food-intake.

Another aspect that is important to control is sleep. The amount of sleep a subject gets the night before the study is highly reflective of their cognitive performance the next day. Depending on a subject's wake time and total sleep time, it will affect the time of the morning diurnal spike in cortisol and subsequently the time of day cortisol decreases. Since we cannot say all subjects received the same amount of sleep the night before the study, this assumption leads to high inter-subject variability at baseline as well as how each subject performs, given their baseline energy level/interest.

To establish control food-intake and sleep, we suggest subjects meet with research staff the day before to be given an actigraph (watch-like device for measuring arousal/sleep and light-intake) and also fill out a sleepiness scale when they arrive to the testing center. Additionally, subjects should meet with a dietician to establish a subject's basal metabolic rate and resting metabolic rate (BMR and RMR) to control food-intake. By knowing a subject's BMR and RMR, specific food (composition known) can be given to the subject.

In reference to the catheter placement, there should be a relaxation period (at least ~ 45 minutes) after the catheter placement. The purpose of the relaxation period post catheter placement is to let subject's relax mentally as well as physiologically. It is known that catheter placements can cause spikes in some subject's cortisol levels and because of this fact, it is important to let subjects have a relaxation period post catheter placement to let cortisol come back to baseline. The number of blood draws and times they are taken should be addressed and defined since the hormone levels can change very quickly.

We suggest using a frequently sampled procedure, so we generate a more phasic outcome. This, along with a shorter study design, will create a more interpretable assessment of blood samples, so we would know each subject's hormone levels at multiple time points. To establish a cleaner baseline EEG signal, we suggest having subjects sit still with periods of eyes open, blinking, closed, and looking in multiple directions. This will result in a lower noise to signal ratio.

REFERENCES

Ahern, G. L., and G. E. Schwartz. 1985. "Differential Lateralization for Positive and Negative Emotion in the Human Brain: EEG Spectral Analysis," *Neuropsychologia 23*:745–756.

Barberis, C., and E. Tribollet. 1996. "Vasopressin and Oxytocin Receptors in the Central Nervous System," *Critical Reviews in Neurobiology 10*:19–154.

Baker, F. C., I. M. Colrain, and J. Trinder. 2008. "Reduced Parasympathetic Activity During Sleep in the Symptomatic Phase of Severe Premenstrual Syndrome," *Journal of Psychosomatic Research 65*:13–22.

Bartholomew, K., and L. M. Horowitz. 1991. "Attachment Styles among Young Adults: A Test of a Four-Category Model," *Journal of Personality and Social Psychology 61*(2):226–244.

Baumgartner, T., M. Heinrichs, A. Vonlanthen, U. Fischbacher, and E. Fehr. 2008. "Oxytocin Shapes the Neural Circuitry of Trust and Trust Adaptation in Humans." Available online at *Neuron* http://www.cell.com/neuron/fulltext/S0896-6273(08)00327-9. Accessed March 1, 2016.

Benedek, M., and C. Kaernbach. 2010. "A Continuous Measure of Phasic Electrodermal Activity," *Journal of Neuroscience Methods 190*(1):80–91.

Berscheid, E., M. Snyder, and A. Omoto. 2004. "Measuring Closeness: The Relationship Closeness Inventory (RCI) Revisited." In *The Handbook of Closeness and Intimacy,* pp. 81–101, D. J. Mashek, A. Aron, and L. Erlbaum, Eds. Lawrence Erlbaum Associates, Mahwah, NJ.

Bigley, G. A., and J. L. Pearce. 1998. "Straining for Shared Meaning in Organization Science: Problems of Trust and Distrust," *The Academy of Management Review 23*(3):405–421.

Blau, P. M. 1986. *Exchange and Power in Social Life*. 2nd ed., pp. 1–352. Transaction Publishers, New Brunswick, NJ, and London, United Kingdom.

Bodenmann, G., B. Ditzen, U. Ehlert, B. Gabriel, M. Heinrichs, and M. Schaer. 2009. "Intranasal Oxytocin Increases Positive Communication and Reduces Cortisol Levels During Couple Conflict," *Biological Psychiatry 65*:728–731.

Cacioppo, J. T. 2004. "Feelings and Emotions: Roles for Electrophysiological Markers," *Biological Psychology 76*(1–2):235–243.

Carter, S. C. 1998. "Neuroendocrine Perspectives on Social Attachment and Love," *Psychoneuroendocrinology 23*:779–818.

Castaldo, S. 2008. "Trust in Market Relationships." In *An Interpretative Model*, M. Buri, and M. Moro Eds. Edward Elgar Publishing, Cheltenham, United Kingdom.

Chernenko, S. 2012. "ECG Processing R Peaks Detection." *Medical Digital Signal Processing Software Development.* Available online at http://www.librow.com/cases/case-2/. Accessed February 18, 2016.

Coan, J. A., and J. J. B. Allen. 2004. "Frontal EEG Asymmetry as a Moderator and Mediator of Emotion," *Biological Psychology* 67:7–49.

Coan, J. A., and J. J. B. Allen. 2003. "Frontal EEG Asymmetry and the Behavioral Activation and Inhibition Systems," *Psychophysiology* 40:106–114.

Coan, J. A., J. B. Allen, and P. E. McKnight. 2006. "A Capability Model for Individual Differences in Frontal EEG Asymmetry," *Biological Psychology* 72(2):198–207.

Coan, J. A., J. J. B. Allen, and M. Nazarian. 2004. "Issues and Assumptions on the Road from Raw Signals to Metrics of Frontal EEG Asymmetry in Emotion," *Biological Psychology* 76(1–2): 183–218.

Costa, P. T., and R. R. McCrea. 1992. "Revised NEO Personality Inventory NEO PI-R and NEO Five-Factor Inventory NEO-FFI." In *Psychological Assessment Resources*. Hogrefe Publishing, Oxford, United Kingdom.

Cox J. C. 2002. "Trust, Reciprocity, and Other-Regarding Preferences: Groups vs. Individuals and Males vs. Females." In *Advances in Experimental Business Research,* R. Zwick and A. Rapoport, Eds. Kluwer Academic Publishers, Boston, MA.

Cox J. C. 2004. "How to Identify Trust and Reciprocity," *Games and Economic Behavior* 46:260–281.

Cox J. C. and C. A. Deck 2005. "On the Nature of Reciprocal Motives," *Economic Inquiry* 43(3):623– 635.

Davidson, R. J. 2004. "What Does the Prefrontal Cortex 'Do' Affect: Perspectives on Frontal EEG Asymmetry Research," *Biological Psychology* 67(1–2):219–234.

Davidson, R. J. 1984. "Affect, Cognition, and Hemispheric Specialization." In *Emotions, Cognition, and Behavior*, pp. 320–365, C. E. Izard, J. Kagan, and R. Zajonc, Eds. Cambridge University Press, New York, NY.

Davidson, R. J. 1988. "EEG Measures of Cerebral Asymmetry: Conceptual and Methodological Issues," *International Journal of Neuroscience* 39:71–89.

Davidson, R. J. 1993. "Cerebral Asymmetry and Emotion: Conceptual and Methodological Conundrums," *Cognition and Emotion* 7:115–138.

Davidson, R. J. 1998. "Affective Style and Affective Disorders: Perspectives from Affective Neuroscience," *Cognition and Emotion* 12:307–330.

Davidson, R. J., P. Ekman, C. Saron, J. Senulis, and W. Friesen. 1990. "Approach/Withdrawal and Cerebral Asymmetry: Emotional Expression and Brain Physiology: I," *Journal of Personality and Social Psychology* 58(2):330–341.

Delorme A., and S. Makeig. 2004. "EEGLAB: An Open Source Toolbox for Analysis of Sign-Trial EEG Dynamics Including Independent Component Analysis," *Journal of Neuroscience Methods* 134:9–21.

Fehr, E. 2008. "The Effect of Neuropeptides on Human Trust and Altruism: A Neuroeconomic Perspective." In *Hormones and Social Behaviour*, pp. 47–56, D. Pfaff, C. Kordon, P. Chanson, and Y. Christen, Eds. Springer-Verlag GmbH, Heidelberg, Germany.

Fehr, E. 2009. "On the Economics and Biology of Trust," *Journal of the European Economic Association 7*:235–266.

Fehr, E., U. Fischbacher, and M. Kosfeld. 2005. "Neuroeconomic Foundations of Trust and Social Preferences: Initial Evidence," *The American Economic Review 95*:346–351.

Franken, R. E., K. J. Gibson, and G. L. Rowland. 1991. "Sensation Seeking and the Tendency to View the World as Threatening," *Personality and Individual Differences 13*(1):31–38.

Gimpl, G., and F. Fahrenholz. 2001. "The Oxytocin Receptor System: Structure, Function, and Regulation*," Physiological Reviews 81*:629–683.

Goldstein, D. S. 2010. "Neuroscience and Heart-Brain Medicine: The Year in Review," *Cleveland Clinic Journal of Medicine 77*(Suppl. 1):S34–S39.

Goldstein, D. S., O. Bentho, M. Y. Park, and Y. Sharabi. 2011. "Low-Frequency Power of Heart Rate Variability is not a Measure of Cardiac Sympathetic Tone but May be a Measure of Modulation of Cardiac Autonomic Outflows by Baroreflexes," *Experimental Physiology 96*:1255–1261.

Gouin, J. P., C. S. Carter, H. Pournajafi-Nazarloo, R. Glaser, W. B. Malarkey, T. J. Loving, J. Stowell, and J. K. Kiecolt-Glaser. 2010. "Marital Behavior, Oxytocin, Vasopressin, and Wound Healing," *Psychoneuroendocrinology 35*:1082–1090.

Hammon, P. S., S. Makeig, H. Poizner, E. Todorov, and V. R. de Sa. 2008. "Predicting Reaching Targets from Human EEG," *IEEE Signal Processing Magazine 25*(1):69–77.

Heinrichs, M., T. Baumgartner, C. Kirschbaum, and U. Ehlert. 2003. "Social Support and Oxytocin Interact to Suppress Cortisol and Subjective Responses to Psychosocial Stress," *Biological Psychiatry 54*:1389–1398.

Hosmer, L. T. 1995. "Trust: the Connecting Link Between Organizational Theory and Philosophical Ethics," *The Academy of Management Review 20*(2):379–403.

Insel, R., L. and J. Young. 2001. "The Neurobiology of Attachment," *Nature Reviews Neuroscience 2*:129–136.

Kasperson, R. 1986. "Six Propositions on Public Participation and their Relevance for Risk Communication," *Risk Analysis 6*:275–281.

Kasperson, R., D. Golding, and S. Tuler. 1992. "Social Distrust as a Factor in Siting Hazardous Facilities and Communicating Risks," *Journal of Social Issues 48*:161–187.

Kosfeld, M., M. Heinrichs, P. J. Zak, U. Fischbacher, and E. Fehr. 2005. "Oxytocin Increases Trust in Humans," *Nature 435*:673–676.

Kramer, R. M. 1999. "Trust and Distrust in Organizations: Emerging Perspectives, Enduring Questions," *Annual Review of Psychology 50*:569–598.

Malik, M. 1996. "Heart Rate Variability: Standards of Measurement, Physiological Interpretation, and Clinical Use," *European Heart Journal 17*:354–381.

Mayer R. C., J. H. Davis, and F. D. Schoorman. 1995. "An Integrative Model of Organizational Trust," *Academy of Management Review 20*(3):709–734.

Mayer, R. C., and J. H. Davis. 1999. "The Effect of the Performance Appraisal System on Trust for Management: A Field Quasi-Experiment," *Journal of Applied Psychology 84*(1):123–136.

Meeran, K., A. Hatterersly, G. Mould, and S.R. Bloom. 1993. "Venipuncture Causes Rapid Rise in Plasma ACTH," *British Journal of Clinical Practice 47*(5):246–7.

Mitov, I. P. 1998. "A Method for Assessment and Processing of Biomedical Signals Containing Trend and Periodic Component," *Medical Engineering and Physics 20*(9):660–668.

Peters, R., V. Covello, and D. MacCallum. 1997. "The Determinants of Trust and Credibility in Environmental Risk Communication: An Empirical Study," *Risk Analysis 17*:43–54.

Poundstone, W. 1992. "Prisoner's Dilemma," Anchor Books, New York, NY.

Rousseau D. M., S. B. Sitkin, R. S. Burt, and C. Camerer. 1998. "Not so Different after All: A Cross-Discipline View of Trust," *Academy of Management Review 23*(3): 393–404.

Schneider, T. R. 2008. "Evaluations of Stressful Transactions: What's in an Appraisal," *Stress and Health 24*:151–158.

Spielberger, C. D., R. L. Gorsuch, and R. E. Lushene. 1970. "Manual for the State-Trait Inventory," C. D. Spielberger, R. L. Gorsuch, R. E. Lushene, P. R. Vagg, and G. A. Jackobs, Eds. Consulting Psychologist Press, Palo Alto, CA.

Spielberger, C. D., R. L. Gorsuch, R. Lushene, P. R. Vagg, and G. A. Jacobs. 1983. "Manual for the State-Trait Anxiety Inventory," Consulting Psychologists Press, Palo Alto, CA.

Stephenson, M. 2000. "Development and Validation of the Stephenson Multigroup: Acculturation Scale (SMAS)," *American Psychological Association, Inc. 12*(1):77–85.

Trinder, J., J. Kleiman, M. Carrington, S. Smith, S. Breen, N. Tan, and Y. Kim. 2001. "Autonomic Activity during Human Sleep as a Function of Time and Sleep Stage," *Journal of Sleep Research 10*:253–264.

Watson, D., L. A. Clark, and A. Tellegan. 1988. "Development and Validation of Brief Measures of Positive and Negative Affect: The PANAS Scales," *American Psychological Association, Inc. 54*(6):1063–1070.

Zak, P. J. 2008. "The Neurobiology of Trust," *Scientific American 298*:88–95.

Zak, P. J. 2005. "Trust: A Temporary Human Attachment Facilitated by Oxytocin," *Behavioral and Brain Sciences 28*:368–369

Zak, P. J. 2007. "The Neuroeconomics of Trust." In *Renaissance in Behavioural Economics: Harvey Leibenstein's Impact of Contemporary Economic Analysis,* pp. 105–145, Frantz Routledge, Ed. Taylor and Francis Group, New York, NY.

Zand, D. E. 1972. "Trust and Managerial Problem Solving," *Administrative Science Quarterly* *17*(2):229-239.

		Form Approved OMB No. 0704-01-0188

REPORT DOCUMENTATION PAGE

1. REPORT DATE *(DD-MM-YYYY)* April 2016	2. REPORT TYPE Final	3. DATES COVERED *(From - To)*

4. TITLE AND SUBTITLE Test and Evaluation of TRUST: Tools for Recognizing Useful Signals of Trustworthiness	5a. CONTRACT NUMBER
	5b. GRANT NUMBER
	5c. PROGRAM ELEMENT NUMBER

6. AUTHORS Jamie R. Lukos Matthew A. Yanagi Wayne Ensign Patrick Longhini Visarath In	5d. PROJECT NUMBER
	5e. TASK NUMBER
	5f. WORK UNIT NUMBER

7. PERFORMING ORGANIZATION NAME(S) AND ADDRESS(ES) SSC Pacific 53560 Hull Street San Diego, CA 92152–5001	8. PERFORMING ORGANIZATION REPORT NUMBER TR 3007

9. SPONSORING/MONITORING AGENCY NAME(S) AND ADDRESS(ES) Office of the Director of National Intelligence Intelligence Advanced Research Projects Agency Washington, DC 20511	10. SPONSOR/MONITOR'S ACRONYM(S) ODNI IARPA
	11. SPONSOR/MONITOR'S REPORT NUMBER(S)

12. DISTRIBUTION/AVAILABILITY STATEMENT
Approved for public release.

13. SUPPLEMENTARY NOTES
This is work of the United States Government and therefore is not copyrighted. This work may be copied and disseminated without restriction.

14. ABSTRACT
This study focuses on the measurement of trustworthiness. The report focuses on testing, research and evaluation of a new research method for measuring and requiring trust between individuals. Not only did this study attempt to understand the holistic neural, psychophysiological, psychological, and behavioral underpinnings of the nature of trust, but more broadly, enhance understanding of the social dynamic of human interaction vital to the success of everyday life, especially in the defense and intelligence community context. The study was adapted from a well-evaluated game theory paradigm (Prisoner's Dilemma). The Prisoner's Dilemma puts study participants in a situation where they must decide to trust or not trust an assigned partner. Their decisions and the decisions of their partners, to trust or not trust are determined by the amount of monetary compensation participants were given at the end of the experimental session. The study goal was to evaluate the extent to which particular behavioral, psychological, physiological, and neural signals are related to trust between two people. Many areas were studied for this report, including frontal alpha power asymmetry, electroencephalography (EEG), high- and low-frequency and RR interval of heart rate, electrocardiography (ECG), skin conductance levels and Galvanic Skin Response (GSR), oxytocin and cortisol concentrations, and psychological state (questionnaires). These areas were investigated using three different methodological transformations: one examining raw signals, and two adjusting the signals to baseline: minus baseline and divided by baseline. Applied throughout the report are six hypotheses derived from Social Exchange Model. The six hypotheses are provided in the report.

15. SUBJECT TERMS
Mission area: Psychological Research
trust, distrust, Prisoners Dilemma, oxytocin, cortisol, RR interval, ECG, GSR

16. SECURITY CLASSIFICATION OF:			17. LIMITATION OF ABSTRACT	18. NUMBER OF PAGES	19a. NAME OF RESPONSIBLE PERSON Matthew Yanagi
a. REPORT	b. ABSTRACT	c. THIS PAGE			19B. TELEPHONE NUMBER *(Include area code)*
U	U	U	U	157	(619) 553-7562

Standard Form 298 (Rev. 8/98)
Prescribed by ANSI Std. Z39.18

INITIAL DISTRIBUTION

Approved for public release.